1461

NOT FOR PUBLICATION

NEANDC(J)-116/U

INDC(JPN)-102/U

PROGRESS REPORT

(JULY 1984 TO JUNE 1985 INCLUSIVE)

SEPTEMBER 1985

EDITOR
S. KIKUCHI
JAPANESE NUCLEAR DATA COMMITTEE

JAPAN ATOMIC ENERGY RESEARCH INSTITUTE
TOKAI RESEARCH ESTABLISHMENT
TOKAI-MURA, IBARAKI-KEN, JAPAN

NOT FOR PUBLICATION

NEANDC(J)-116/U

INDC(JPN)-102/U

PROGRESS REPORT

(JULY 1984 TO JUNE 1985 INCLUSIVE)

SEPTEMBER 1985

EDITOR

S. KIKUCHI

JAPANESE NUCLEAR DATA COMMITTEE

JAPAN ATOMIC ENERGY RESEARCH INSTITUTE

TOKAI RESEARCH ESTABLISHMENT

TOKAI-MURA, IBARAKI-KEN, JAPAN

Editor's Note

This is a collection of reports which have been submitted to the Japanese Nuclear Data Committee at the committee's request. The request was addressed to the following individuals who might represent or be in touch with groups doing researches related to the nuclear data of interest to the development of the nuclear energy program.

Although the editor tried not to miss any appropriate addressees, there may have been some oversight. Meanwhile, contribution of a report rested with discretion of its author. The coverage of this document, therefore, may not be uniform over the related field or research.

In this progress report, each individual report is generally reproduced as it was received by the JNDC Secretariat, and editor also let pass some simple obvious errors in the manuscripts if any.

This edition covers a period of July 1, 1984 to June 30, 1985. The information herein contained is of a nature of "Private Communication". Data contained in this report should not be quoted without the author's permission.

TABLE OF CONTENTS

ELEMENT S	A	QUANTITY	ENERGY MIN	MAX	LAB	TYPE	DOCUMENTATION REF	VOL	PAGE	DATE	COMMENTS
H	002	N, PROTON	50+7		YOK	THEO-PROG	NEANDC-J116		79	SEP 85	SHIRATO+.FADDEEV ANAL OF P-SPEC.FIG
LI	006	N EMISSION	42+6	14+7	TOH	EXPT-PROG	NEANDC-J116		83	SEP 85	CHIBA+.PRESENTED AT 1985 SANTA FE
LI	006	N EMISSION	42+6	14+7	TOH	EXPT-PROG	NEANDC-J116		85	SEP 85	CHIBA+.TBP IN NST
LI	007	N EMISSION	42+6	14+7	TOH	EXPT-PROG	NEANDC-J116		83	SEP 85	CHIBA+.PRESENTED AT 1985 SANTA FE
LI	007	N EMISSION	54+6	14+7	TOH	EXPT-PROG	NEANDC-J116		85	SEP 85	CHIBA+.TBP IN NST
LI	007	N, TRITON	14+7		YOK	EXPT-PROG	NEANDC-J116		81	SEP 85	FURUTATE+.DA/DE SIG IN FIGS
BE	009	EVALUATION	10-5	20+7	JAE	EVAL-PROG	NEANDC-J116		37	SEP 85	SHIBATA.PUBLISHED AS JAERI-M 84-226
B	010	N EMISSION	14+7		TOH	EXPT-PROG	NEANDC-J116		84	SEP 85	BABA+.PRESENTED AT 1985 SANTA FE
B	011	N EMISSION	14+7		TOH	EXPT-PROG	NEANDC-J116		84	SEP 85	BABA+.PRESENTED AT 1985 SANTA FE
C	012	N EMISSION	14+7	18+7	TOH	EXPT-PROG	NEANDC-J116		84	SEP 85	BABA+.PRESENTED AT 1985 SANTA FE
N	014	N EMISSION	14+7		TOH	EXPT-PROG	NEANDC-J116		84	SEP 85	BABA+.PRESENTED AT 1985 SANTA FE
O	016	N EMISSION	14+7		TOH	EXPT-PROG	NEANDC-J116		84	SEP 85	BABA+.PRESENTED AT 1985 SANTA FE
F	019	N EMISSION	14+7		TOH	EXPT-PROG	NEANDC-J116		84	SEP 85	BABA+.PRESENTED AT 1985 SANTA FE
AL	027	DIFF ELASTIC	12+7	14+7	JAE	EXPT-PROG	NEANDC-J116		33	SEP 85	SUGIMOTO+.D-D TOF.20-140 DEG.NDG
AL	027	DIFF INELAST	12+7	14+7	JAE	EXPT-PROG	NEANDC-J116		33	SEP 85	SUGIMOTO+.D-D TOF.20-140 DEG.NDG
AL	027	N, PROTON	14+7		KTO	EXPT-PROG	NEANDC-J116		53	SEP 85	KOBAYASHI+.REAC+6LI.D,76.13+-3.49 MB
AL	027	N, ALPHA	14+7	20+7	JPN	EXPT-PROG	NEANDC-J116		5	SEP 85	KUDO+.D-T.ACT.ABSL SIG.FIG GIVN
AL	027	N, ALPHA	15+7		KYU	EXPT-PROG	NEANDC-J116		65	SEP 85	FUKAHORI+.HE PROD SIG=120+-11 MB
SI		TOTAL	20-3	20-1	JPN	EXPT-PROG	NEANDC-J116		70	SEP 85	AIZAWA+.PRESENTED AT 1985 SANTA FE
SI		N EMISSION	14+7		TOH	EXPT-PROG	NEANDC-J116		84	SEP 85	BABA+.PRESENTED AT 1985 SANTA FE

ELEMENT S	A	QUANTITY	ENERGY MIN	MAX	LAB	TYPE	DOCUMENTATION REF	VOL	PAGE	DATE	COMMENTS
SI	028	DIFF ELASTIC	13+7		JAE	EXPT-PROG	NEANDC-J116		34	SEP 85	YAMANOUTI+.D-D TOF.DWBA CC ANAL.NDG
SI	028	DIFF INELAST	13+7		JAE	EXPT-PROG	NEANDC-J116		34	SEP 85	YAMANOUTI+.D-D TOF.DWBA CC ANAL.NDG
SI	028	N, GAMMA	57+5	81+5	TIT	EXPT-PROG	NEANDC-J116		90	SEP 85	SHIMIZU+.TOF,WG.NDG
SI	028	N, GAMMA	57+5	81+5	TIT	THEO-PROG	NEANDC-J116		91	SEP 85	KITAZAWA+.CORE-PARTICLE MODEL CALC.
CA	042	N, PROTON	13+7	15+7	JAE	EXPT-PROG	NEANDC-J116		20	SEP 85	OISHI+.D-T,ACT.FIG GIVN
CA	044	N, PROTON	13+7	15+7	JAE	EXPT-PROG	NEANDC-J116		20	SEP 85	OISHI+.D-T,ACT.FIG GIVN
CA	044	N,N PROTON	13+7	15+7	JAE	EXPT-PROG	NEANDC-J116		20	SEP 85	OISHI+.D-T,ACT.FIG GIVN
CA	044	N, ALPHA	13+7	15+7	JAE	EXPT-PROG	NEANDC-J116		20	SEP 85	OISHI+.D-T,ACT.FIG GIVN
MN	055	RES INT ABS	50-1		KTO	EXPT-PROG	NEANDC-J116		56	SEP 85	KOBAYASHI+.REL AU-197,14.0B+-3.33PC
FE	056	N, PROTON	14+7	20+7	JPN	EXPT-PROG	NEANDC-J116		5	SEP 85	KUDO+.D-T.ACT.ABSL SIG.FIG GIVN
CO	059	N, 2N	14+7	15+7	JAE	EXPT-PROG	NEANDC-J116		16	SEP 85	IKEDA+.D-T,ACT,REL AL(N,A).FIG GIVN
NI	058	N, 2N	14+7	15+7	JAE	EXPT-PROG	NEANDC-J116		16	SEP 85	IKEDA+.D-T,ACT,REL AL(N,A).FIG GIVN
NI	058	N, 2N	14+7		KTO	EXPT-PROG	NEANDC-J116		53	SEP 85	KOBAYASHI+.REAC+6LI.D,25.36+-0.84 MB
NI	058	N, PROTON	14+7		KTO	EXPT-PROG	NEANDC-J116		53	SEP 85	KOBAYASHI+.REAC+6LI.D,416.6+-13.9 MB
GE		TOTAL	15-3	30-1	JPN	EXPT-PROG	NEANDC-J116		73	SEP 85	SUETOMI+.TBP IN NST.
ZR	090	N, 2N	14+7		KTO	EXPT-PROG	NEANDC-J116		53	SEP 85	KOBAYASHI+.REAC+6LI.D,626.4+-20.8 MB
ZR	090	N, 2N	14+7	15+7	JAE	EXPT-PROG	NEANDC-J116		16	SEP 85	IKEDA+.D-T,ACT,REL AL(N,A).FIG GIVN
NB		TOTAL	24+4		JPN	EXPT-PROG	NEANDC-J116		70	SEP 85	AIZAWA+.PRESENTED AT 1985 SANTA FE
NB	093	N, 2N	14+7	15+7	JAE	EXPT-PROG	NEANDC-J116		16	SEP 85	IKEDA+.D-T,ACT,SIG TO ISOM.FIG GIVN
NB	093	N, 2N	14+7		KTO	EXPT-PROG	NEANDC-J116		53	SEP 85	KOBAYASHI+.REAC+6LI.D,471.1+-15.6 MB

ELEMENT S	A	QUANTITY	ENERGY MIN	ENERGY MAX	LAB	TYPE	DOCUMENTATION REF	VOL	PAGE	DATE	COMMENTS
MO	092	N, PROTON	15+7		NAG	EXPT-PROG	NEANDC-J116		75	SEP 85	KATOH+.ACT SIG TO ISOM=68.1+-1.5 MB
MO	092	N, PROTON	13+7	15+7	JAE	EXPT-PROG	NEANDC-J116		24	SEP 85	IKEDA+.D-T,ACT.SIG TO ISOM.FIG GIVN
MO	092	N,N PROTON	15+7		NAG	EXPT-PROG	NEANDC-J116		75	SEP 85	KATOH+.ACT SIG TO ISOM=64.7+-17.6MB
MO	092	N, ALPHA	13+7	15+7	JAE	EXPT-PROG	NEANDC-J116		24	SEP 85	IKEDA+.D-T,ACT.SIG TO ISOM.FIG GIVN
MO	092	N, ALPHA	15+7		NAG	EXPT-PROG	NEANDC-J116		75	SEP 85	KATOH+.ACT SIG=27.5+-0.8 MB
MO	092	N,N ALPHA	14+7	15+7	NAG	EXPT-PROG	NEANDC-J116		75	SEP 85	KATOH+.ACT SIG=0.16+-0.03MB AT 15MEV
MO	092	N,N ALPHA	13+7	15+7	JAE	EXPT-PROG	NEANDC-J116		24	SEP 85	IKEDA+.D-T,ACT.SIG TO ISOM.FIG GIVN
MO	094	N, 2N	15+7		NAG	EXPT-PROG	NEANDC-J116		75	SEP 85	KATOH+.ACT SIG=6.40+-0.33 MB
MO	094	N, 2N	13+7	15+7	JAE	EXPT-PROG	NEANDC-J116		24	SEP 85	IKEDA+.D-T,ACT.SIG TO ISOM
MO	095	N, PROTON	15+7		NAG	EXPT-PROG	NEANDC-J116		75	SEP 85	KATOH+.32.+-.8MB(GS),5.81+-.39MB(MS)
MO	095	N, PROTON	13+7	15+7	JAE	EXPT-PROG	NEANDC-J116		24	SEP 85	IKEDA+.D-T,ACT.TO ISOM AND GS.FIG
MO	096	N, PROTON	15+7		NAG	EXPT-PROG	NEANDC-J116		75	SEP 85	KATOH+.ACT SIG=24.1+-0.5 MB
MO	096	N, PROTON	13+7	15+7	JAE	EXPT-PROG	NEANDC-J116		24	SEP 85	IKEDA+.D-T,ACT.FIG GIVN
MO	096	N,N PROTON	15+7		NAG	EXPT-PROG	NEANDC-J116		75	SEP 85	KATOH+.4.31+-.14MB(GS)1.6+-.11MB(MS)
MO	096	N,N PROTON	13+7	15+7	JAE	EXPT-PROG	NEANDC-J116		24	SEP 85	IKEDA+.D-T,ACT.TO ISOM AND GS
MO	097	N, PROTON	15+7		NAG	EXPT-PROG	NEANDC-J116		75	SEP 85	KATOH+.ACT SIG=18.09+-0.45 MB
MO	097	N, PROTON	13+7	15+7	JAE	EXPT-PROG	NEANDC-J116		24	SEP 85	IKEDA+.D-T,ACT.FIG GIVN
MO	097	N,N PROTON	15+7		NAG	EXPT-PROG	NEANDC-J116		75	SEP 85	KATOH+.ACT SIG=3.82+-0.11 MB
MO	097	N,N PROTON	13+7	15+7	JAE	EXPT-PROG	NEANDC-J116		24	SEP 85	IKEDA+.D-T,ACT.
MO	098	N, PROTON	15+7		NAG	EXPT-PROG	NEANDC-J116		75	SEP 85	KATOH+.ACT SIG=5.71+-0.11 MB

ELEMENT S A	QUANTITY	ENERGY MIN	MAX	LAB	TYPE	DOCUMENTATION REF	VOL	PAGE	DATE	COMMENTS
MO 098	N, PROTON	13+7	15+7	JAE	EXPT-PROG	NEANDC-J116		24	SEP 85	IKEDA+.D-T,ACT.
MO 098	N,N PROTON	15+7		NAG	EXPT-PROG	NEANDC-J116		75	SEP 85	KATOH+.ACT SIG=2.15+-0.07 MB
MO 098	N,N PROTON	13+7	15+7	JAE	EXPT-PROG	NEANDC-J116		24	SEP 85	IKEDA+.D-T,ACT.
MO 098	N, ALPHA	13+7	15+7	JAE	EXPT-PROG	NEANDC-J116		24	SEP 85	IKEDA+.D-T,ACT.
MO 098	N, ALPHA	15+7		NAG	EXPT-PROG	NEANDC-J116		75	SEP 85	KATOH+.ACT SIG=5.80+-0.11 MB
MO 100	N, 2N	15+7		NAG	EXPT-PROG	NEANDC-J116		75	SEP 85	KATOH+.ACT SIG=1470+-100 MB
MO 100	N, 2N	13+7	15+7	JAE	EXPT-PROG	NEANDC-J116		24	SEP 85	IKEDA+.D-T,ACT.FIG GIVN
MO 100	N, ALPHA	15+7		NAG	EXPT-PROG	NEANDC-J116		75	SEP 85	KATOH+.ACT SIG=3.19+-0.07 MB
MO 100	N, ALPHA	13+7	15+7	JAE	EXPT-PROG	NEANDC-J116		24	SEP 85	IKEDA+.D-T,ACT.
IN 115	N, GAMMA	14+5	57+5	JPN	EXPT-PROG	NEANDC-J116		9	SEP 85	HINO+.D-T.ABSL SIG TO ISOM.FIG GIVN
SN 122	RESON PARAMS	15+3	30+4	JAE	EXPT-PROG	NEANDC-J116		28	SEP 85	NAKAJIMA+.PRESENTED AT 1985 SANTA FE
BA 135	TOTAL	40+2	40+3	JAE	EXPT-PROG	NEANDC-J116		32	SEP 85	MIZUMOTO+.PRESENTED AT 1985 SANTA FE
BA 135	N, GAMMA	40+2	40+3	JAE	EXPT-PROG	NEANDC-J116		32	SEP 85	MIZUMOTO+.PRESENTED AT 1985 SANTA FE
BA 137	TOTAL	40+2	90+3	JAE	EXPT-PROG	NEANDC-J116		32	SEP 85	MIZUMOTO+.PRESENTED AT 1985 SANTA FE
BA 137	N, GAMMA	40+2	90+3	JAE	EXPT-PROG	NEANDC-J116		32	SEP 85	MIZUMOTO+.PRESENTED AT 1985 SANTA FE
CE 142	RESON PARAMS	10+2	50+4	JAE	EXPT-PROG	NEANDC-J116		29	SEP 85	OHKUBO+.PRESENTED AT 1985 SANTA FE
TA 181	TOTAL	24+4	10+6	JAE	EXPT-PROG	NEANDC-J116		30	SEP 85	TSUBONE+.PUBLISHED IN NSE 88 579.
W 183	RESON PARAMS	50+0	11+3	JAE	EXPT-PROG	NEANDC-J116		31	SEP 85	OHKUBO+.PUBLISHED IN NST 21 805.
AU 197	N, 2N	14+7	15+7	JAE	EXPT-PROG	NEANDC-J116		16	SEP 85	IKEDA+.D-T,ACT,REL AL(N,A).FIG GIVN
TH 232	RES INT CAP	50-1		KTO	EXPT-PROG	NEANDC-J116		56	SEP 85	KOBAYASHI+.REL AU-197,86.28+-3.57PC

ELEMENT S	A	QUANTITY	ENERGY MIN	MAX	LAB	TYPE	DOCUMENTATION REF	VOL	PAGE	DATE	COMMENTS
TH	232	FISSION	50+5	70+6	TOH	EXPT-PROG	NEANDC-J116		85	SEP 85	KANDA+.PRESENTED AT 1985 SANTA FE
U	233	FISSION	50+5	70+6	TOH	EXPT-PROG	NEANDC-J116		85	SEP 85	KANDA+.PRESENTED AT 1985 SANTA FE
U	234	FISSION	50+5	70+6	TOH	EXPT-PROG	NEANDC-J116		85	SEP 85	KANDA+.PRESENTED AT 1985 SANTA FE
U	235	FISSION	NDG		KYU	EVAL-PROG	NEANDC-J116		69	SEP 85	UENOHARA+.SIMULTANEOUS EVAL.NDG
U	238	TOTAL	24+4	10+6	JAE	EXPT-PROG	NEANDC-J116		30	SEP 85	TSUBONE+.PUBLISHED IN NSE 88 579.
U	238	RES INT CAP	50-1		KTO	EXPT-PROG	NEANDC-J116		56	SEP 85	KOBAYASHI+.REL AU-197,277B+-4.28PC
PU	239	FISSION	NDG		KYU	EVAL-PROG	NEANDC-J116		69	SEP 85	UENOHARA+.SIMULTANEOUS EVAL.NDG
PU	240	FISSION	NDG		KYU	EVAL-PROG	NEANDC-J116		69	SEP 85	UENOHARA+.SIMULTANEOUS EVAL.NDG
BK	249	EVALUATION	10-5	20+7	JAE	EVAL-PROG	NEANDC-J116		38	SEP 85	KIKUCHI.PUBLISHED AS JAERI-M 85-138
CF	249	EVALUATION	10-5	20+7	JAE	EVAL-PROG	NEANDC-J116		38	SEP 85	KIKUCHI.PUBLISHED AS JAERI-M 85-138
MANY		EVALUATION	NDG		KYU	EVAL-PROG	NEANDC-J116		68	SEP 85	KANDA+.PRESENTED AT 1985 SANTA FE
MANY		N EMISSION	14+7		KYU	THEO-PROG	NEANDC-J116		60	SEP 85	KUMABE+.PUBLISHED IN PL/B 140 272.
MANY		N, PROTON	FISS		JPN	THEO-PROG	NEANDC-J116		41	SEP 85	HORIBE.PRESENTED AT 1985 SANTA FE
MANY		N, ALPHA	FISS		JPN	THEO-PROG	NEANDC-J116		41	SEP 85	HORIBE.PRESENTED AT 1985 SANTA FE
MANY		FISSION	NDG		KYU	THEO-PROG	NEANDC-J116		64	SEP 85	OHSAWA+.PUBLISHED IN NST 21 887.
MANY		LVL DENSITY	NDG		KYU	THEO-PROG	NEANDC-J116		67	SEP 85	UENOHARA+.PRESENTED AT 1985 SANTA FE

The content table in the CINDA format was compiled by the JNDC CINDA group;

R. Nakasima (Hosei Univ.), Y. Kawarasaki (JAERI),
M. Sakamoto (JAERI), M. Kawai (NAIG).
H. Kitazawa (Tokyo Inst. of Tech.), T. Nakagawa (JAERI)

I. ELECTROTECHNICAL LABORATORY

Quantum Technology Division

I-1 Precise Determination of Neutron Energy in d+T Neutron Field

K. Kudo , T. Michikawa and T. Kinoshita

The d+T neutron source has been often used for cross section measurements in the neutron energy from 14MeV to 15MeV and also applied in the research field of neutron therapy. These fields sometimes require the precise measuring techniques to determine the mean neutron energy as well as the neutron fluence. It is especially important to know the neutron energy in a reaction cross section measurement. For example, the $^{56}Fe(n,p)^{56}Mn$ reaction, which is widely used for fluence determination and was also adopted as a transfer instrument in the first international intercomparison of the 14.8MeV neutron fluence(1). However, its cross section varies about -1.7%/100keV around the 14.8MeV energy and hence it requires fairly accurate knowledge of the neutron energy as well as that of the neutron fluence.

Several methods have been proposed to measure the mean energy of neutrons produced by low energy deuterons incident on a solid Ti-T target(2)~(5). Since the tritium depth distribution in the target gradually varies depending on the irradiation condition of the target, it is highly desirable to measure the accurate energy distribution of the d+T neutrons for the precise neutron fluence determination with the uncertainty around ±1%.

The ^{3}He proportional counter has been used as a convenient monitor(6) to separate the undesirable d+D neutrons, which gradually increase with deuteron bombardment on a Ti-T target, in the d+T neutron field in the energy range from 14MeV to 20MeV(7). Furthermore, it has good characteristics to determine the mean neutron energy for the monoenergetic neutron field by analyzing the pulse height spectrum of the ^{3}He recoil edge.

An 220keV deuteron beam was guided on a Ti-T target (Amersham International PLC, TRT11 $\sim$0.4mg/cm^{2} on a 0.25mm thick Cu backing) inclined by 45° to the beam direction and the mean neutron energies of 14.0, 14.6 and 14.8MeV are obtained by changing the irradiation angles of 0°, 45° and 96° respectively. The ^{3}He detector (Texas Nuclear 9341; 2.54cm diameter and 15.24cm effective length) is composed of 400kPa ^{3}He and 200kPa Kr gases . The d+T neutron source was located on the axis of the cylinder and at 35cm from the front edge of the detector.

The pulse height spectra originated from the ^{3}He recoil part obtained in the measurements are shown in Fig.1, and the irradiated neutron fluence was about $2x10^{11}$ n/sr at each angle monitored by the associated α particle method(5). The channels corresponding to the half maximum of the ^{3}He recoil edges could be determined very precisely with the uncertainties less than ±1.5 ch., although the peak channels could not be determined with the uncertainties less than ±5 ch.

To determine the mean neutron energy, the calibration of energy axis has been done by using the two reference points; the 0 ch. of the pulse height analyzing system and the channel corresponding to 14.0MeV neutrons at 96°, as used in the energy calibration by T.B. Ryves[(3)]. The results are shown in Fig.2 with those obtained by other standard methods, and the agreements are fairly well. The mean energies at this energy range measured by the ^{3}He proportional detector can be estimated with an accuracy of better than 40keV.

References

(1) V.D. Huynh, Metrologia **16** (1980) 31.

(2) V.E. Lewis and E.J. Axton, Nucl. Instr. and Meth. **159** (1979) 401.

(3) T.B. Ryves and K.J. Zieba, Nucl. Instr. and Meth. **167** (1979) 449.

(4) V.E. Lewis and K.J. Zieba, Nucl. Instr. and Meth. **174** (1980) 141.

(5) K. Kudo, Y. Kawada, T. Michikawa and T. Kinoshita, Bul. Electrotechnical Lab. **47** (1983) 923.

(6) T. Kosako, M. Nakazawa, H. Wakabayashi and A. Sekiguchi, UTNL-R R-0038 (1976).

(7) K. Kudo, T. Michikawa, T. Kinoshita, Y. Hino and Y. Kawada, to be published in the Proceedings of IAEA Advisory Group Meeting on Nucl. Standard Reference Data held at Geel in November of 1984.

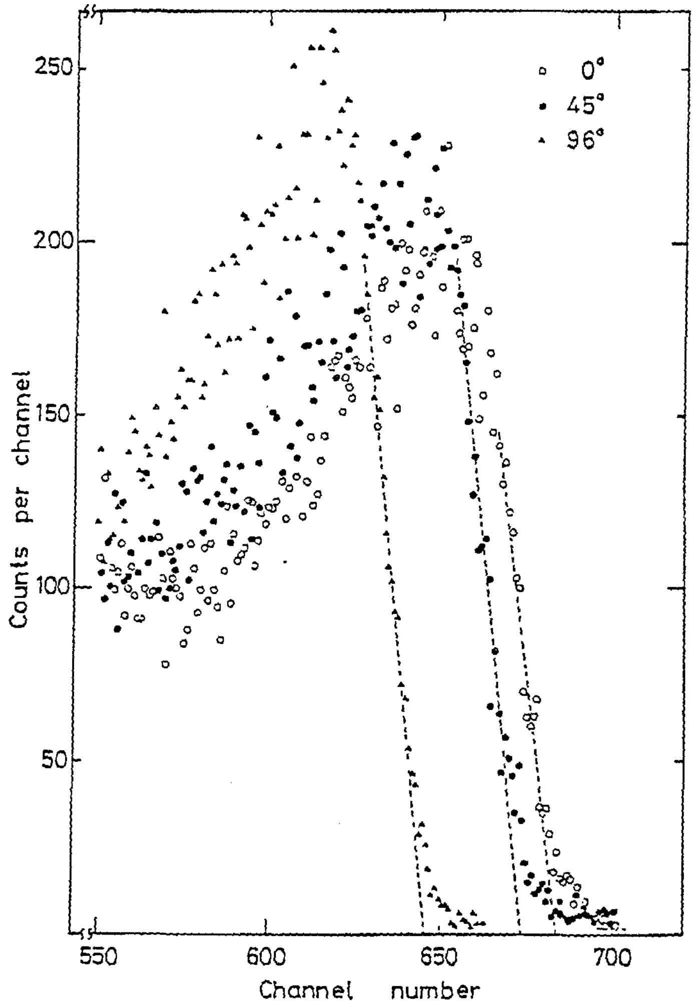

Figure 1. Pulse height spectra of ^{3}He recoil part induced by d+T neutrons emitted to the directions of 0°, 45° and 96° respectively.

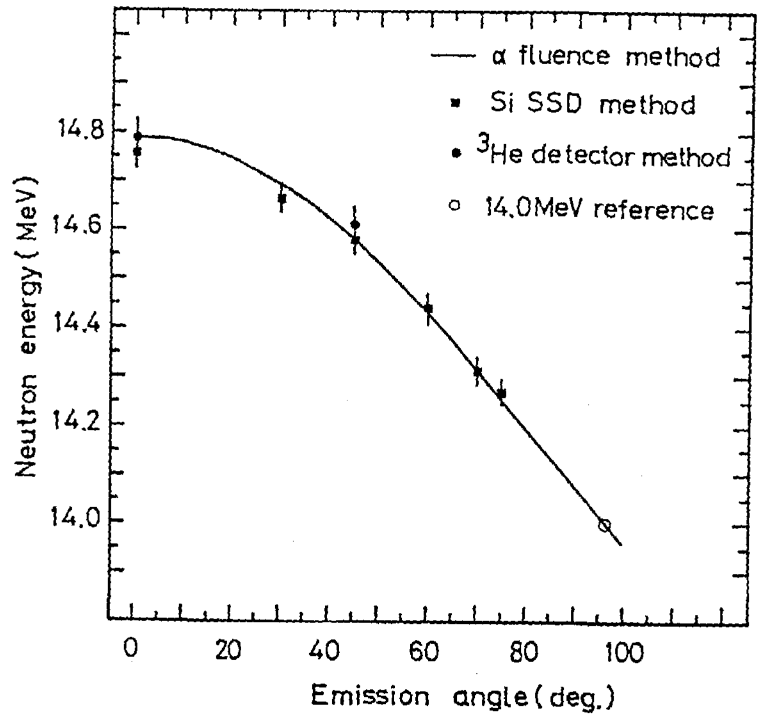

Figure 2. Mean neutron energy distributions versus neutron emission angle measured by several standard methods, the associated α fluence ratio method at 89° and 131°, the Si(n,α) reaction method and the ^{3}He proportional detector method.

I-2 Cross Section Measurements of $^{56}Fe(n,p)^{56}Mn$ and $^{27}Al(n,\alpha)^{24}Na$ Between 14.0 and 19.9MeV

K.Kudo, T.Michikawa, T.Kinoshita, Y.Hino and Y.Kawada

The cross section of $^{27}Al(n,\alpha)^{24}Na$ reaction in the neutron energy range of the threshold to 20MeV is one of the standard reference data recommended by the IAEA, and the $^{56}Fe(n,p)^{56}Mn$ is also often used to measure fast neutron fluxes in neutron fields with comparatively lower intensity, since the produced ^{56}Mn has adequate long half life of 2.58 hours and higher specific activity for the neutron irradiation and the activity measurement.

The cross sections for the $^{27}Al(n,\alpha)^{24}Na$ and $^{56}Fe(n,p)^{56}Mn$ reactions for neutron energies from 14.0 to 19.9MeV have been measured in the neutron standard fields established by using a proton recoil telescope for all energies and an associated α particle method below 15MeV. Activation samples were mainly set at 0 degree to the deuteron beam accelerated by the Pelletron at distances of 55 to 100mm from the target and arranged in the order Al, Fe and Al for each irradiation. The neutron fluxes of 14.8, 14.6 and 14.0MeV are obtained by changing the irradiation angles of 0, 45 and 96 degrees respectively in the case of the incident 220keV deuteron beam from Cockcroft type accelerator.

The absolute activities of iron and aluminum foils were measured by the 4πβ-γ coincidence method using a pure methane gas flow proportional counter positioned between two

7.6cm x 7.6cm NaI(Tl) scintillators as γ monitors. Small corrections Ks, which are related to the effects due to the efficiency of the $4\pi\beta$ counter to γ rays, and specially to the complex decay scheme of the ^{56}Mn, were adopted from our previous measurements[(1),(2)].

The d+D neutrons ranging 2.5MeV to 6.5MeV originated from the deuteron implantation in the Ti-T target build up rapidly at higher energies,and contribute to the additional activities of the ^{24}Na and ^{56}Mn. The neutron yields from the $D(d,n)^{3}He$ reaction have been measured by a calibrated ^{3}He detector(Texas Nuclear 9341). The extra activity by the d+D neutrons were finally calculated by the help of the evaluated $^{27}Al(n,\alpha)^{24}Na$ and $^{56}Fe(n,p)^{56}Mn$ cross sections[(3)].

Secondary neutron spectra at the activation sample position originated from the direct neutron interaction with the copper backing metal and the surrounding aluminum target holder assembly have been calculated numerically taking into account the angular distribution of the $T(d,n)^{4}He$ reaction[(4)] and the differential scattering, inelastic and (n,2n) cross sections of the target assembly.

As the activation samples used in the $^{56}Fe(n,p)^{56}Mn$ cross section measurements were natural iron, the extra ^{56}Mn activity from the $^{57}Fe(n,np+pn+d)^{56}Mn$ reaction should be subtracted from the total ^{56}Mn activity. The calculated response curve of the cross section[(5)] was normalized at 14.7MeV by the Qaim's evaluation[(6)].

The total uncertainties on the cross section by summing in quadrature the systematic and statistic uncertainties are

±1.3 to ±4.0% for the $^{27}Al(n,\alpha)^{24}Na$ reaction and ±1.4 to ±5.6% for the $^{56}Fe(n,p)^{56}Mn$ reaction respectively. The cross section results are given in Fig.1 and 2 with the recent other data. The results show difference of up to 10% in the $^{27}Al(n,\alpha)^{24}Na$ cross section at 19.9MeV, and systematic higher values in the $^{56}Fe(n,p)^{56}Mn$ cross section except at 19.9MeV compared with those of ENDF/B-V(3).

References

(1) Y. Kawada, Int. J. Appl. Radiat. Isotopes **20** (1969) 413.

(2) K. Kudo, Nucl. Instr. Meth. **141** (1977) 325.

(3) Evaluated Neutron Data File, ENDF/B-V (1979).

(4) H. Liskien and A. Paulsen, Nucl. Data Table **11** (1973) 569.

(5) T. Asami(JAERI), private communication

(6) S.M. Qaim, Nucl. Phys. **A325** (1979) 255.

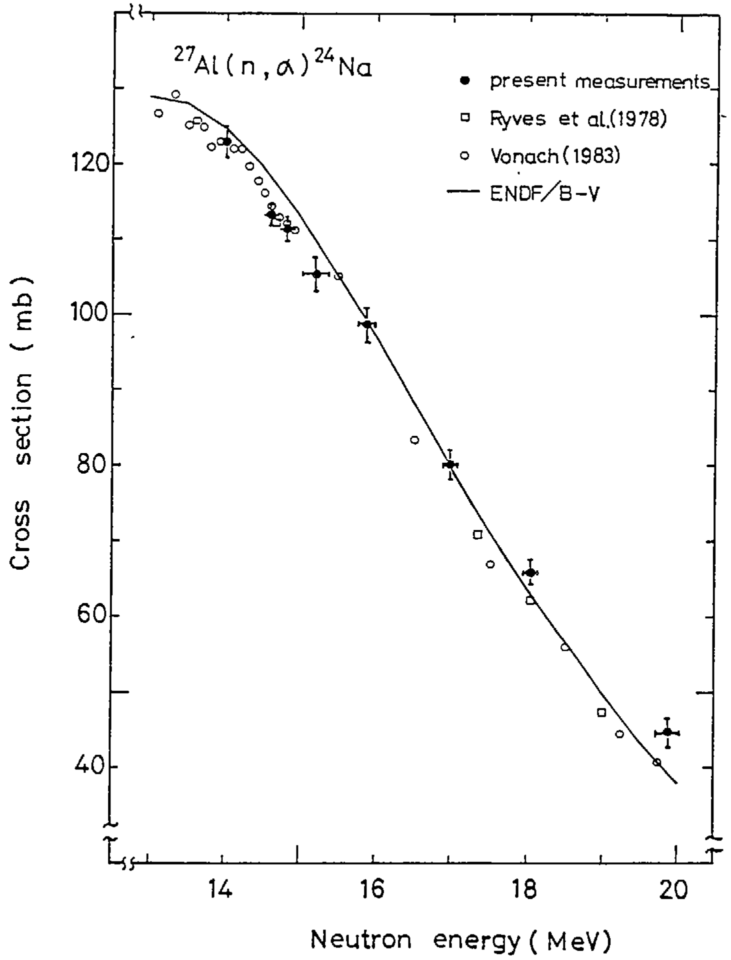

Figure 1. Neutron cross section of

$^{27}Al(n,\alpha)^{24}Na$ reaction

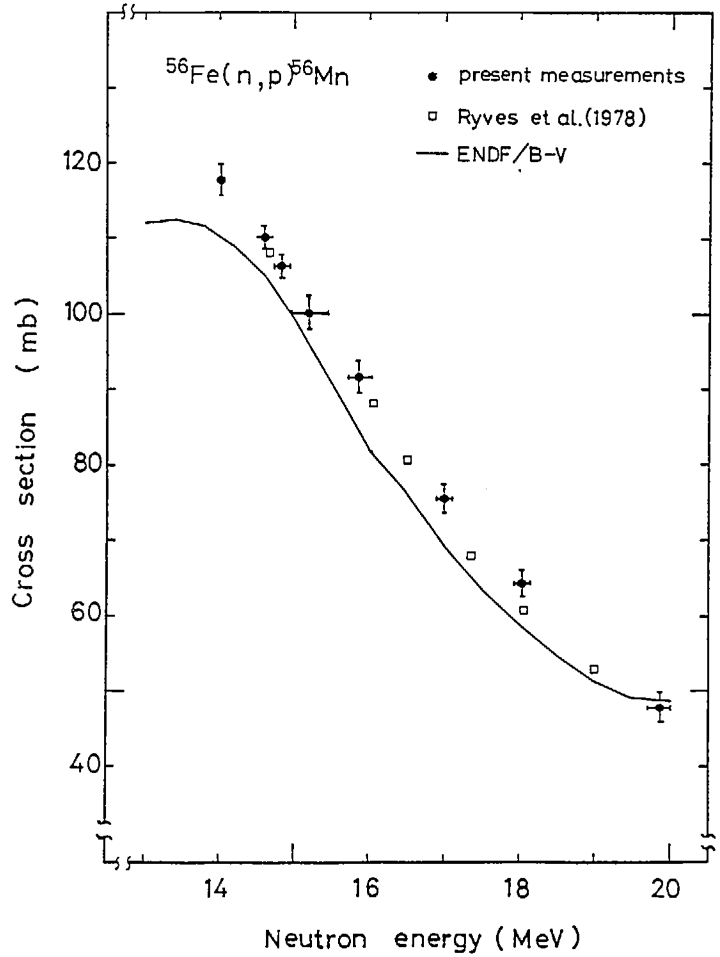

Figure 2. Neutron cross section of

$^{56}Fe(n,p)^{56}Mn$ reaction

I-3 $^{115}In(n,\gamma)^{116m}In$ Reaction Cross Section Measurement at Neutron Energies of 144 and 565 keV

Y. Hino, T. Michikawa, T. Kinoshita, K. Kudo and Y. Kawada

Precise $^{115}In(n,\gamma)^{116m}In$ reaction cross sections at neutron energies of 144 and 565 keV were measured in connection with the international intercomparison of fast neutron fluence standards. The Bureau International des Poids et Mesures (BIPM) has organized fast neutron fluence intercomparison at five energies between 144 keV and 14.8 MeV. For the two lowest energies, 144 and 565 keV, $^{115}In(n,\gamma)^{116m}In$ reaction was used as transfer method.[1) The participating laboratories were asked to determine the neutron flux density at the location of indium foil and to report the number of counts per gram and per neutron fluence. The result is expressed as

$$K = \frac{A_o}{\bar{\phi}} \cdot \frac{1}{m \cdot f_t \cdot f_a \cdot f_s \cdot (1-\exp(-\lambda T))} , \qquad (1)$$

where A_o is the β count rate of indium foil at the end of irradiation and $\bar{\phi}$ is the average flux density at the foil position over the duration of the irradiation time T, m is the mass of the foil, ft, fa and fs are correction factors for time-variation of neutron flux, attenuation of neutrons, and scattering effect, respectively. While the cross section of σ can be expressed as

$$\sigma = \frac{N_a}{\bar{\phi}} \cdot \frac{1}{N_o \cdot f_t \cdot f_a \cdot f_s \cdot (1-\exp(-\lambda T))} , \qquad (2)$$

where N_a is the number of atoms produced by the reaction and N_o is the number of atoms included in the indium foil. The relationship between N_a and A_o is expressed as

$$\lambda \cdot N_a \cdot \varepsilon_\beta = A_o \ , \qquad (3)$$

where λ is the decay constant and ε_β is the β-counting efficiency. When ε_β is decided, N_a is immediately obtained from the formula 3 and also the cross section is derived from the formula 2. In order to obtain the β efficiency, the 4πβ-γ coincidence method has been adopted. When N is the total number of decay, and N_β, N_γ and N_c is the count rate of β, γ and coincidence channel, respectively, the simplified relationship of these count rates after usual corrections are as follows.

$$N_\beta = N \cdot \varepsilon_\beta \qquad (4\text{-}1)$$

$$N_\gamma = N \cdot \varepsilon_\gamma \qquad (4\text{-}2)$$

$$N_c = N \cdot \varepsilon_\beta \cdot \varepsilon_\gamma \qquad (4\text{-}3)$$

Then ε_β can be calculated as

$$\varepsilon_\beta = \frac{N_c}{N_\gamma} = \frac{N \cdot \varepsilon_\beta \cdot \varepsilon_\gamma}{N \cdot \varepsilon_\gamma} \ . \qquad (5)$$

Although these simplified formula is not applicable for complex decay nuclide, ^{116m}In can be regarded as a simple decay nuclide if 1294 keV and 2112 keV gamma rays could be separated from other gamma-rays. The 4πβ-γ detection system with a pure Ge detector was used to make coincidence measurement with selected gamma-rays. Figure 1 shows the block diagram of this system.

Indium foils of some different thicknesses (20 mg/cm^2 $\sim$ 70 mg/cm^2) were irradiated with thermal neutrons in order to have enough count rate for this coincidence measurement. A 4 Ci Am-Be neutron source was put into the center position of graphite pile and indium foils were irradiated at the points of 30 cm and 70 cm distances from the source. In order to certify the efficiency values obtained from thermal neutron irradiation, a 36 mg/cm^2 foil was irradiated by 565 keV neutrons. The result of ε_β from 565 keV neutrons is in good agreement with thermal neutron data.

Figure 2 shows the cross section curve of ^{115}In(n,γ) reaction from the third edition of BNL-325[2)] in comparison with the present results and ENDF/B-V[3)]. The present results show very good agreement with the evaluated line of BNL-325 but ENDF/B-V data shows smaller values in 500 keV energy region.

The final result of this international intercomparison is not yet reported, but in the moment, the K values of 144 keV neutrons from 4 participating laboratories converge within 5% and within 4% for 565 keV neutrons from 6 laboratories. The disagreement of the present result with ENDF/B-V for 565 keV neutrons is about 11% which exceed the confidence level of present intercomparison. The present results are only two points of neutron energies but offer the reliable reference points for evaluation in connection with the international intercomparison of fast neutron standards.

References:

1) T.B. Ryves, Report to BIPM CCEMRI(III) 79-7 (1979)

2) BNL 325, Third Edition, Neutron Cross Sections Vol. 2 (1976)

3) Evaluated Neutron Data File, ENDF/B-V

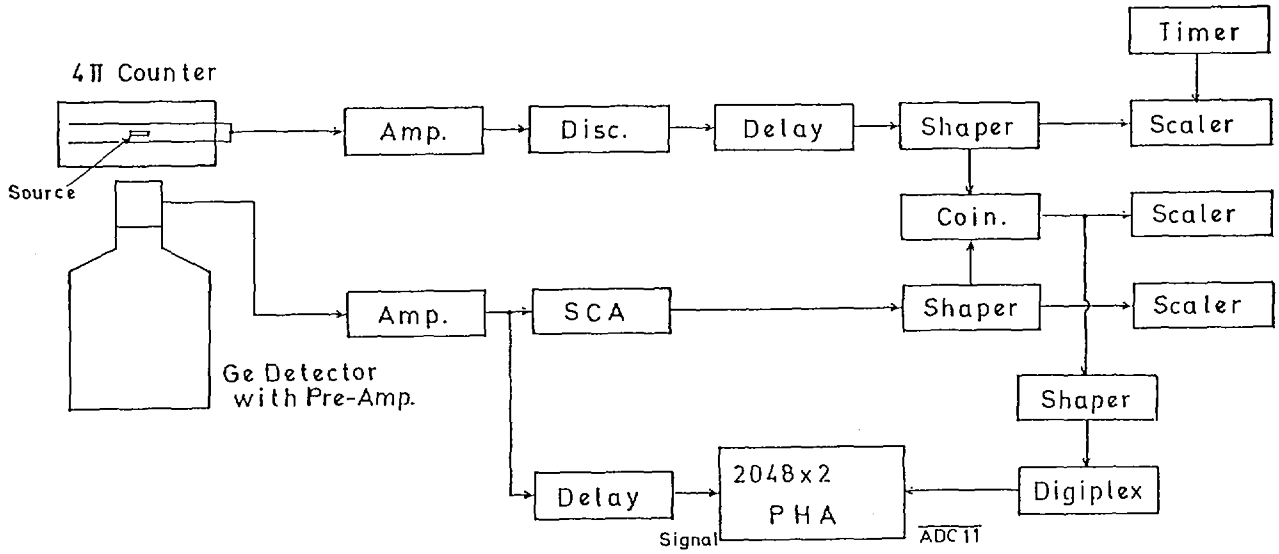

Fig. 1. Block diagram of 4πβ-γ(Ge) detection system

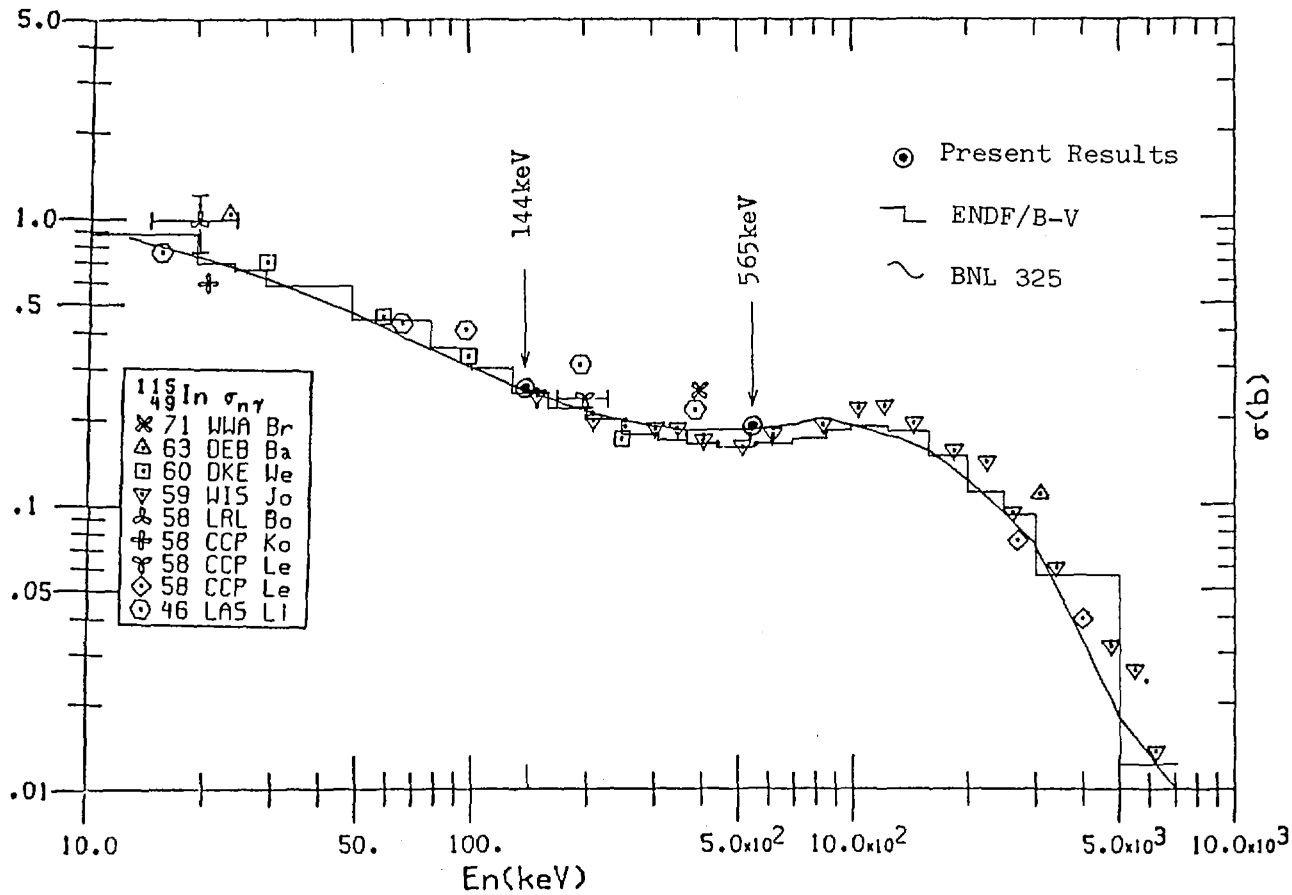

Fig. 2. Comparison of the measured ^{115}In(n,γ) reaction cross sections with evaluated data

Decay Data of ^{64}Cu

Y.KAWADA

The principal decay data for ^{64}Cu were determined by $4\pi\beta(PC)-\gamma$ coincidence techniques and photon spectrometry. The probability of electron capture was assessed from consistent results of three experiments; (1) measurements by the slope-to-intercept ratio method based on the $4\pi X-\gamma$ coincidence counting gated with the 1.34 MeV γ-rays, (2) K-X ray measurements with a calibrated low energy photon spectrometer (LEPS), and (3) 4π β-ray emission rate measurements using sandwiched sources. Method (1) is practically independent of the decay parameters. The emission rate per decay of the positrons decay and of the 1.34 MeV γ-rays were measured with a calibrated Ge γ-ray spectrometer. From these measurements, the branching fractions of positron decay, negatron decay and electron capture and the γ-intensity per decay could be evaluated with uncertainties between 1.0 and 1.2 percent except for an about 4 percent uncertainty for the γ fraction.

The decay data of ^{64}Cu as determined in the present work are summarized in Table 1 together with the K capture to positron ratio. They are compared with earlier results and evaluations in Table 2. They are evidently in good agreement with the compilation of Martin and Blichert-Toft[1] as well as those cited in Table of Isotopes 6th edition[2]. There are, however, considerable discrepancies with the results in NDS[3,4] , Table of Isotopes 7th edition[5] and the Table de Radionucléides(LMRI)[6], although some of the stated uncertainties are large enough to bridge the differences. On the other hand the values obtained with a mass spectrometer by Reynolds[7] are in a good agreement with the present results. However, since the earlier value of the K-fluorescence yield was considerably lower than that recently quoted, critical comparisons with older data are somewhat meaningless at least for some of the parameters.

The present results are consistent with the recent detailed work by Christmas et al.[8]. The data on $p_{\beta+}$ and p_{γ} are in excellent agreement. The consistency of these independently measured results would support the reliability of the present and the Christmas' data.

The detail was submitted to Int. J. Appl. Rad. Isotopes.

References

1) Martin M.J. and Blichert-Toft P.H. Nucl. Data Tables 8, 47 (1970)

2) Lederer C.M., Hollander J.M. and Perlman I."Table of Isotopes, 6th Ed.",Wiley, N.Y. p198 (1967)

3) Auble R.L. Nucl. Data Sheets 12, 305 (1974)

4) Halbert M.L. Nucl. Data Sheets 28, 179 (1979)

5) Lederer C.M. and Shirley V.S.(Ed.)"Table of Isotopes, 7th Ed.",Wiley-Interscience, N.Y.,p197 (1978)

6) Lagoutine F.,Coursol N. and Legrand J."Table de Radionucléides", LMRI, Sacley (1984)

7) Reynolds J.H. Phys. Rev. 79, 789 (1950)

8) Christmas P., Judge S.M., Ryves T.B., Smith D. and Winkler G. Nucl. Instrum. Methods 215, 397 (1983)

Table 1 Summary of the present results(1σ C.L.). The data are expressed as percent except for $p_{\beta-}/p_{\beta+}$ and $K_1/p_{\beta+}$

Method	$p_{EC1}+p_{EC2}$	p_{EC1}	p_{EC2}, P_{γ}	$p_{\beta+}+p_{\beta-}$	$p_{\beta+}$	$p_{\beta-}$	$p_{\beta-}/p_{\beta+}$	$K_1/p_{\beta+}$
Slope/Intercept	43.9 ±0.9	43.4 ±0.9		56.1 ±0.9		38.2 ±0.9	2.13 ±0.05	2.14 ±0.03
K X/n_o (LEPS)	43.5 ±0.8	43.0 ±0.8		56.5 ±0.8		38.6 ±0.8	2.15 ±0.05	2.12 ±0.03
Total β/n_o (4πβ-Annihi.)	43.9 ±1.1	43.4 ±1.1		56.1 ±1.1		38.2 ±1.1	2.13 ±0.07	2.14 ±0.03
γ-Spectrometry (Ge Detector)			0.487 ±0.020		17.93 ±0.20			
Weighted Mean	43.73 ±0.52	43.24 ±0.53	0.487 ±0.020	56.27 ±0.52	17.93 ±0.20	38.34 ±0.56	2.138 ±0.032	2.13 ±0.02

Table 2 Comparison with published results and evaluations. The data are shown in percent except those for $p_{\beta-}/p_{\beta+}$.

Author/Ref.	Method	$p_{EC1}+p_{EC2}$	p_{EC1}	p_{EC2}, P_{γ}	$p_{\beta+}+p_{\beta-}$	$p_{\beta+}$	$p_{\beta-}$	$p_{\beta-}/p_{\beta+}$
Table of Isotopes (6th Ed.)[(2)]	Compilation	(43.5)	43	0.5	57	19	38	(2.0)
Table of Isotopes (7th Ed.)[(5)]	Compilation	41.1 ±2.2	40.5 ±2.2	0.6 ±0.2	(58.9)	19.3 ±0.7	39.6 ±2.0	(2.05)
Nucl. Data Sheets ('74 Ed.)[(3)]	Evaluation							
Nucl. Data Sheets ('79 Ed.)[(4)]	Evaluation	45.0	(44.52)	0.48	(55.0)	17.9	37.1	
Nucl. Data Tables[(1)]	Evaluation	(43.5)	43 ±2	0.55 ±0.08	(56.4)	18.4 ±0.8	38 ±2	2.07
Reynolds[(7)]	Mass Spec.	43.2 ±2.0				18.6 ±1.2	38.2 ±1.6	
Christmas et al.[(8)]	Mag. Spec. 4πβ(LS)-γ 4πβ(PC)-γ Ge γ Spec.	43.10 ±0.46		0.471 ±0.011		17.86 ±0.14	39.04 ±0.33	2.187 ±0.007
Present Work	See Text	43.73 ±0.52	43.24 ±0.53	0.487 ±0.020	56.27 ±0.52	17.93 ±0.20	38.34 ±0.56	2.138 ±0.032

II. JAPAN ATOMIC ENERGY RESEARCH INSTITUTE

A. Fusion Reactor Physics Laboratory
Department of Reactor Engineering

II-A-1 Measurement of Some (n,2n) Activation Cross Sections for 13.5 - 15.0 MeV Neutrons†

Y. Ikeda, K. Oishi,** H. Maekawa, T. Nakamura,
H. Miyade,* K. Kawade,* H. Yamamoto,* and T. Katoh*

Cross sections for the (n,2n) reaction of ^{58}Ni, ^{59}Co, ^{90}Zr, ^{93}Nb and ^{197}Au were systematically measured for the neutron energy range from 13.5 to 15.0 MeV by using the intense d-T neutron source, FNS. The cross sections were obtained relative to that of ^{27}Al(n,α)^{24}Na. The source strength of d-T neutrons was about 3×10^{12} n/s at the target. Foils of Ni, Co, Zr, Nb and Au, each sandwiched by Al foils, were placed around the target, at the

---

† The content of this paper is submitted to Int. Conf. on Nuclear Data for Basic and Applied Science, Santa Fe, New Mexico, U.S.A., May 13-17, 1985.

* Nagoya University

** Shimizu Construction Co., Ltd.

angles of 0 - 130° to the incident d^{+} beam.(310 keV, 15mA) After irradiation, γ-ray spectra were measured by Ge detectors. The reaction rate of each element was deduced from the measured γ-ray counts and decay data which are listed in Table 1. The uncertainty of the reference cross section was assigned to be ± 3 %. All the data were obtained within the accuracy of about ± 5 %. The results are shown in Figs. 1 - 5 together with previous evaluated and/or experimental data.

^{58}Ni(n,2n)^{57}Ni

Present results are higher than the ENDF/B-V in the energy range above 14.5 MeV. The difference at 15 MeV amounts to about 20 %. In the energy region below 14.0 MeV, the ENDF/B-V gives higher value in contrary to the case of higher energy region. Present data are in good agreement with recent data of this reaction reported by Winkler[1)] in the whole energy range.

^{59}Co(n,2n)^{58mg}Co

In comparison with the ENDF/B-V, the present data are 15 % lower in the whole energy range. The present data, however, are in good agreement with recent evaluation of this cross section in the JENDL-2.

^{90}Zr(n,2n)^{89}Zr

The present data agree with the IRDF-82[2)] dosimetry file and Winkler's data[3] in the experimental errors.

^{93}Nb(n,2n)^{92m}Nb

The present data are in good agreement with the data evaluated by Nethaway[3)], whereas it is lower than the data of Ref-4 by $\sim$ 5 %.

^{197}Au(n,2n)^{196}Au

The present data give slightly lower value than the data of Ref-4.

References

1) G. Winkler, et al.: Proc. Int. Conf. on Nuclear Data for Sci. & Technol., Antwerp, 400 (1982).

2) D. E. Cullen, et al.: IAEA-NDS'-42/R (1982).

3) D. R. Nethaway : J. Inorg. Nucl. Chem. 40, 1285 (1978).

4) R. L. Greenwood : ANL/FPP/TM-115 (1978).

TABLE I Associated decay properties

Reaction	$T_{1/2}$	E_g(keV)	I_g(%)
$^{27}Al(n,a)^{24}Na$	15.02h	1369	100
$^{58}Ni(n,2n)^{57}Ni$	36.0 h	1378	77.6
$^{59}Co(n,2n)^{58}Co$	70.78h	811	99.44
$^{90}Zr(n,2n)^{89}Zr$	78.4 h	909	99.01
$^{93}Nb(n,2n)^{92m}Nb$	10.14d	935	99.2
$^{197}Au(n,2n)^{196}Au$	6.18d	365	87.6

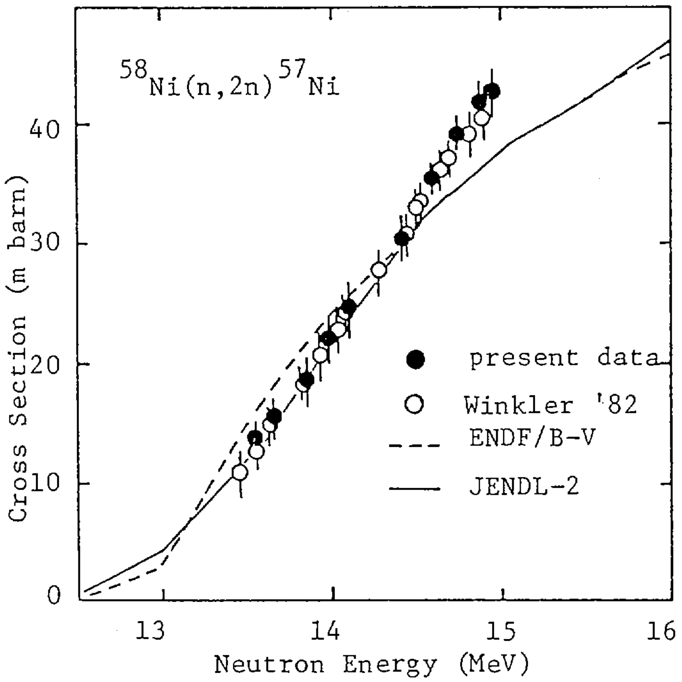

Fig 1 Cross section of $^{58}Ni(n,2n)^{57}Ni$

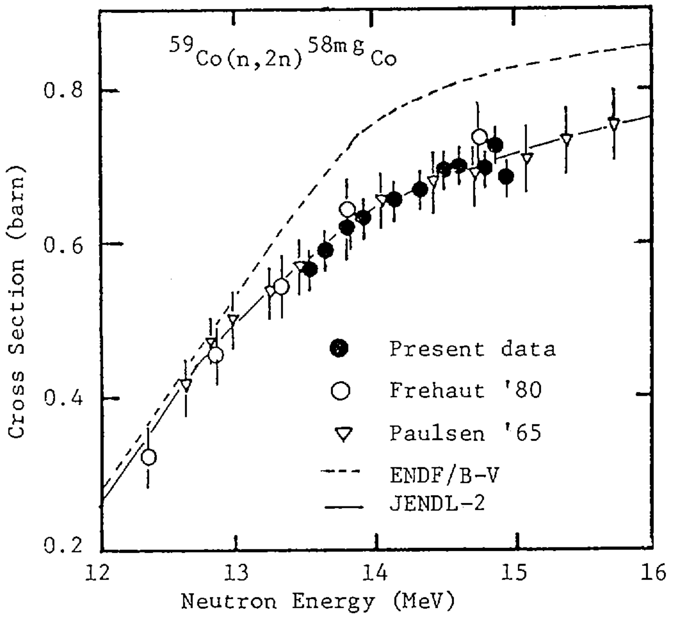

Fig. 2 Cross section of $^{59}Co(n,2n)^{58m+g}Co$

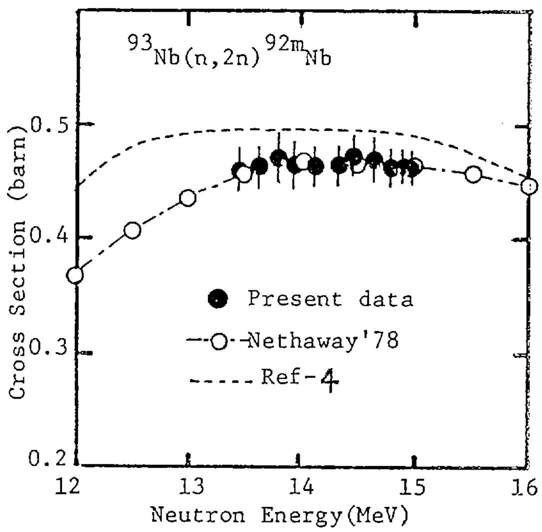

Fig. 3 Cross section of $^{93}Nb(n,2n)$-^{92m}Nb

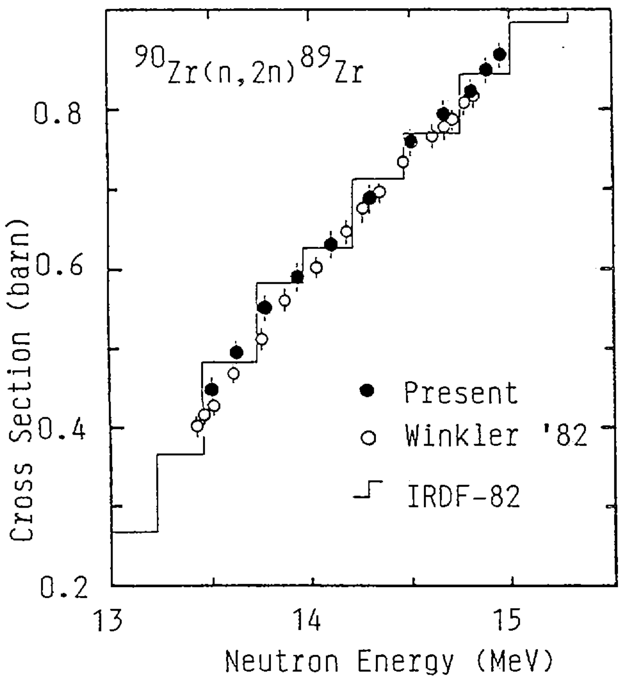

Fig. 4 Cross section of $^{90}Zr(n,2n)^{89}Zr$

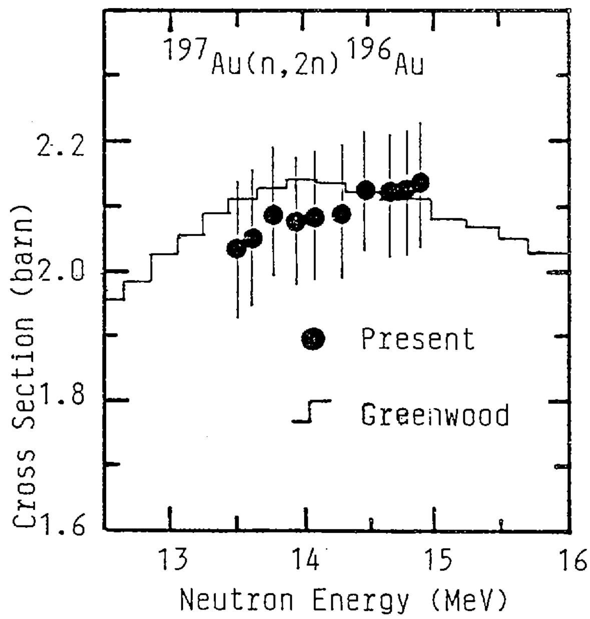

Fig. 5 Cross section of $^{197}Au(n,2n)$-^{196}Au

II-A-2 Measurement of the Neutron Activation Cross Section of Calcium Isotopes by D-T Neutrons.

K. Oishi*, Y. Ikeda and T. Nakamura

To estimate the activation of structural materials in fusion facilities exactly, experimental measurement of the neutron activation cross sections of components of those materials is required. Calcium is not only one of the main components of concrete as a structural material, but can be an impurity in blanket materials.

In this study, activation cross sections of the ^{42}Ca(n,p), ^{44}Ca(n,p), ^{44}Ca(n,α), and ^{44}Ca(n,np) reactions (See Table 1) have been measured using separated isotopes of calcium.

The D-T neutrons were generated in the tritium target at the end of the 80° beam line of the FNS. Samples of about 50 mg were wrapped in cartridge papers, and emplaced around the target at eight measurement positions, where the incident neutron energy ranged from 13.4 MeV to 14.9 MeV. Irradiation time varied between 1 hour and 6 hours, according to the half-life. Nb foils were used to monitor the neutron flux. The measured neutron flux was $8.5 \times 10^7 \sim 1.9 \times 10^8$ n / cm^2•sec.

Results are shown in Fig. 1 to Fig. 4. Since all samples were irradiated in the same irradiation field, highly precise data with small relative error could be obtained. For the

---

* Shimizu Construction Co. Ltd.

$^{42}Ca(n,p)$ reaction, using present data as an input cross section for the THIDA[1] calculation in an integral experiment[2], agreement between experiment and calculation has been improved.

References

1) Iida H. and Igarashi M. : JAERI-M 8019 (1978)

2) Oishi K., et al. : Preprint of Annual Meeting of the Atomic Energy Society of Japan, B39 (1985)

Table 1 Measured Reactions

Reaction	$T_{1/2}$	Eγ(keV)	Iγ(%)
$^{42}Ca(n,p)^{42}K$	12.36 h	1524.7	17.9
$^{44}Ca(n,p)^{44}K$	22.15 m	115.70	58.1
$^{44}Ca(n,\alpha)^{41}Ar$	1.83 h	1293.6	99.2
$^{44}Ca(n,np)^{43}K$	22.4 h	372.9	86.7

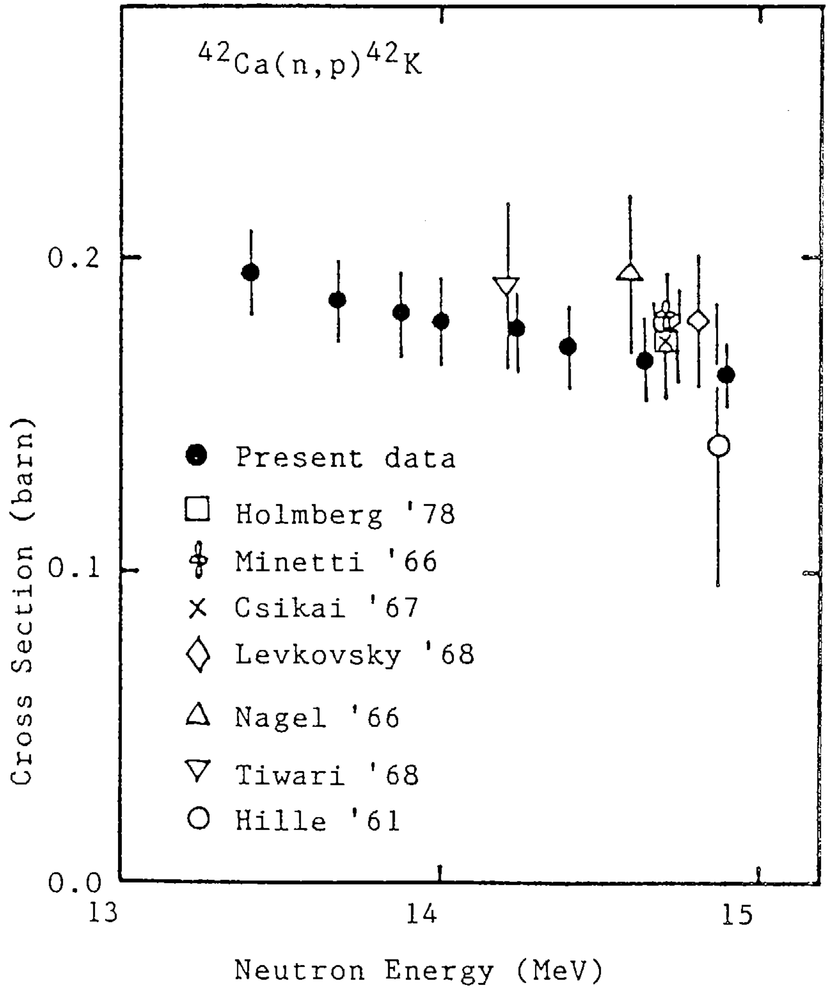

Fig.1 Cross Section of $^{42}Ca(n,p)^{42}K$

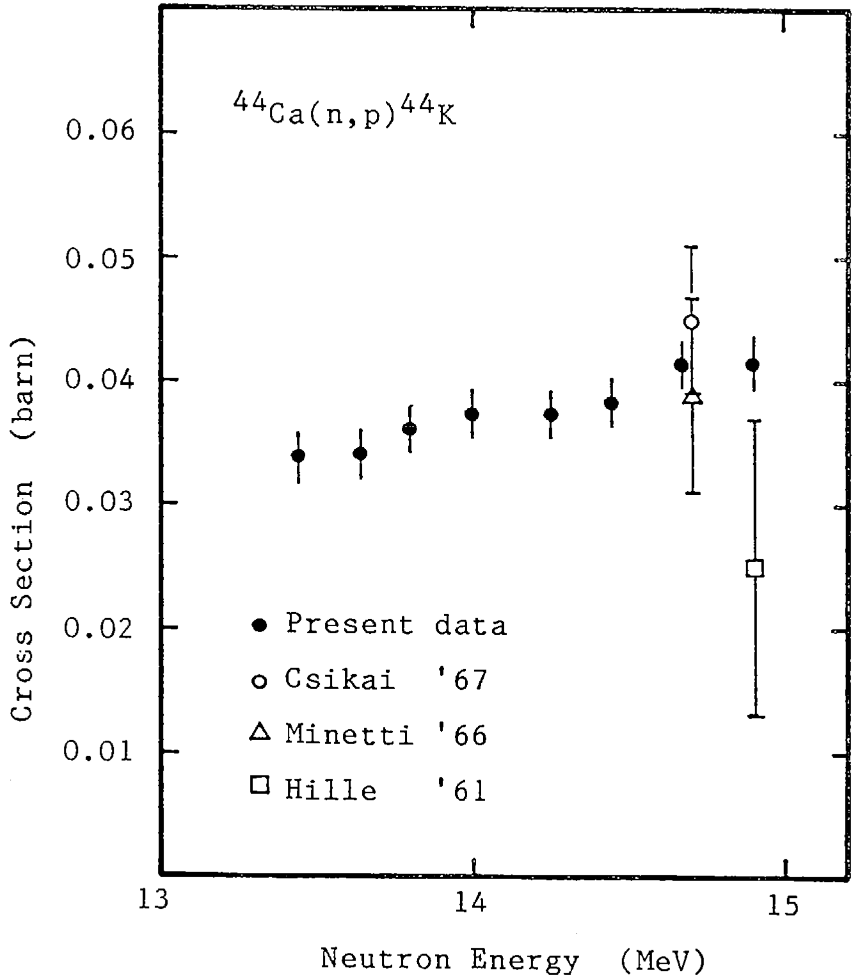

Fig.2 Cross Section of $^{44}Ca(n,p)^{44}K$

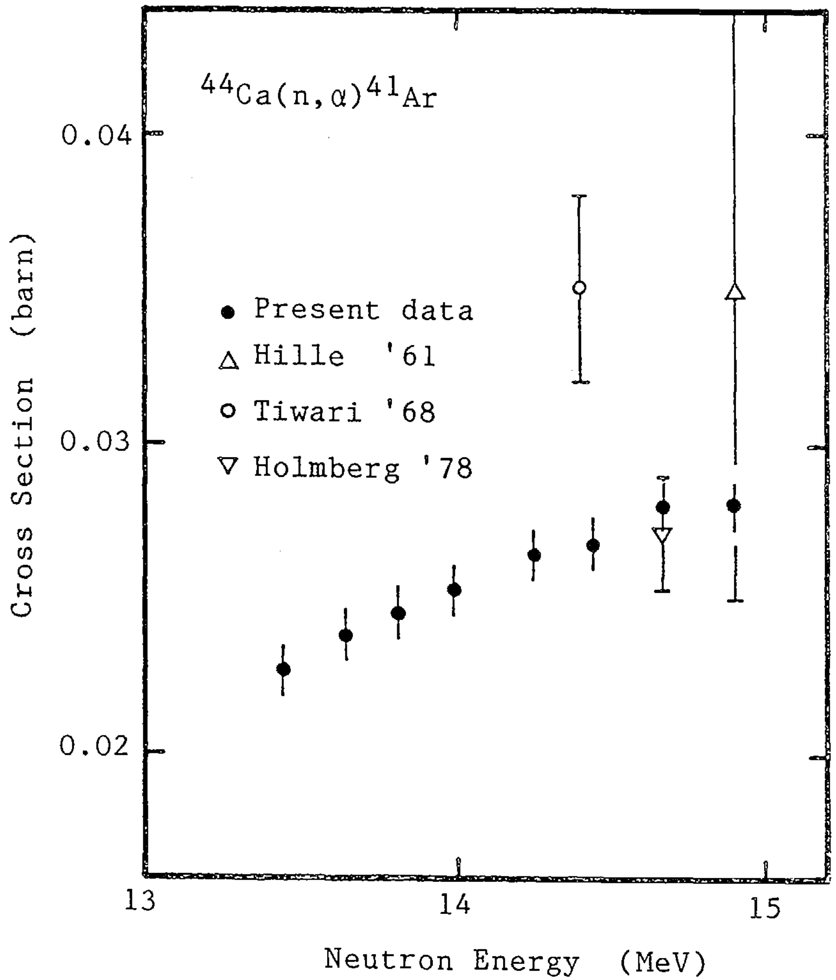

Fig.3 Cross Section of $^{44}Ca(n,\alpha)^{41}Ar$

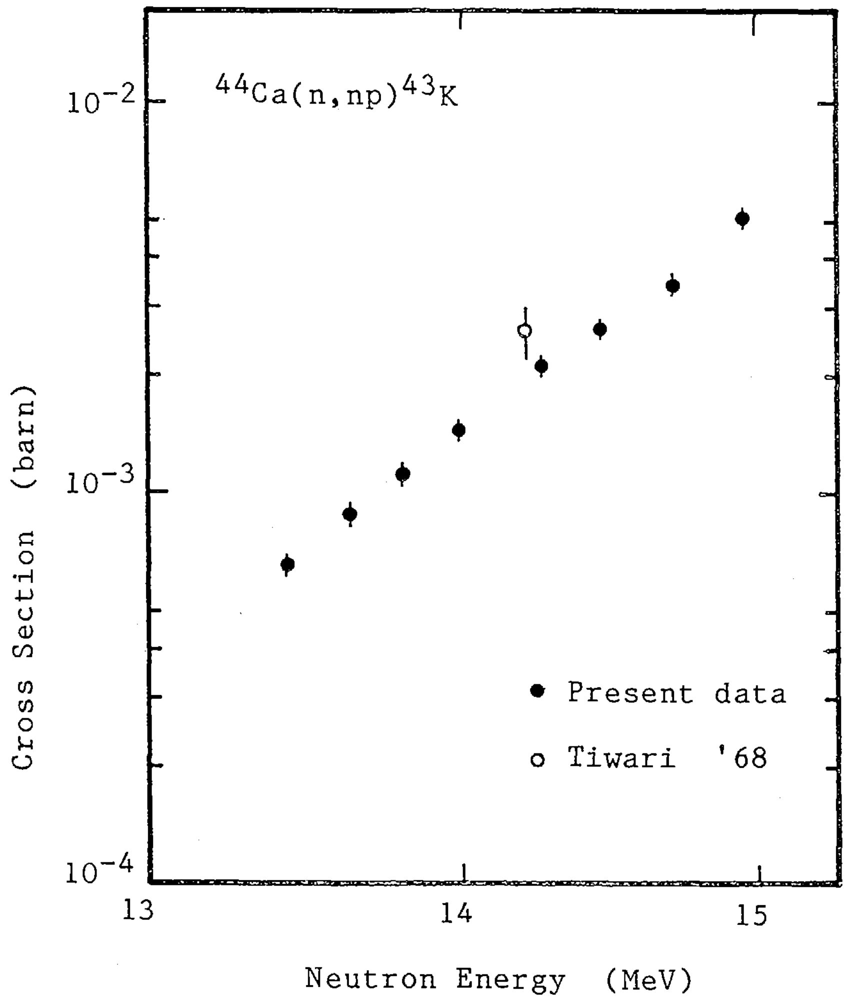

Fig.4 Cross Section of $^{44}Ca(n,np)^{43}K$

II-A-3 A Series of Measurement on Cross Sections of Activation Reaction in Fusion Reactor Structural Materials

Y. Ikeda, H. Miyade*, K. Kawade*, H, Yamamoto*,
T. Katoh*, K. Oishi**, H. Maekawa and T. Nakamura

The activation cross sections of isotopes of molybdenum were measured for the neutron energy range from 13.4 to 15.0 MeV by using the FNS facility. The reaction types and associated decay properties of each reaction product are summarized in Table 1. Since the isotopes have adjacent mass numbers, the same radioactive products are sometimes produced by different reactions such as (n,p) and (n,np). So, the separated isotopes were used to isolate the individual reaction cross section. The samples were prepared by wrapping each isotope of about 50 mg in a cartridge paper, the effective area being 1 cm^2. The niobium foils of the same size as the samples were employed to monitor the neutron flux. The samples were positioned at 10 cm in radius centered the target with the support made of styrene foam.

The D-T neutrons were generated at the tritium target mounted on the target assembly at the end of the 80° beam line, which was newly fabricated for the irradiation experiment. The incident deuterium ion energy and intensity were 330 keV and 1.5 mA, respectively.

---

* Nagoya University

** Shimizu Construction Co., Ltd.

The neutron yield was about 2×10^{11}n/s at the target.

After irradiation, gamma-rays emitted from the produced activities were measured by Ge detectors. Reaction rates were deduced from the gamma-ray counts with necessary corrections. The cross section for each reaction was obtained relative to that of ^{93}Nb(n,2n)^{92m}Nb. The errors were estimated to be ± 6 % including the monitor errors of cross section error.

The results for ^{92}Mo(n,p), ^{95}Mo(n,p), ^{96}Mo(n,p), ^{97}Mo(n,p) and ^{100}Mo(n,2n) are shown in Figs. 1 to 5, respectively, in comparisn with previous experimental data. As can be seen, the present results cover systematically rather wide energy range in comparisn with other data previonsly reported. In addition, errors of the present data are relatively small in comparison with the other data. Further efforts will be continued on the other objective materials.

Table 1 Reaction type and decay properties

Target Nucleus	Reaction	Product	Half-life	Gamma-ray Energy(keV)	Branching Ratio (%)
^{92}Mo	(n,p)	^{92m}Nb	10.15 d	934.5	99.2
	(n,α)	^{89}Zr	3.27 d	909.2	99.0
	(n,n'α)	^{88}Zr	83.4 d	393.7	97.3
^{94}Mo	(n,2n)	^{93m}Mo	6.95 h	684.7	99.68
^{95}Mo	(n,p)	^{95m}Nb	3.61 d	235.7	25.5
		^{95g}Nb	34.98 d	765.8	99.8
^{96}Mo	(n,p)	^{96}Nb	23.4 h	778.2	96.8
	(n,n'p)	^{95m}Nb	3.61 d	235.7	25.5
		^{95g}Nb	34.98 d	765.8	99.8
^{97}Mo	(n,p)	^{97}Nb	1.20 h	657.9	98.2
	(n,n'p)	^{96}Nb	23.4 h	778.2	96.8
^{98}Mo	(n,p)	^{98}Nb	51.3 m	787.2	93.2
	(n,n'p)	^{97}Nb	1.20 h	657.9	98.2
	(n,α)	^{95}Zr	64.03 d	756.7	54.6
^{100}Mo	(n,2n)	^{99}Mo	2.75 d	739.6	12.6
	(n,α)	^{97}Zr	16.9 h	743.4	92.8

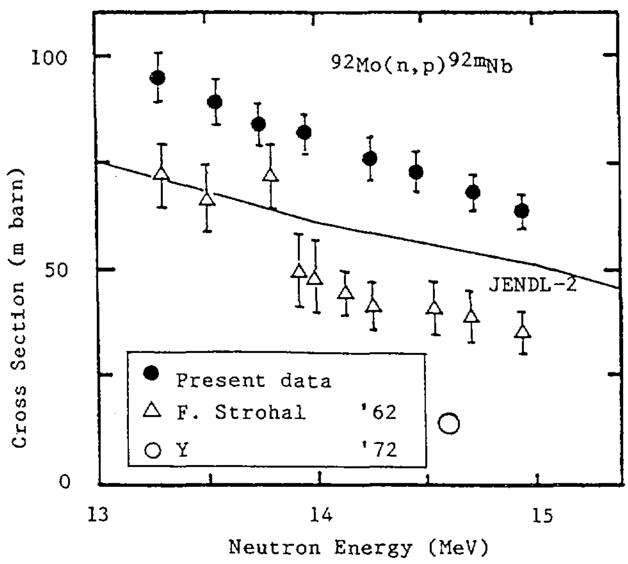

Fig. 1 Cross section of $^{92}Mo(n,p)^{92m}Nb$

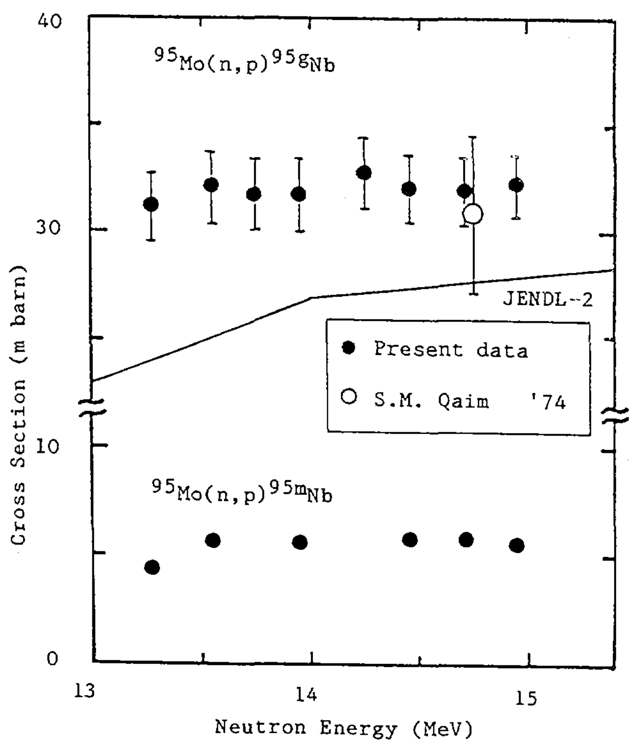

Fig. 2 Cross section of $^{95}Mo(n,p)$-$^{95m,g}Nb$

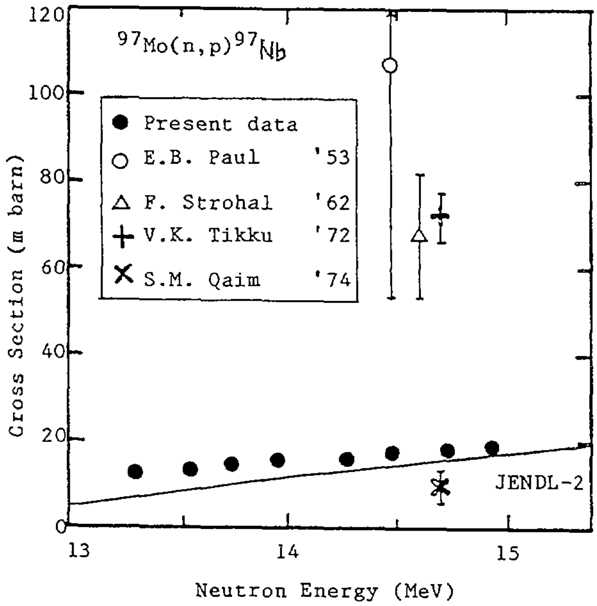

Fig. 3 Cross section of $^{97}Mo(n,p)^{97}Nb$

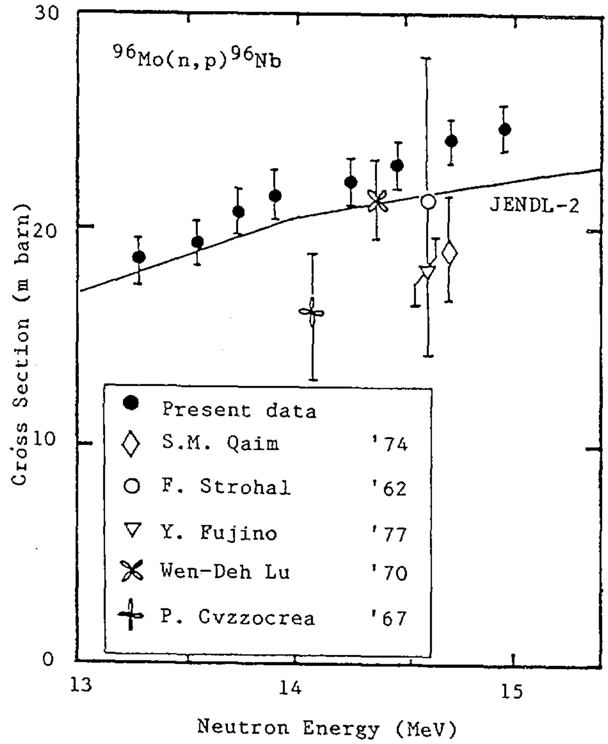

Fig 4 Cross section of $^{96}Mo(n,p)^{96}Nb$

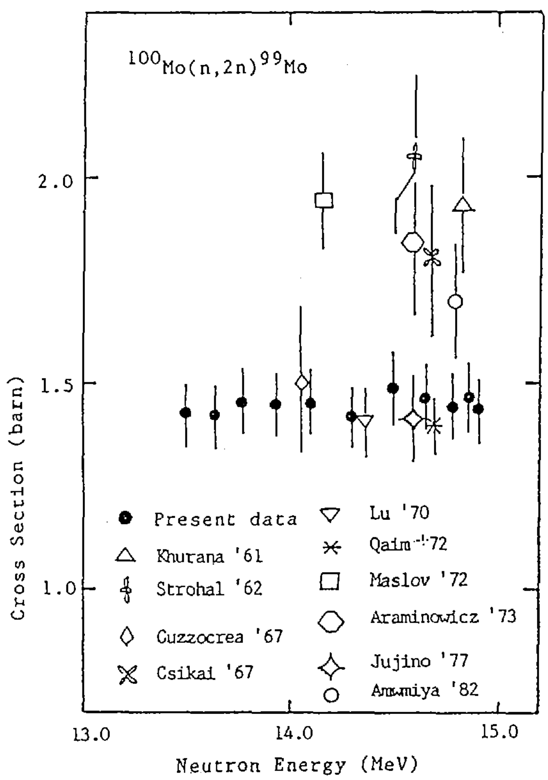

Fig. 5 Cross section of $^{100}Mo(n,2n)^{99}Mo$

B. Linac Laboratory, Department of Physics

II-B-1 Neutron Resonance Parameters of ^{122}Sn

Yutaka Nakajima, Makio Ohkubo, Yutaka Furuta, Masayoshi Sugimoto and Yuuki Kawarasaki

A paper on this subject was presented at the International Conference on Nuclear Data for Basic and Applied Science held in Santa Fe, New Mexico, U.S.A. on May 13 - 17, 1985 with the follpwing abstract:

Neutron transmission measurements were carried out on an oxide sample enriched to 92.20 % ^{122}Sn at a 190-m station with the neutron time-of-flight method. The resonance energies and neutron widths were determined for 21 resonances between 1.5 and 30 keV by a shape analysis and the following average resonance parameters for s-wave neutrons were obtained: $D = 1.17 ^{+0.09}_{-0.08}$ keV, $S_0 \times 10^4 = 0.30 ^{+0.12}_{-0.08}$, $R' = 5.60 \pm 0.05$ fm. The s-wave neutron strength function of ^{122}Sn is greater than the theoretical prediction of the doorway state model.

II-B-2 NEUTRON RESONANCE PARAMETERS OF ^{142}Ce

Makio OHKUBO, Motoharu MIZUMOTO, Yutaka NAKAJIMA,
Masayoshi SUGIMOTO, Yutaka FURUTA and Yuuki KAWARASAKI

Neutron transmission and capture measurements have been made on natural cerium and separated isotope ^{142}Ce at the TOF facility of the Japan Atomic Energy Research Institute linear accelerator. Neutron total cross sections of ^{140}Ce and ^{142}Ce are obtained from 0.1 to 100 keV energy region. The resonance analysis were made on the transmission data, and the parameters of the resonances of ^{142}Ce isotope were newly obtained up to 50 keV. The s-wave strength function S_0, and average level spacing D_0 were deduced to be $S_0=(2.7\pm0.6)\times10^{-4}$, and $D_0=0.75\pm0.12$ keV below 50 keV. Resonance parameters of N=82 nucleus ^{140}Ce are also determined in the same energy region, and S_0 is deduced to be $S_0= 1.1\times10^{-4}$ below 50 keV except a region including a very large resonance at 21.6 keV. Preliminary results have been reported in the International Conference on "Nuclear Data for Basic and Applied Science" held at Santa Fe, USA, in May 1985.

II-B-3 Neutron Total Cross Sections of ^{181}Ta and ^{238}U from 24.3 keV to 1 MeV and Average Resonance Parameters

Izumi Tsubone*, Yutaka Nakajima, Yutaka Furuta and Yukinori Kanda**

A paper on this subject was published in J. Nucl. Science and Eng. 88(1984) 579-591 with the following abstract:

The neutron total cross sections of ^{181}Ta and ^{238}U have been obtained in the energy range from 24.3 keV to 1 MeV by means of neutron transmission measurements using the Japan Atomic Energy Research Institute linac. The measurements were carried out with the iron-filtered neutron beam technique and the time-of-flight method, using an NE-110 plastic scintillator as a neutron detector at a 100 m station. For ^{238}U, correction for the resonance self-shielding effect was taken into account below 270 keV by measuring transmission of four samples of different thicknesses. By fitting average R-matrix calculations to the observed total cross sections, the neutron strength functions S_{ℓ} and distant level parameters R_{ℓ}^{∞} for s-, p-, and d-wave were deduced to be: R_0^{∞}=-0.003±0.03, S_1x10^4= 0.57±0.31, R_1^{∞}=-0.01±0.03, S_2x10^4=1.22±0.12,and R_2^{∞}=-0.15±0.3 for ^{181}Ta, and R_0^{∞}=-0.072±0.028, S_1^{∞}x10 =1.68±0.28 ,R_1^{∞}=0.23±0.08, S_2x10^4=0.70±0.34 and R_2^{∞}=-0.33±0.13 for ^{238}U. The effective s-wave scattering radii were 7.90±0.03 and 9.30±0.04 fm for ^{181}Ta and ^{238}U, respectively.

---

* On leave from Kyushu University as a research student in Japan Atomic Energy Research institute.

** Kyushu University, department of Energy Conversion Engineering.

II-B-4 Neutron Resonance Parameters of ^{183}W up to 1.1 keV

Makio OHKUBO and Yuuki KAWARASAKI

A paper on this subject was published in "Journal of Nuclear Science and Technology" in Vol 21,805-813,(Nov.1984) with the following abstract.

Neutron transmission, scattering and capture experiments on the separated isotope ^{183}W were carried out in the resonance region, using a time-of-flght spectrometer of the Japan Atomic Energy Research Institute linear accelerator. A ^{6}Li-glass and a ^{7}Li-glass detectors were used in pair wise to determine the spins by detecting scattered neutrons and capture gamma rays. Resonance parameters, E, $2g\Gamma_n$ were deduced up to 1.1 keV by analyzing the transmission data. Average level spacing D and s-wave strength function S_0 were derived to be D = 13.3 ± 1 eV, S_0 =(1.24 ± 0.22)x10^{-4} below 1.1 keV. Spins of 41 resonances were determined up to 900 eV from the capture and scattering experiments. The result on spin values supports the (2J+1) law on level density. The dependence of Γ_γ on spin values is inferred. Frequent appearence of spacing of 173 eV betweent two arbitrary levels is discussed.

II-B-5

Neutron radiative capture and transmission measurements of ^{135}Ba and ^{137}Ba

M. Mizumoto, M. Sugimoto, M. Ohkubo, Y. Nakajima,

Y. Furuta and Y. Kawarasaki

A paper on this subject was presented at the International Conference on Nuclear Data for Basic and Applied Science, May 13-17, 1985, Santa Fe with an abstract as follows:

The neutron capture and total cross sections of ^{135}Ba and ^{137}Ba were measured at the 55 m station of the JAERI Electron Linear Accelerator. Measurements were carried out with a 500 l liguid scintillation detector and a ^{6}Li glass detector. Resonance energies and neutron widths for ^{135}Ba and ^{137}Ba were determined from 400 eV to 4 keV and from 400 eV to 9 keV, respectively. The s-wave strength functions and average level spacings were obtained to be $S_0 = (0.96 \pm 0.30) \times 10^{-4}$, $D_0 = 44 \pm 6$ eV for ^{135}Ba and $S_0 = (0.16 \pm 0.07) \times 10^{-4}$ for ^{137}Ba. The average capture cross sections for ^{135}Ba were deduced from 4 to 300 keV.

II-B-6 Measurements of Fast Neutron Scattering Cross Sections of Aluminum

M. Sugimoto, Y. Yamanouti, Y. Furuta, M. Mizumoto,
S. Nishihara* and M. Hyakutake**

Neutron scattering cross section measurements of aluminum at 13 MeV were carried out using the JAERI tandem fast neutron time-of-flight spectrometer. The neutrons produced by the $D(d,n)^3He$ reaction and scattered from the 3 cm diam by 4 cm aluminum were detected by the four 20 cm diam by 35 cm NE213 scintillators. The new technique was applied to improve the time resolution of the large volume detectors. This technique uses the method to process the list mode event data to attain the time-compensated spectrum in the wide range of the scattered neutron energy. The details of the measurements and the new technique were described elsewhere[1]. The differential cross sections to the g.s., (0.84 + 1.01 MeV), 2.21 MeV and (2.73 + 2.98 + 3.04 MeV) levels were obtained at 15 angles through 20 - 140 deg. The excitation functions at 60 and 100 deg were also measured in the energy range 12.3 - 13.5 MeV.

Reference:

1) M. Sugimoto, Y.Yamanouti, Y. Furuta, M. Mizumoto, S. Nishihara and M. Hyakutake, JAERI-M 85-104 (1985) 185.

---

* Present Address: Mitsubishi Electrics Co., Osaka.

** Department of Nuclear Engineering, Kyushu University.

II-B-7 Scattering of 12.8 MeV neutrons from ^{28}Si

Y.Yamanouti, M.Sugimoto, Y.Furuta, M.Mizumoto and M.Hyakutake*

Differential cross sections for the scattering of 12.8 MeV neutrons from ^{28}Si were measured in order to get deeper understanding of the reaction mechanism in the energy region above 10 MeV and collective properties of the low-lying excited states of ^{28}Si. Scattered neutrons were observed by a newly constructed time-of-flight spectrometer with an array of four 20 cmϕ x 35 cm NE213 liquid scintillator detectors. Monoenergetic neutrons were generated in a gas cell filled with deuterium gas by the $^{2}H(d,n)^{3}He$ reaction as a neutron source reaction. Neutron time-of-flight spectra were taken at scattering angles from 15° to 140°. Inelastic scattering cross sections of neutrons leading to the first 2^+ state at 1.779 MeV and the 4^+ state at 4.617 MeV were measured simultaneously with the elastic scattering cross sections. The relative efficiencies for the neutron detector were determined by measuring the known angular distribution of neutrons from the $^{2}H(d,n)^{3}He$ reaction.

The experimental cross sections were analyzed by the optical model, the DWBA theory and the coupled-channel formalism. The experimental cross sections for the 0^+, 2^+ and 4^+ states of ^{28}Si were well reproduced by the coupled-channel calculation based on the rotational model with the oblate quadrupole deformation.

---

* Department of Nuclear Engineering,Kyushu University

C. Nuclear Data Center, Department of Physics and Working Groups of Japanese Nuclear Data Committee

II-C-1 Activities of Japanese Nuclear Data Committee

The Japanese Nuclear Data Committee(JNDC) was convened once in 1984 fiscal year to discuss plans of working-group activities as well as to examine the activities made in the last fiscal year. The Steering Committee met eight times in this period to promote plans of the Committee and Subcommittees, to discuss every problem on the activities of the Working Groups, and to furnish advice to the JAERI Nuclear Data Center(JAERI/NDC) on the business of the secretariat.

The Counseling Committee met twice to check and review the activities of the JNDC from the viewpoint of long-term strategy. They made a report on a subject that the JNDC must do in the near future to satisfy potential requirements to the nuclear data. They recommended also the JNDC Chairman to promote international cooperation with the Asian-Pacific countries as well.

Working Groups of the JNDC held the meetings seventy-eight times totally from April 1984 to March 1985. They worked in cooperation with the JAERI/NDC to evaluate nuclear cross-section data for the JENDL-3.

Evaluation of the nuclear structure data for A=118, 120 and 122 was finished, and the data were compiled to submit to the NNDC(BNL). Work for the second version of the Nuclear Data Library for the summation calculation of the decay heat has been promoted.

The covariance data and the processing codes were made for the adjustment of the group cross sections composed of the JENDL-2 data. They have done the benchmark tests for the shielding problems with the iron data, and for the transmission experiments with the 14 MeV neutrons.

A Seminar on Nuclear Data was held on November 13 to 15, 1984 at Tokai Research Establishment of JAERI. The JNDC had made plans to invite some experts from the Asian-Pacific countries. Although it could not be realized, four papers were contributed from China and Australia.

The Seminar was comprised of the following seven sessions: (1) Introduction of Nuclear data activities in Japan, China and Australia, (2) Nuclear data for fuel cycle, (3) Nuclear data for reactor design, (4) Nuclear data evaluation, (5) Fission phenomena, (6) Utilization of nuclear data in various fields, and (7) Poster session entitled Nuclear Data Files Available from the JAERI/NDC.

II-C-2 Evaluation of Neutron Nuclear Data of ^{9}Be

Keiichi SHIBATA

A paper on this subject was published as JAERI-M 84-226 with the following abstract:

Neutron nuclear data of ^{9}Be have been evaluated for JENDL-3 in the energy range from 10^{-5} eV to 20 MeV. Evaluated quantities are the total, elastic and inelastic scattering, photon-production, (n,γ), (n,p), (n,d), (n,t) and (n,α) reaction cross sections and the angular and energy distributions of neutrons. The total cross section below 830 keV was calculated with the R-matrix theory. The statistical model was applied to the prediction of the inelastic scattering and charged-particle emission cross sections. The (n,2n) reaction cross section is given by the sum of the inelastic scattering and (n,α_1) reaction cross sections.

II-C-3 Evaluation of Neutron Nuclear Data for ^{249}Bk and ^{249}Cf*

Yasuyuki KIKUCHI and Tsuneo NAKAGAWA

A paper on this subject is in the press as JAERI-M 85-138. The following is abstract of the paper.

Neutron nuclear data of ^{249}Bk and ^{249}Cf have been evaluated in the energy range from 10^{-5} eV to 20 MeV. Evaluated quantities are the total, elastic and inelastic scattering, fission, capture, (n,2n), (n,3n) and (n,4n) reaction cross sections, the resolved and unresolved resonance parameters, the angular and energy distributions of the emitted neutrons, and the average number of neutrons emitted per fission. The fission cross sections were evaluated mainly on the basis of measured data. The other cross sections were calculated with the optical and statistical models because of scarce measured data.

---

* This work was performed under contracts between Power Reactor and Nuclear Fuel Development Corporation and Japan Atomic Energy Research Institute.

II-C-4 Present Status of the Compilation for JENDL-3

Nuclear Data Center

The data evaluation and compilation for the Japanese Evaluated Nuclear Data Library Version 3, JENDL-3 are now in progress towards the completion in 1987. Before the compilation of JENDL-3, however, we decided to compile the preliminary version of JENDL-3 to use urgently the evaluated data of some nuclides for analyses of integral experiments in fusion neutronics. Though the JENDL-2 data have been confirmed to be applicable for calculations of cores and shieldings in fission reactors, it has been pointed out that they were not always adequate for uses in fusion researches. For the preliminary version, therefore, the data in higher neutron-energies were reevaluated and further recent experimental data of the angle- and energy- distributions for neutron emission were taken into account.

JENDL-3 Preliminary Version 1, JENDL-3PR1[1)] contains eight nuclides which are used for data analyses in Japan-U.S. Technology Cooperation on Fusion Neutronics: ^{6}Li, ^{7}Li, ^{9}Be, ^{12}C, ^{16}O, Cr, Fe and Ni. JENDL-3PR1 was compiled in 1984. The data of ^{6}Li and ^{7}Li in this file were wholly reevaluated, including photon-production data newly. The data for ^{9}Be and ^{12}C also were wholly reevaluated. The details of the evaluations for these data have been described elsewhere[2)-5)]. The data of ^{16}O were newly evaluated for this version by Working Group on Nuclear Data for Fusion in JNDC. For Cr, Fe and Ni, the inelastic scattering data of JENDL-2 were revised[6)] in higher energies to consider accurately the direct and precompound processes.

Among the above JENDL-3PR1 data the evaluated data for ^{6}Li, ^{7}Li and ^{12}C were revised further in taking account of recent experimental results on double differential cross sections for neutron emission (DDX). For ^{6}Li and ^{7}Li the inelastic scattering data (cross sections and angular distributions) were revised sharply to fit to the experimental DDX data and the (n,2n) reaction data were also modified partly[7]. For ^{12}C the cross section and angular distribution for the inelastic scattering to the third level (9.63 MeV) were revised to fit to the recent experimental data.

These evaluated data for ^{6}Li, ^{7}Li and ^{12}C were compiled as JENDL-3PR2 recently. These data are not final and are expected to be made some additional improvements before the compilation of JENDL-3.

References:

1) K. Shibata and Y. Kikuchi, submitted to Santa Fe Conference (1985).
2) K. Shibata, JAERI-M 84-198 (1984).
3) K. Shibata, JAERI-M 84-204 (1984).
4) K. Shibata, JAERI-M 84-226 (1984).
5) K. Shibata, JAERI-M 83-221 (1983).
6) Y. Kikuchi et al., to be published in J. Nucl. Sci. Tech.
7) S. Chiba et al., submitted to Santa Fe Conference (1985).

III. Kinki University

Department of Reactor Engineering

III-1 The Feasibility of the Empirical Rule for the Estimation of Fission Neutron Spectrum Averaged Cross Sections for the (n,p) and (n,α) Reactions

Osamu Horibe

A paper on this subject is submitted to the Int. Conf. on Nuclear Data for Basic and Applied Science, Santa Fe, New Mexico, U.S.A., May 13-17, 1985, with the following abstract:

We have proposed the empirical rule useful to estimate the fission averaged cross sections of the (n,p) and (n,α) reactions. The feasibility of this rule is further approved by the fact that the newly measured values of the (n,p) reaction cross sections on ^{43}Ca, ^{96}Mo, ^{132}Ba and ^{140}Ce, and of the (n,α) reaction cross sections on ^{45}Sc, ^{50}Ti and ^{54}Fe coincide with values predicted by this rule. The hitherto known values of these cross sections were erroneous and then deviated from this rule.

IV. KYOTO UNIVERSITY

Research Reactor Institute

IV-1 Pa values of ^{95}Rb, ^{95}Sr and ^{95}Y

K. Okano, Y. Funakoshi* and Y. Kawase

Using the ^{95}Rb samples mass-separated by KUR-ISOL, the absolute γ-ray emission probabilities (Pa) of main γ rays following the β^- decays of ^{95}Rb, ^{95}Sr and ^{95}Y have been measured. The Pa values for the ^{95}Rb 352.2 keV, ^{95}Sr 685.9 keV and ^{95}Y 954.2 keV γ rays have been determined as 49.2±3.1, 21.8±1.8 and 15.9±0.7 per 100 decays, respectively, by a filiation method. The Pa value of 0.547±0.004 for the 756.7 keV γ ray of 64.0d ^{95}Zr was used as standard. The results obtained are compared with previous values in Tables 1-2.

The Pa values obtained in this work for the ^{95}Rb 352.2 keV and ^{95}Sr 685.9 keV γ rays are in good agreement with previous results (see Table 1) if the new Pa value obtained in this work for the ^{95}Y 954.2 keV γ ray is adopted as standard instead of the value[1)] 0.19±0.02 which was used as standard in the previous works. There exist large discrepancies among the Pa values for the ^{95}Y 954.2 keV γ ray as can be seen in Table 2.

---

* Present Address: National Laboratory for High Energy Physics

The reason of these discrepancies is not clear.

The log f_1t value of the first-forbidden unique β^- transition of ^{95}Y to the ground state of ^{95}Zr has been determined as 8.62±0.04.

References:

1) P. Cavallini and J. Blachot, Radiochem. Radioanal. Lett. 21 (1975) 157

2) Kratz et al., Z. Phys. A Atoms and Nuclei 312 (1983) 43

3) W. Herzog and W. Grimm, Z. Phys. 266 (1974) 397

4) B. Pfeiffer et al., Proc. 4th Int. Conf. on Nuclei far from Stability, CERN 81-09 (1981) p. 423

5) R. E. Larson and C. M. Gordon, Nucl. Phys. 88 (1966) 481

6) J. Van Klinken et al., Phys. Rev. 154 (1967) 1116

7) P. Cavallini et al., J. Phys. (Paris) 34 (1973) 675

8) Niizeki and Tamura, J. Phys. Soc. Jap. 52 (1983) 3743

9) K. Luksch, Nucl. Data Sheets 38 (1983) 1

Table 1. Absolute emission probabilities (Pa) for the 352.2keV γ ray in the decay of ^{95}Rb and the 685.9keV γ ray in the decay of ^{95}Sr.

Reference	Method and detector	Pa value
	^{95}Rb 352.2keV γ ray	
Kratz et al. (1983)[2]	Filiation method, Ge(Li)	0.57±0.04
This work	Filiation method, Ge(Li)	0.492±0.031
	^{95}Sr 685.9keV γ ray	
Herzog and Grimm (1974)[3]	Cumulative fission yields and Pa values of ^{93}Sr and ^{94}Sr	0.24±0.02
Pfeiffer et al. (1981)[4]	Filiation method, Ge(Li)	0.28±0.04
This work	Filiation method, Ge(Li)	0.218±0.018

Table 2. Absolute emission probability (Pa) for the 954.2 keV γ ray and β branching to the ground state of ^{95}Zr in the decay of ^{95}Y.

Reference	Method and detector	Pa value	β branching (%)
Larson and Gordon (1966)[5]	Analysis of β-ray spectra, plastic scintillator	$\approx 0.27^{a}$	≈ 40
Klinken et al. (1967)[6]	$4\pi\beta$-plastic, NaI(Tl)	0.09±0.02	82±5
Cavallini et al. (1973)[7]	Filiation method, Ge(Li)	0.132±0.010	70±4
Cavallini and Blachot (1975)[1]	Filiation method, Ge(Li)	0.19±0.02	57^{b}
Niizeki and Tamura (1983)[8]	$4\pi\beta$-anthracene, Ge(Li)	0.111 ± 0.022^{a}	75±5
This work	Filiation method, Ge(Li)	0.159±0.007	64.5 ± 1.6^{c} 64.1 ± 1.6^{a}

[a] Calculated using the γ-ray decay scheme of Niizeki and Tamura (1983)[8].

[b] Luksch (1983)[9].

[c] Calculated using the γ-ray decay scheme of Cavallini et al (1973)[7].

IV-2 Half-lives of ^{95}Sr, ^{139}Cs and ^{141}Cs

K. Okano, Y. Kawase and Y. Funakoshi*

Precise half-lives of fission-product nuclides ^{95}Sr, ^{139}Cs and ^{141}Cs have been determined using samples mass-separated by KUR-ISOL. Special care was paid to reduce contaminations and backgrounds in the Ge(Li) γ-ray peaks. Measurements were performed by using a 64K MCA in a configuration of 4K×16 or 2K×32 multi-spectrum scaling mode. The results obtained are listed in table 1 and are compared with previous results.

Reference:

1) W. Herzog and W. Grimm, Z. Phys. 266 (1974) 397

2) I. Amarel, R. Bernas, R. Foucher, J. Jastrzebski, A. Johnson and J. Teillac, Phys. Lett. 24B (1967) 402

3) T. Tamai, J. Takada, R. Matsushita and Y. Kiso, Inorg. Nucl. Chem. Lett. 9 (1973) 245

4) B. Grapengiesser, E. Lund and G. Rudstam, J. Inorg. Nucl. Chem. 36 (1974) 2409

5) B. Grappengigsser, E. Lund and G. Rudstam, Proc. Internatl. Conf. Properties of Nuclei Far from the Region of β-stability, Leysin (1970), CERN 70-30, p. 1093

6) G. C. Carlson, W. C. Schick, Jr, W. L. Talbert, Jr and F. K. Wohn, Nucl. Phys. A125 (1969) 267

7) B. Ehrenberg and S. Amiel, Phys. Rev. C6 (1972) 618

* Present Address: National Laboratory for High Energy Physics

8) N. P. Archer and G. L. Keech, Can. J. Phys. 44 (1966) 1823

9) W. L. Talbert, Jr., A. B. Tucker and G. M. Day, Phys. Rev. 177 (1969) 1805

10) E. Lund and G. Rudstam, Phys. Rev. C13 (1976) 1544

Table 1. Half-lives of ^{95}Sr, ^{139}Cs and ^{141}Cs

Nuclide	Present results	Previous results	Reference
^{95}Sr	23.3±0.3 sec	24.4±0.2 sec	(1)
		26±1 sec	(2)
		25.9±1.6 sec	(3)
		26.8±1.5 sec	(4)
^{139}Cs	9.36±0.15 min	9.53±1.0 min	(5)
		9.27±0.05 min	(6)
		9.76±0.08 min	(7)
		9.0±0.15 min	(8)
^{141}Cs	24.5±0.4 sec	24.9±0.2 sec	(9)
		24.7±0.4 sec	(6)
		25.6±0.3 sec	(4)
		22.2±0.4 sec	(10)

IV-3

Measurement and Analysis of Energy Spectra of Neutrons in Structural Materials for Reactors

Itsuro Kimura, Shu A. Hayashi, Katsuhei Kobayashi, Shuji Yamamoto, Hiroshi Nishihara*, Satoshi Kanazawa*, Takamasa Mori**, Masayuki Nakagawa** and Ahmet Saim Selvi***

In order to assess evaluated nuclear data of main structural materials for fission and fusion reactors, measurement and analysis of energy spectra of neutrons mainly in the keV region in sample piles or scattered by sample slabs have been continuously carried out.

(1) The final result of the neutron spectrum in a spherical manganese pile was published recently[1]. Good agreement can be seen in the general shape between calculated and measured angular spectra from a few keV to a few MeV. As far as can be concluded from the intercomparison, the nuclear data for Mn in ENDF/B-IV may be applicable to reactor design, however, several improvements for its resonance parameters can be recommended. A little more improvements are recommended for that in JENDL-2 from this intercomparison.

(2) The final result of the neutron spectrum in a metallic lithium pile was also published recently[2]. In the energy region above 600 keV, both calculations with JENDL-2 and

* Department of Nuclear Engineering, Kyoto University

** Reactor System Research Laboratory, JAERI

*** Present Address : Physics Department, Ege University Izmir, Turkey

JENDL-3PR1 give slightly harder spectra than the measured one, while the ENDF/B-IV calculation predicts a better shape of the spectrum. The overalll shape of the spectrum the ^{7}Li resonance is well predicted by the JENDL-2 and JENDL-3PR1 calculations, though the flux calculated with JENDL-2 is lower by 20 % than the measured one. The ENDF/B-IV calculation overestimates the decrease of the flux below about 300 keV. In addition, the contribution of the angular distribution of elastically scattered neutrons from ^{7}Li has been discussed.

(3) The final results of the measurement and analysis of neutron distribution in lithium fluoride and polytetrafluoroethylene piles are now in print for the publication[3].

In these cases, an additional photoneutron source in the sample materials (F) has been markedly observed, so that we have tried to carry out a 2-D transport calculation. However the distortion of the neutron spectra caused by the photoneutron source in the sample materials is estimated to be less than 10 % below a few MeV for both piles. The spectra calculated with the JENDL-2 and ENDF/B-IV data show generally good agreement with the measured ones for both piles. However, the calculation underestimates the fluxed around several 100 keV and overestimates below 100 keV. Overall shapes of the spectra below 100 keV are better predicted by the JENDL-2 data than by the ENDF/B-IV ones. The reevaluations of the ratio of the inelastic and elastic scattering cross sections below 1 MeV and the resonance cross section below 100 keV are necessary to reduce the discrepancies observed.

(4) The final result of the neutron spectrum in a spherical

copper pile was submitted to Ann. Nucl. Energy[4] and was presented at the International Conference on Nuclear Data for Basic and Applied Science at Santa Fe in May 1985[5].

Better agreement can be seen in the general shape between the calculated angular spectrum with ENDF/B-IV and the measured one from a few keV to a few MeV than the case with JENDL-2. The JENDL-2 data have no resonance parameters in the energy range from 35 keV to 500 keV, while the ENDF/B-IV data have those in this range. From about 10 keV to 30 keV the total cross section data in ENDF/B-IV are 30 - 60 % larger than our new data which we obtained by a subsidiary measurement. If the total cross section data in ENDF/B-IV are decreased in this region, the calculated spectrum would approach to the measured one.

(5) The results of the neutron spectra in iron, nickel, chromium and stainless steel piles will be written as a final paper and it will be submitted to a jounal, soon.

(6) In this research series, the part of the works concerning new reactor materials, such as Mo, Nb, Ti, Li and fluorine compounds (LiF and $(CF_2)_n$) was reported by one of the members[6].

(7) An old measured neutron spectrum in a spherical thoria pile by this group[7] has been rechecked by comparison with the calculated ones with ENDF/B-IV, ENDF/B-V and JENDL-2. A preliminary result shows that the best agreement can be seen for the case of ENDF/B-IV and the data of inelastic scattering play an important role in the shape of neutron spectra. Therefore we are trying to check the inelastic scattering data in these three evaluated data files.

(8) The neutron spectrum in a spherical pile of silicon was measured and analyzed recently. A preliminary result was presented at the Santa Fe Conference[5]. Two calculated spectra with ENDF/B-IV and JENDL-2 satisfactorily agree each other from 10 keV to several MeV, but they predict considerably lower neutron flux below the cross section minimum at 144 keV than the measured one. We are trying to seek the reason of this discrepancy.

References :

1) A. S. Selvi, et al.: Atomkernenergie-Kerntechnik, 45, 183 (1984).

2) T. Mori, et al.: Annu. Rep. Res. Reactor Inst., Kyoto Univ., 17, 22 (1984).

3) T. Mori, et al.: J. Nucl. Sci. Technol., in print.

4) S. A. Hayashi, et al.: Submitted to Annals of Nucl. Energy.

5) I. Kimura, et al.: To be published in radiation effects (Proc. Intern. Conf. on Nuclear Data for Basic and Applied Science at Santa Fe in May 1985).

6) T. Mori : JAERI-M 85-049 (1985).

7) H. Nishihara, et al.: J. Nucl. Sci. Technol., 14, 426 (1977).

IV-4

Activation Cross Sections Measured with 14.1 MeV Neutrons from ^{6}LiD Converters

Katsuhei Kobayashi and Itsuro Kimura

With a ^{6}LiD converter placed in a thermal neutron field, 14.1 MeV neutrons can be produced through the following reactions;

$$^{6}Li + n_{th} \longrightarrow {}^{4}He + T + 4.8\ MeV$$

$$D + T \longrightarrow {}^{4}He + n(14.1\ MeV)$$

The conversion ratio from thermal neutrons to 14.1 MeV neutrons is said to be $1 \sim 2 \times 10^{-4}$.[1)]

In the present experiment, ^{6}LiD powder of about 75 g was packed in an aluminum case 10 cm square and 1 cm thick to prepare a ^{6}LiD converter. Activation foils were sandwiched between a pair of the ^{6}LiD converters, and these samples and converters were installed in a large irradiation room of the KUR thermal neutron facility, as seen in Fig.1. After the irradiation, the induced activities were measured with a calibrated Ge(Li) detector.

In the present measurement, the cross sections at 14.1 MeV for the $^{27}Al(n,p)^{27}Mg$, $^{58}Ni(n,p)^{58}Co$, $^{58}Ni(n,2n)^{57}Ni$, $^{90}Zr(n,2n)^{89}Zr$ and $^{93}Nb(n,2n)^{92m}Nb$ reactions were measured relative to that for the $^{27}Al(n,\alpha)^{24}Na$ reaction, whose reference value was taken from ENDF/B-V data. The results obtained are summarized in Table 1, where the 14.1 MeV neutron spectrum averaged cross sections and the correlation matrix are also given. This uncertainty analysis was carried out by the same method as before[2)]. The results from the evaluated data and their

C/E ratios are also shown in the table. It can be seen from the present results that the cross section for the $^{58}Ni(n,2n)$ ^{57}Ni reaction from ENDF/B-V is lower by about 5 % near 14.1 MeV, and the evaluated values for the $^{90}Zr(n,2n)^{89}Zr$ and ^{93}Nb $(n,2n)^{92m}Nb$ reactions also seem to be rather lower.

References:

1) W. H. Miller, et al.: Nucl. Instr. Meth., 216, 219 (1983).

2) K. Kobayashi, et al.: J. Nucl. Sci. Technol., 19, 341 (1982).

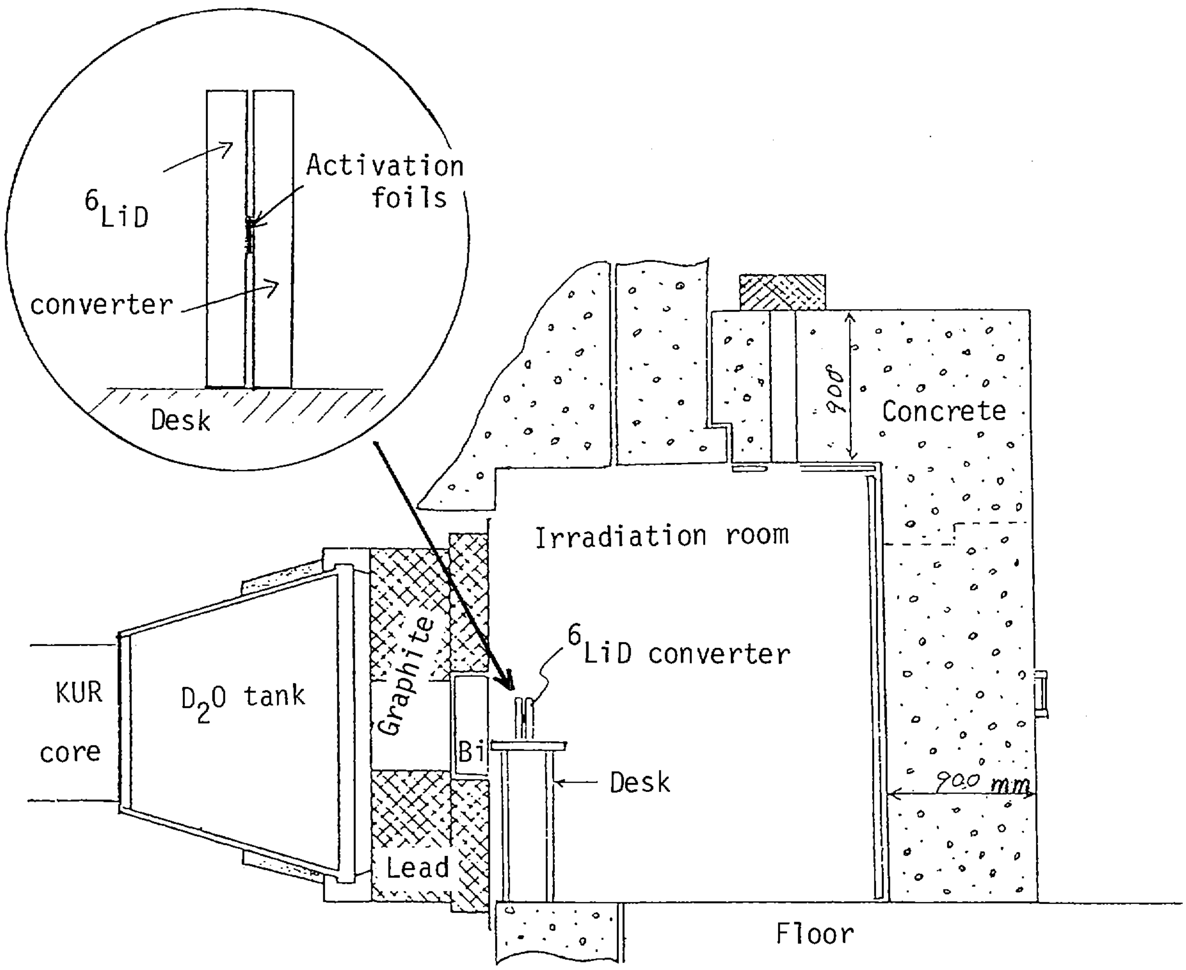

Fig. 1 Experimental arrangement with ^{6}LiD converters at the KUR thermal neutron facility

Table 1 Present result of the measured cross sections and comparison with the evaluated value

Reaction	Cross section (mb)	Correlation matrix (x 100)						ENDF/B-V	C / E
$^{27}Al(n,\alpha)^{24}Na$	121.2 ± 3.72	100						121.2 mb	1.000
$^{27}Al(n,p)^{27}Mg$	76.13 ± 3.49	68	100					76.89	1.010
$^{58}Ni(n,p)^{58}Co$	416.6 ± 13.9	92	67	100				412.4	0.9899
$^{58}Ni(n,2n)^{57}Ni$	25.36 ± 0.84	92	66	90	100			23.99	0.9460
$^{90}Zr(n,2n)^{89}Zr$	626.4 ± 20.8	92	66	91	90	100		598.3 *	0.9551
$^{93}Nb(n,2n)^{92m}Nb$	471.1 ± 15.6	92	67	92	90	91	100	452.5 #	0.9604

* G. Winkler (1982)
\# B. Strohmaier (1982)

IV-5

Measurement of Resonance Integrals for the $^{55}Mn(n,\gamma)^{56}Mn$, $^{232}Th(n,\gamma)^{233}Th$ and $^{238}U(n,\gamma)^{239}U$ Reactions

Katsuhei Kobayashi, Itsuro Kimura, Shuji Yamamoto
Ryota Miki* and Tetsuo Itoh*

The research reactor UTR-KINKI, whose nominal power is 1 W, has separate cores with MTR-type fuels. Between the cores, there exists a graphite reflector 70 cm thick (Fig.1). A stringer 9.5 cm square, 122 cm long at the center of the reflector can be pulled out to make an experimental hole, where the neutron spectrum has been experimentally and theoretically verified to be a standard 1/E neutron spectrum field[1].

In the present study, we have measured resonance integrals for the $^{55}Mn(n,\gamma)^{56}Mn$, $^{232}Th(n,\gamma)^{233}Th$ and $^{238}U(n,\gamma)^{239}U$ reactions relative to that for the $^{197}Au(n,\gamma)^{198}Au$ reaction. Characteristics of the sample foils are shown in Table 1. Each sample was covered with a cadminium case 0.5 mm thick, and each run for the irradiation of the sample and gold foils was performed for 150 minutes at the center of the graphite reflector.

After the irradiation, induced activities were measured with a Ge gamma-ray spectrometer, whose detection efficiencies were calibrated with the standard gamma-ray sources.

Concerning the correlation of neutron self-shielding

* Atomic Energy Research Institute, Kinki University
3-2-1 Kowakae, Higashi-osaka, Osaka-fu, Japan

effects in each sample foil, a Monte Carlo calculation by VIM code[2] has been applied. We have experimentally checked the validity of the correction method by counting the activities from the five foils which were superposed together.

In the data processing to obtain the resonance integrals, we have considered data correlations due to the uncertainties from the each error element, such as counting statistics, detector efficiency, neutron self-shielding correction and so on, as we did before[3].

Table 2 summarizes the present result of the resonance integrals and the correlation matrix. In the last two columns, evaluated values are given to compare with the measurement. The data for the $^{55}Mn(n,\gamma)^{56}Mn$ and $^{238}U(n,\gamma)^{239}U$ reactions are, in general, close to the measurement, however, the data for the $^{232}Th(n,\gamma)^{233}Th$ reaction, the JENDL-2 value seems to be lower by about 7 %. Recent data (86.1 b) by Olsen[4] agrees very well with our present measurement.

References:

1) R. Miki and K. Tsuchihashi, Unpublished.
2) R. N. Blomquist, et al.: ORNL/RSIC 44 (1980).
3) K. Kobayashi, et al.: J. Nucl. Sci. Technol., 19, 341 (1982).
4) D. K. Olsen, et al.: ORNL/TM-8056 (1982).

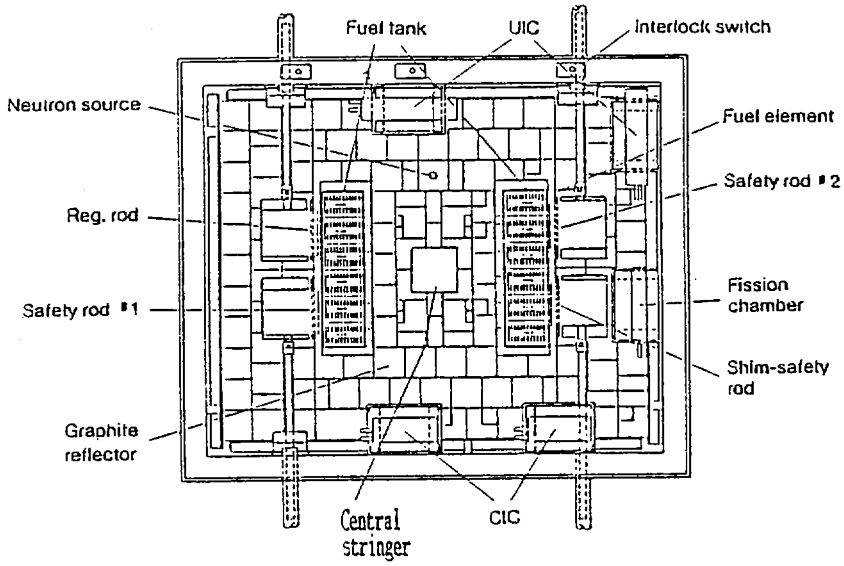

Fig. 1 Core configuration of UTR-KINKI

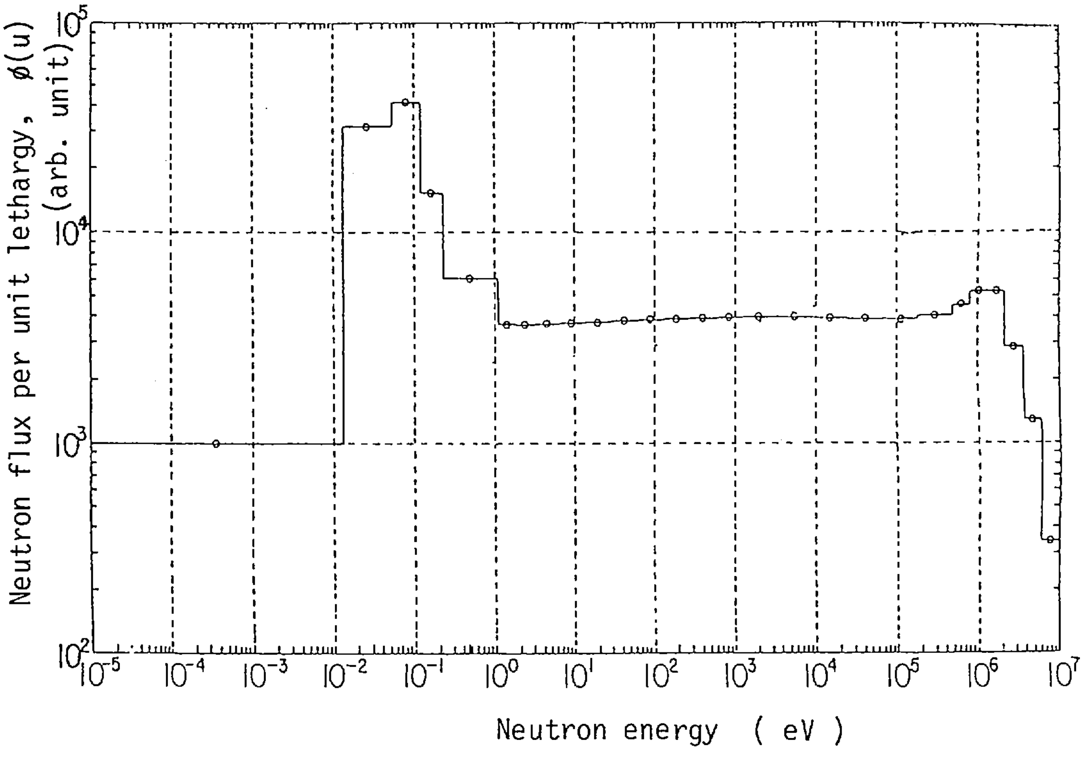

Fig. 2 Neutron spectrum at the core center of UTR-KINKI

Table 1 Characteristics of sample foils used

Sample foil	Reaction	Diameter	Thickness	Comment
Gold	$^{197}Au(n,\gamma)^{198}Au$	12.7 mm	0.050 mm	
Manganese	$^{55}Mn(n,\gamma)^{56}Mn$	12.7	0.2	Alloy,Mn:Cu=84:16
Thorium	$^{232}Th(n,\gamma)^{233}Th$	12.7	0.127	^{233}Pa measured
Uranium	$^{238}U(n,\gamma)^{239}U$	12.7	0.127	^{239}Np measured

Table 2 Resonance integrals and correlation coefficients

Reaction	Resonance integrals (barn)	Error (%)	Correlation coefficient				Evaluation (barn)	JENDL-2
$^{197}Au(n,\gamma)$	1550 *	1.81 *	1.00				1550 $\pm$ 2.8 *	- - -
$^{55}Mn(n,\gamma)$	14.0	3.33	0.54	1.00			14.0 $\pm$ 0.3**	14.63
$^{232}Th(n,\gamma)$	86.2	3.57	0.50	0.74	1.00		85 $\pm$ 3 *	79.93
$^{238}U(n,\gamma)$	277	4.28	0.42	0.70	0.67	1.00	277 $\pm$ 3 *	279.0

* S. F. Mughabghab, "Neutron Cross Sections", Vol.1, Part B (1984).

** S. F. Mughabghab, "Neutron Cross Sections", Vol.1, Part A (1981).

V. KYUSHU UNIVERSITY

A. Department of Nuclear Engineering Faculty of Engineering

V-A-1

Comment on Application of Statistical Multi-Step Direct Emission Theory to a Neutron-Emitting Reaction

I. Kumabe, M. Haruta, M. Hyakutake and M. Matoba

A paper on this subject was published in Physics Letters 140B (1984) 272 with an abstract as follows:

The statistical multi-step direct emission theory formulated by Feshbach, Kerman and Koonin(FKK) was applied to the analysis of 14 MeV (n,n') scattering on ^{93}Nb and Ag. It is concluded that the FKK theory as it stands disagrees with experimental data, because of anomalously large multi-step cross sections due to the resonance-like behaviour of non-DWBA matrix elements which are entered in the calculation.

V-A-2

Shell and Odd-Even Effects on Alpha-Particle Energy Spectra from (p,α) Reaction on Nuclei around Z=50

I. Kumabe, Y. Inenaga, M. Hyakutake, N. Koori,
Y. Watanabe, K. Ogawa and K. Orito

In order to clarify the shell effect and the odd-even effect in the pre-equilibrium process on the (p,α) reaction, we have undertaken to measure systematically and accurately the double differential cross sections of the (p,α) reaction which is analogous one with the (n,α) reaction. By the analogy with the (p,α) reaction, we expect to clarify the shell effect and odd-even effect on the 14 MeV (n,α) reaction.

In a previous paper[1)], we have reported a study of the energy spectra of α-particles emitted from the (p,α) reaction on ^{90}Zr, $^{92,94,96,98,100}Mo$, ^{93}Nb, ^{106}Pd and Ag for 18 MeV protons and on some of them for 15 MeV protons.

In the present work the energy spectra of α-particles emitted from the (p,α) reaction on ^{112}Cd, ^{118}Sn, ^{120}Sn, Sb, ^{128}Te and ^{130}Te for 18 MeV protons and on some of them for 15 MeV protons have been measured.

The 15 and 18 MeV proton beams from the tandem Van de Graaff accelerator at Kyushu University were analyzed by a beam analyzing magnet and brought into a scattering chamber. The α-particle detecting system was mounted on a turntable inside the scattering chamber. The detecting system consisted of a ΔE-E counter telescope of two silicon surface barrier detectors having a thickness of 15 μm and 300 μm, respectively. Emitted α-particles were identified and separated from other reaction products by means of an Osaka Denpa MPS-1230 Particle Identifier.

The α-particle spectra were measured at the angles ranging 20° to 160° in steps of 20°. The energy spectra of α-particles integrated over angle are shown in Fig.1.

An analysis of these spectra is now in process under the assumption of three nucleon pick-up process.

Reference:

1) I. Kumabe et al., NEANDC(J)-106/U p.48 (1984).

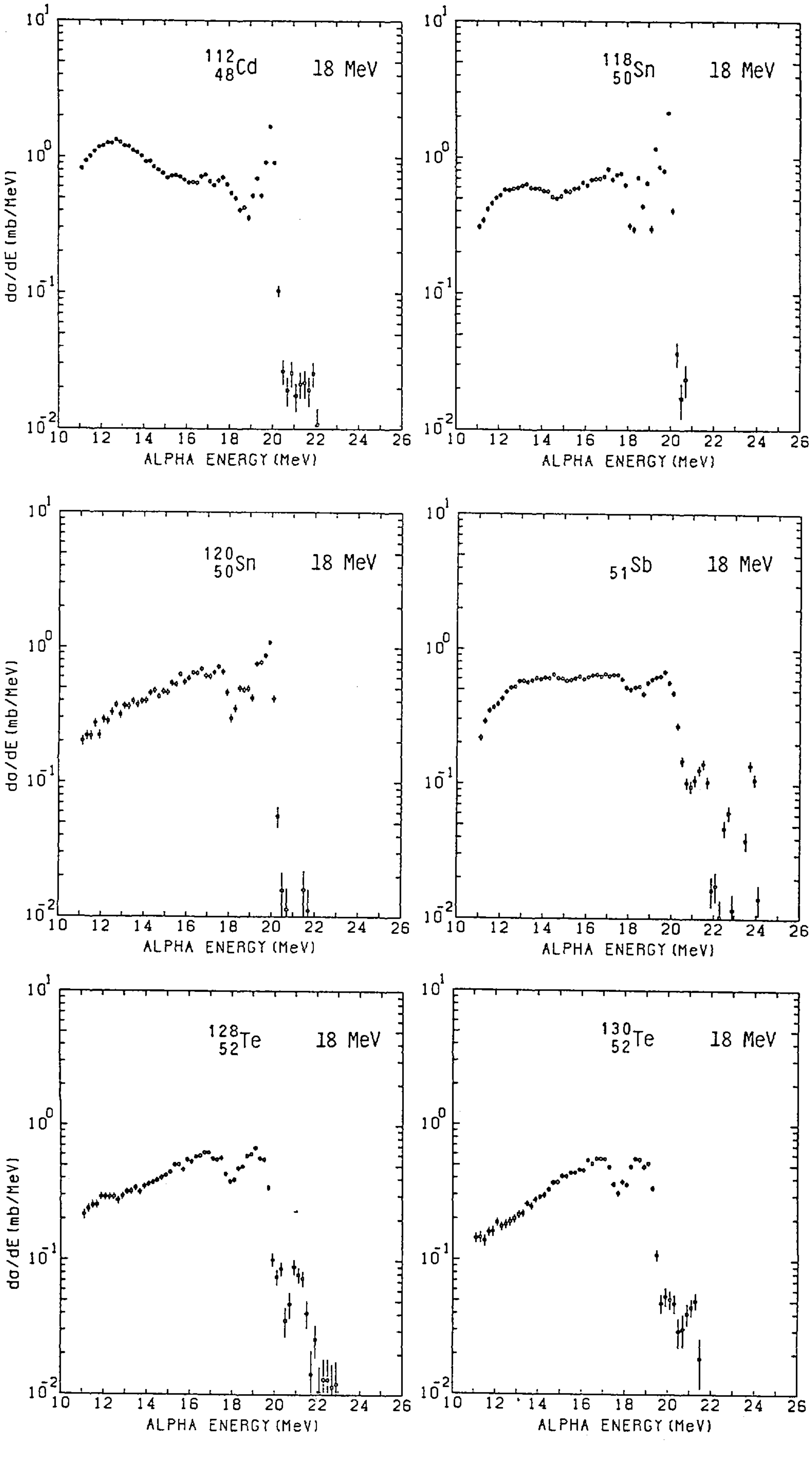

$^{112}_{48}Cd$ 18 MeV
$^{118}_{50}Sn$ 18 MeV
$^{120}_{50}Sn$ 18 MeV
$_{51}Sb$ 18 MeV
$^{128}_{52}Te$ 18 MeV
$^{130}_{52}Te$ 18 MeV
dσ/dE (mb/MeV)
ALPHA ENERGY (MeV)

Fig.1

V-A-3 **Systematic Analysis of Fission Cross Sections of Actinides by Means of Double-Humped Barrier Model**

T. Ohsawa, Y. Shigemitsu, M. Ohta and K. Kudo

A paper on this subject was published in Journal of Nuclear Science and Technology, Vol. 21, p. 887 (1984) with an abstract as follows :

Neutron-induced fission cross sections of 24 actinide nuclei were analyzed in terms of the double-humped fission barrier model to deduce the barrier heights. Good fits were obtained by assuming that the first barrier is mass-symmetric and axially asymmetric, while the second barrier is mass-asymmetric and axially symmetric. Systematic trends were observed in the barrier heights of the actinide nuclei; the first barrier height as a function of neutron number tends to be peaked at $N \simeq 147$, whereas the second barrier height increases linearly as a function of $(1-x)^3 A^{2/3}$, where x is the fissility. By decomposing the barrier heights into liquid-drop and shell correction parts, the surface energy coefficient was deduced to be 17.55 MeV. This value is consistent with existing values obtained from nuclear mass systematics. This fact corroborates the theoretical conjecture that the shell correction is damped at larger deformations corresponding to the second barrier. Near constancy of the fission barrier heights for actinides (fission barrier anomaly) was interpreted in terms of the three-component analysis.

B. Energy Conversion Engineering

Interdisciplinary Graduate School

of Engineering Sciences

V-B-1

Measurement of He Production Cross Section with He Accumulation Method+

T. Fukahori*, Y. Kanda*, K. Mori*, H. Tobimatsu*,
Y. Maeda*, T. Nakamura**, and Y. Ikeda**

In design of fusion and fast reactors, gas production in structural materials by fast neutron irradiation is a serious problem, because it causes embrittlement of structural materials. Especially He production is important because of low solubility and high migration in metals.

In order to study He production in metals, measurement of He production cross section is required. A He accumulation method is one of the most useful means to measure the He production cross section. For this work, a He atom measurement system has been constructed.

The He production cross section of ^{27}Al has been measured relative to $^{27}Al(n,\alpha)^{24}Na$[1] at 14.8 MeV with He accumulation method. The Al samples were irradiated with FNS at JAERI. As a preliminary result, He production cross section of ^{27}Al at 14.8 MeV is 120 ± 11 mb. This value is

---

+ This work was performed as co-operation program between Kyushu Univ. and JAERI.

* Department of Energy Conversion Engineering, Kyushu University, Kasuga, Fukuoka 816, Japan

** Department of Reactor Engineering, Tokai Research Establishment, JAERI

similar to Grimes et al.'s result, 121 ± 25 mb[2] which was obtained by emitted charged-particle measurement than Kneff et al.'s, 144 ± 7 mb[3] by He accumulation method.

References

1) H. Vonach, "Nuclear Data Standards for Nuclear Measurements", INTERNATIONAL ATOMIC ENERGY AGENCY (1983. VIENNA) p59

2) D. W. Kneff et al., J. Nucl. Mater., 103&104 (1981) 1451

3) S. M. Grimes et al., Phys. Rev., C19 (1979) 2127

V-B-2 **Estimation of Level Density Parameters and Energy Shifts with Bayesian Method**

Y. Uenohara, Y. Kanda, T. Yugawa and Y. Yoshioka

A paper on this subject was presented at the International Conference on Nuclear Data for Basic and Applied Science, held at Santa Fe, in May 13-17, 1985 with an abstract as follow:

Bayesian method has been applied to estimate level density parameters and energy shifts of Ni, Co, Fe, and Mn isotopes in Hauser-Feshbach model formula so as to reproduce measured cross sections and emitted particle spectra. The computer code GNASH was used to calculate these quantities. Spline functions were used to interpolate experimental data and to reduce computing time. The estimated results are not so different from prior parameters which have been widely used in many studies.

V-B-3 **Simultaneous Evaluation of Fission and Capture Cross Sections and their Covariances for Heavy Nuclei**

Y. Kanda, Y. Uenohara*, T. Murata, M. Kawai**, H. Matsunobu+, T. Nakagawa, Y. Kikuchi and Y. Nakajima++

A paper on this subject was presented at the International Conference on Nuclear Data for Basic and Applied Science, held at Santa Fe, in May 13-17, 1985 with an abstract as follow:

The fission cross sections of ^{235}U, ^{238}U, ^{239}Pu, ^{240}Pu, and ^{241}Pu, and the capture cross sections of ^{197}Au and ^{238}U have been simultaneously evaluated for JENDL-3 in the energy range from 50 keV to 20 MeV. A generalized least squares method has been applied to estimate their cross sections and associated covariances from experimental data of absolute and ratio measurements. The experimental covariances were estimated from the partial errors for each measurement. The partial errors were categorized to a few groups which have specific correlation factors. The correlation only in neutron energies was taken into account. The presently evaluated fission cross sections of ^{235}U and ^{239}Pu are a few percent lower than those of JENDL-2 below 1 MeV.

---

* Department of Energy Conversion Engineering, Kyushu University, Kasuga, Fukuoka 816, Japan

** Nippon Atomic Industry Group Co., Ltd., Kawasaki, Kanagawa 210, Japan

+ Sumitomo Atomic Energy Industries, Ltd., Chiyoda, Tokyo, 101, Japan

++ Japan Atomic Energy Research Institute, Tokai, Ibaraki 319-11, Japan

V-B-4

Influence of Correlation among Different Reaction Data Measured by same Investigator on Simultaneous Evaluation

Y. Uenohara and Y. Kanda

Strong correlation has been usually assumed for experimental cross sections measured in a same experiment. The correlations between different cross section data have been hardly observed by evaluators because experimental conditions were different.

Fission cross sections for many nuclides were measured by groups in KfK, LLNL, and NBS. A large amount of these data strongly influence on the simultaneous evaluations of fission cross sections. The contribution of correlations in different experimental data has been estimated with respect to the previous simultaneous evaluations[1]. In the tests, it was assumed that the ^{235}U(n,f), ^{239}Pu(n,f), and ^{240}Pu(n,f) cross sections, and fission cross section ratio of ^{239}Pu to ^{235}U measured in KfK are correlated positive. These correlations were ignored in the previous evaluations. The evaluated ^{239}Pu(n,f) cross sections are slightly different from the results of the previous work and others agree with them within the evaluated standard deviations.

References:

1) Y. Uenohara and Y. Kanda, Proc. Int. Nat. Conf. "Nuclear Data for Science and Technology", p. 639 held at Antwerp, Sept. (1982)

VI. Musashi Institute of Technology

Atomic Energy Research Laboratory

VI-1 Temperature Dependence of Total Neutron Cross Sections in Thermal and KeV Regions

O. Aizawa, H. Kadotani*, T. Matsumoto and S. Oheda**

A paper on this subject was presented at the International Conference on Nuclear Data for Basic and Applied Science, held at Santa Fe, New Mexico in May 13-17, 1985.

In the paper we have discussed the temperature dependence of total neutron cross section of Si in the thermal energy region and of Nb in the keV energy region.

In the thermal neutron energy region, the inelastic scattering cross sections of Si in crystalline state have been measured at the room and 600°C temperatures. We used the time-of-flight spectrometer installed at TRIGA-II reactor at the Atomic Energy Research Laboratory of Musashi Institute of Technology. The measured cross section was compared with the calculation by THRUSH code in Fig. 1. We adopted the Debye model of the Debye temperature of 640°K for the calculation. We added the absorption cross section to the calculated inelastic scattering cross section for comparison. The agreement between the experiment and the calculation is quite satisfactory in the energy range between 0.002 to 0.2 eV.

---

* Century Research Center Corp.

** Present Address: Century Research Center Corp.

The temperature dependence of the total cross section of Nb was measured by the use of a filtered beam technique to produce the neutron beam with the energy band of 23.3 to 25.3 keV. The cross section was measured again at the room and 600°C temperatures. As the cross section of Nb around 24 keV is in the unresolved region, the measured cross section was analyzed as the EATCS (Effective Average Total Cross Section). Due to the self-shielding effect of the resonance cross section, EATCS depends on sample thickness and temperature.

In Table I, we compared the experiment with the calculated EATCS from the resonance cross section generated by U3R code and the resonance parameters of ENDF/B-IV. The table shows that both values of the sample thickness and of the temperature dependence are qualitatively reasonable. The present experiments and calculations are in good agreement with the other experimental data (see Fig. 2). However, there are large differences between the experiments and the calculations. This means that the evaluated resonance parameters of Nb in ENDF/B-IV are probably not applicable to the present application.

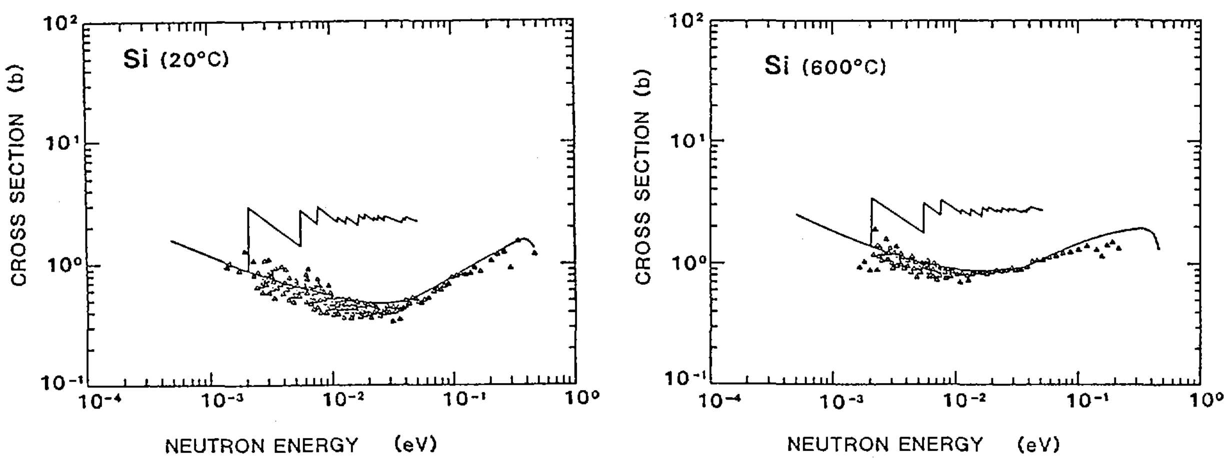

Fig. 1 Total cross section of silicon

TABLE I Effective average total cross section of Nb.

Thickness (cm)	EATCS (24keV) (barn)		EATCS (54keV) (barn)	EATCS (144keV) (barn)
	20 ℃	600 ℃	20 ℃	
2	7.57 ± 0.09	7.85 ± 0.09	8.36 ± 0.04	8.87 ± 0.04
4	7.04 ± 0.08	7.32 ± 0.09	7.42 ± 0.04	8.46 ± 0.03
6	6.68 ± 0.07	6.91 ± 0.08	7.00 ± 0.04	8.05 ± 0.03

U3R-code Calculation for Nb

Thickness (cm)	EATCS (24keV) (barn)	
	20 ℃	600 ℃
2	6.588 max 6.690 min 6.464	6.633 max 6.733 min 6.526
4	6.522 max 6.609 min 6.366	6.592 max 6.671 min 6.448
6	6.461 max 6.547 min 6.288	6.541 max 6.620 min 6.383

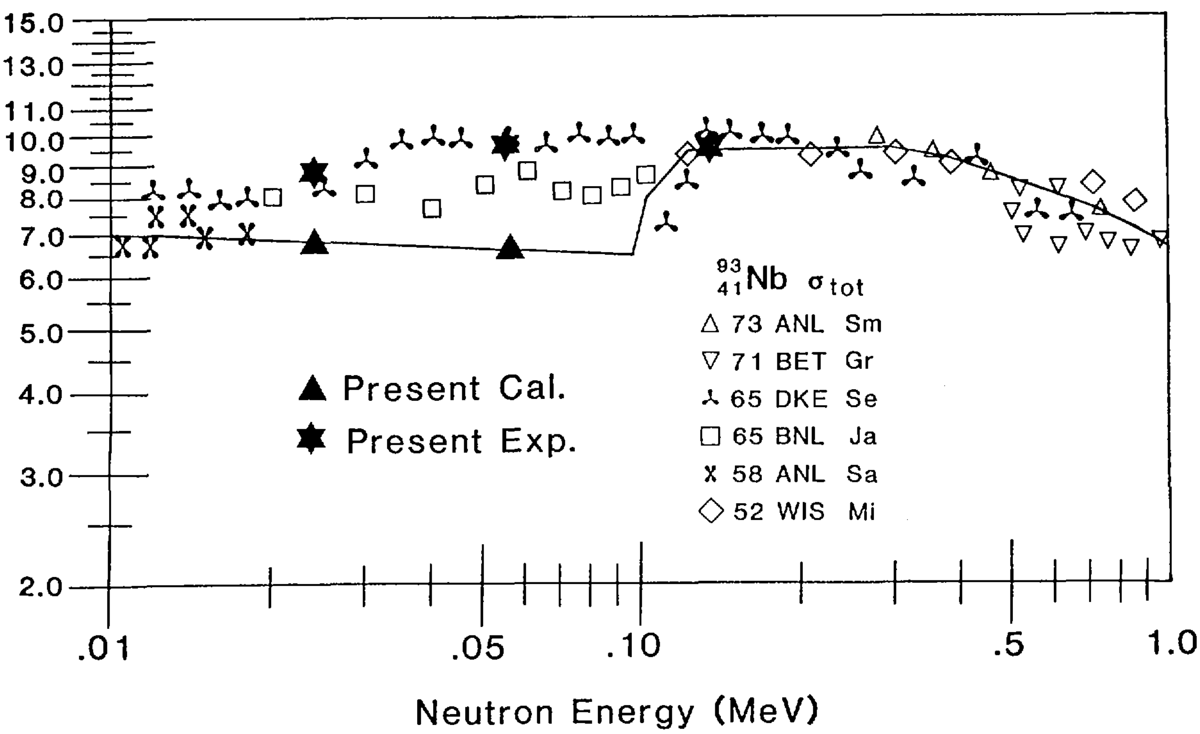

Fig. 2 Total cross section of Nb (BNL-325, 3rd edition)

VI-2 Total neutron cross sections of single- and poly-crystalline germanium

E. Suetomi, O. Aizawa, T. Matsumoto and H. Kadotani*

Total neutron cross sections of germanium have been measured at room temperature in the energy range from 0.0015 to 0.3 eV using a time-of-flight spectrometer of the Musashi Institute of Technology Research Reactor (TRIGA-II, 100 kW). The experiments were performed for single- and poly-crystalline germanium. To study the effect of grain size, the poly-crystalline samples were prepared from pure metal in solid, in crush and in powder forms. Theoretical cross sections were calculated for inelastic and elastic scattering using the THRUSH and the UNCLE-TOM codes, respectively.

The measured total cross sections of single-crystal germanium is compared with the calculation in Fig. 1. The agreement between experiment and calculation is fairly good. However, the calculation is slightly smaller than the experiment at the energy region above 20 meV. In Fig. 2 the total cross section of poly-crystalline germanium (grain size $< 74\mu$) is compared between the experiment and the calculation. In this case the agreement is satisfactory. The short note concerning on this subject has been accepted for publication in Nuclear Science and Technology.

---

* Century Research Center Corp.

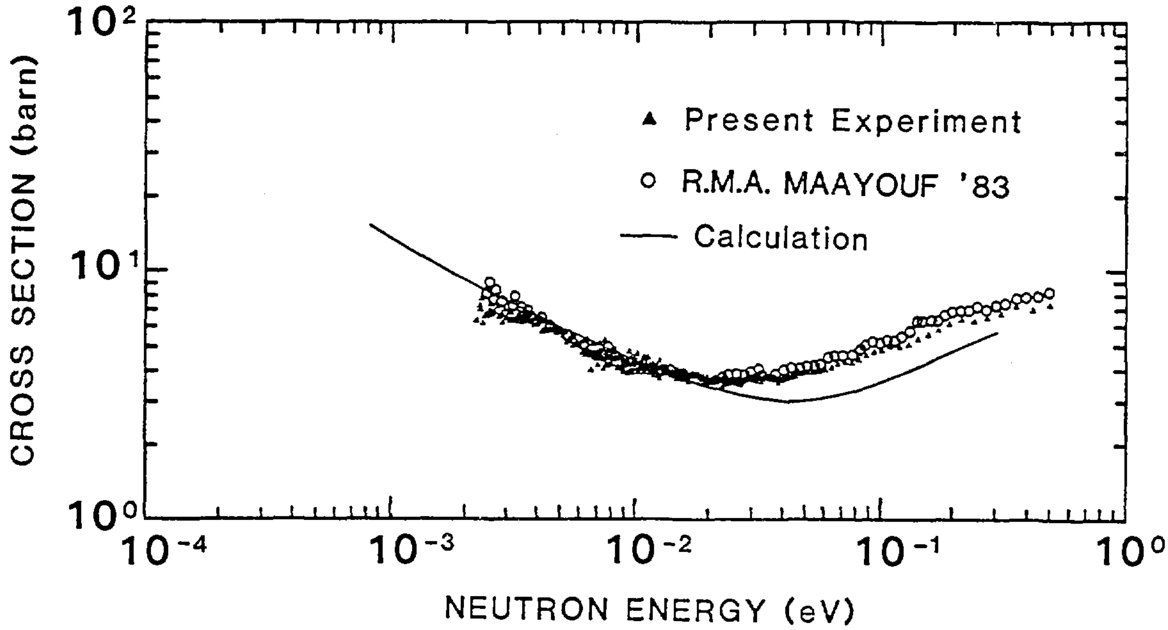

Fig. 1 Total cross section of single-crystal germanium

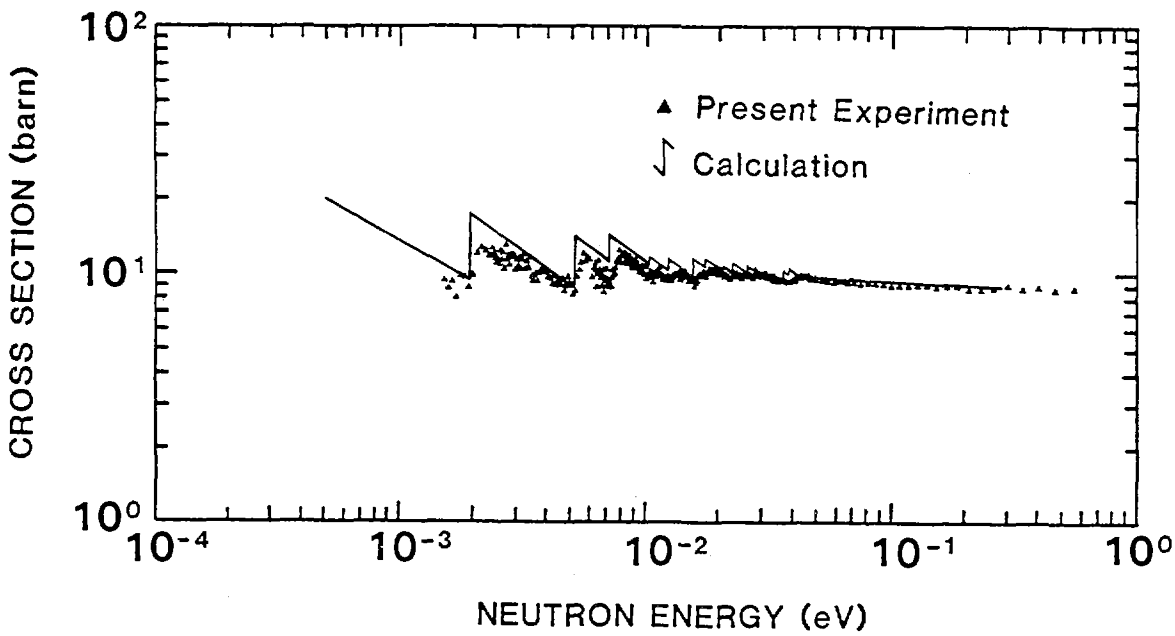

Fig. 2 Total cross section of poly-crystalline germanium

VII. NAGOYA UNIVERSITY

Department of Nuclear Engineering

Faculty of Engineering

VII-1

Measurement of Neutron Activation Cross-section of Molybdenum Isotopes at 14.6 MeV

T. Katoh, K. Kawade, H. Yamamoto, T. Ishii,
M. Yoshida, H. Miyade, H. Atsumi, A. Takahashi*
and T. Iida*

Neutron activation cross-sections of molybdenum isotopes at 14.6 MeV were measured to provide basic data for candidate structural materials of fusion reactors.

Sample materials were irradiated with the fast neutrons generated from the Intense 14 MeV Neutron Source (OKTAVIAN) at Osaka University by the D(T,n)α reaction. The neutron flux was about 10^9 neutrons/$cm^2 \cdot s$. Gamma-rays from produced radioactive elements were measured with a Ge detector to obtain the cross-sections. Activation cross-sections were determined by using the standard cross-section of the $^{93}Nb(n,2n)^{92}Nb$ reaction, which is taken as 464 ± 14 mb.

---

* Department of Nuclear Engineering, Osaka University

Measured cross-sections of molybdenum isotopes are shown in Table 1. Some of data in Table 1 supersede data in previous report (NEANDC(J)-106/U, INDC(JPN)-92/U).

A cross-section of a gas production reaction $^{92}Mo(n,n'\alpha)^{88}Zr$ was also measured, which is small and has not been reported previously. The obtained values for 14.1 and 14.6 MeV neutrons are shown in Table 2.

Table 1. Activation cross sections of Molybdenum isotopes

Reaction	σ (mb)	Reaction	σ (mb)
$^{92}Mo(n,p)^{92m}Nb$	68.1 ± 1.5	$^{96}Mo(n,n'p)^{95g}Nb$	4.31 ± 0.14
$^{92}Mo(n,\alpha)^{89}Zr$	27.5 ± 0.8	$^{97}Mo(n,p)^{97}Nb$	18.09 ± 0.45
$^{92}Mo(n,n'p)^{91m}Nb$	64.7 ± 17.6	$^{97}Mo(n,n'p)^{96}Nb$	3.82 ± 0.11
$^{92}Mo(n,n'\alpha)^{88}Zr$	0.16 ± 0.03	$^{98}Mo(n,p)^{98}Nb$	5.71 ± 0.11
$^{94}Mo(n,2n)^{93}Mo$	6.40 ± 0.33*	$^{98}Mo(n,\alpha)^{95}Zr$	5.80 ± 0.11
$^{95}Mo(n,p)^{95m}Nb$	5.81 ± 0.39	$^{98}Mo(n,n'p)^{97}Nb$	2.15 ± 0.07
$^{95}Mo(n,p)^{95g}Nb$	32.0 ± 0.8	$^{100}Mo(n,2n)^{99}Mo$	1470 ± 100
$^{96}Mo(n,p)^{96}Nb$	24.1 ± 0.5	$^{100}Mo(n,\alpha)^{97}Zr$	3.19 ± 0.07
$^{96}Mo(n,n'p)^{95m}Nb$	1.60 ± 0.11		

* Contribution of the $^{92}Mo(n,\gamma)$ reaction is not considered

Table 2. Cross section of the $^{92}Mo(n,n'\alpha)^{88}Zr$ reaction

En (MeV)	σ (μb)
14.1	50 ± 10
14.6	160 ± 30

VII-2

Emission Rate of the 620 keV Gamma-ray in the Decay of ^{143}La

K. Kawade, H. Yamamoto, T. Ishii, M. Yoshida,

T. Katoh, K. Okano* and Y. Kawase*

Emmision rate of the 620 keV gamma-ray in the decay of ^{143}La was measured as a part of study of decay scheme of fission products. The source of ^{143}La was obtained as a decay product from ^{143}Cs. The source of ^{143}Cs was separated from the fission products of ^{235}U by using an on-line isotope separator (KUR-ISOL) installed at Kyoto University Reactor Facility. The gamma-rays from the activities were measured by using a Ge(Li) detector and a low energy photon spectrometer (LEPS). The emission rate of 620 keV gamma-ray was determined by comparing with the intensity of the 293 keV gamma-ray, which is the gamma-ray from the 293 keV level in ^{143}Pr (see Fig. 1.). The emission rate of the 293 keV gamma-ray is known as 42 %. The obtained value of emission rate of the 620 keV gamma-ray is shown in Table 1. The result is different from the previously reported value (1 %). The present value revises the log ft value of β decay from ^{143}La to the 620 keV level of ^{143}Ce.

---

* Research Reactor Institute, Kyoto University

Table 1. Emission rate of the 620 keV gamma-ray in the decay of ^{143}La.

Detector	η (%)
Ge(Li)	2.62
Ge(Li)	2.51
LEPS	2.72
LEPS	2.66
mean	2.63 ± 0.18

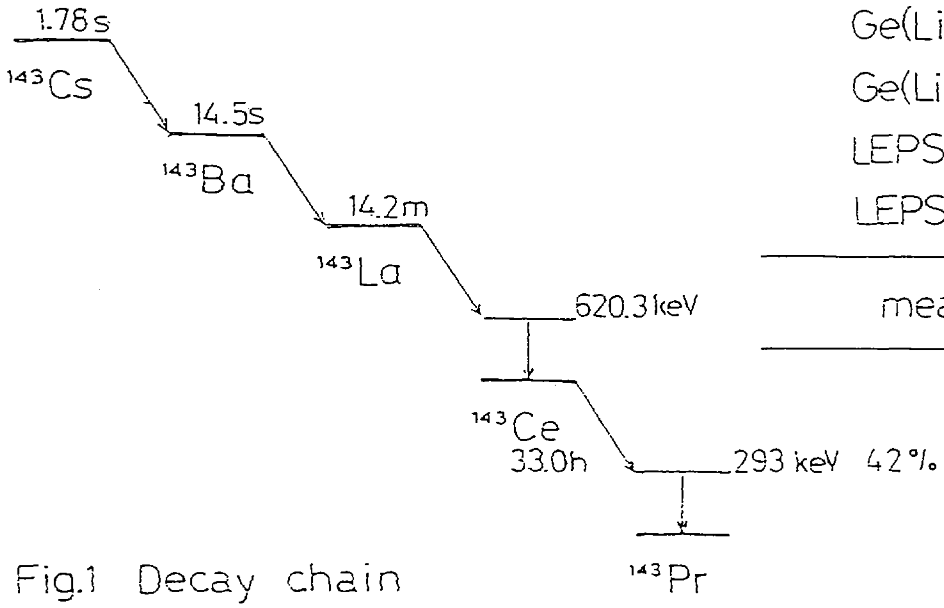

Fig.1 Decay chain

VIII. RIKKYO (ST. PAUL'S) UNIVERSITY

Department of Physics

VIII-1 Reanalysis of the $^{2}H(n,p)2n$ Data at 50 MeV

S. Shirato, Y. Ishibe and K. Shibata*

The breakup proton spectrum from the $^{2}H(n,p)2n$ reaction measured at 49.6 MeV by Stricker et al.[1] was analyzed through the Faddeev calculation code of Shibata et al.[2] in order to derive the neutron-neutron singlet scattering length $^{1}a_{nn}$. This code solves the Faddeev equations using the s-wave Yamaguchi separable two-nucleon interaction by means of the Ebenhoh method. The n-p effective-range parameters adopted in the calculation are as follows: $^{1}a_{np}$=-23.68 fm, $^{1}r_{np}$=2.67 fm, $^{3}a_{np}$=5.404 fm, $^{3}r_{np}$=1.75 fm. The n-n singlet effective range $^{1}r_{nn}$ was fixed as 2.76 fm and the $^{1}a_{nn}$ was varied from -17 fm to -22 fm.

The comparison between the experimental data[1] and the result of the calculation are shown in Fig. 1, where the old result of the impulse approximation calculation using $^{1}a_{nn}$=-22 fm is also reproduced from Ref.1. The most probable value of $^{1}a_{nn}$ was derived to be -19.6 ± 2 fm at a normalization constant of 1.505 and the minimum reduced chi-square of 2.23. This value of $^{1}a_{nn}$ is consistent with our value (-18.3 fm) derived from the 14.1 MeV data[3] as well as the value (-18.5 fm) from the $^{2}H(\pi^{-},\gamma)2n$ reaction[4].

---

* Present address: Nuclear Data Center, Department of Physics, JAERI

References:

1) A. Stricker, Y. Saji, Y. Ishizaki, J. Kokame, H. Ogata, T. Suehiro, I. Nonaka, Y. Sugiyama, S. Shirato and N. Koori, Nucl. Phys. A190 (1972) 284.

2) K. Shibata, T. Narita and S. Igarasi, JAERI-M 83-006 (1983).

3) S. Shirato, K. Saitoh, N. Koori and R. T. Cahill, Nucl. Phys. A215 (1973) 277.

4) B. Gabloud et al., Phys. Rev. Lett. 42 (1979) 1508.

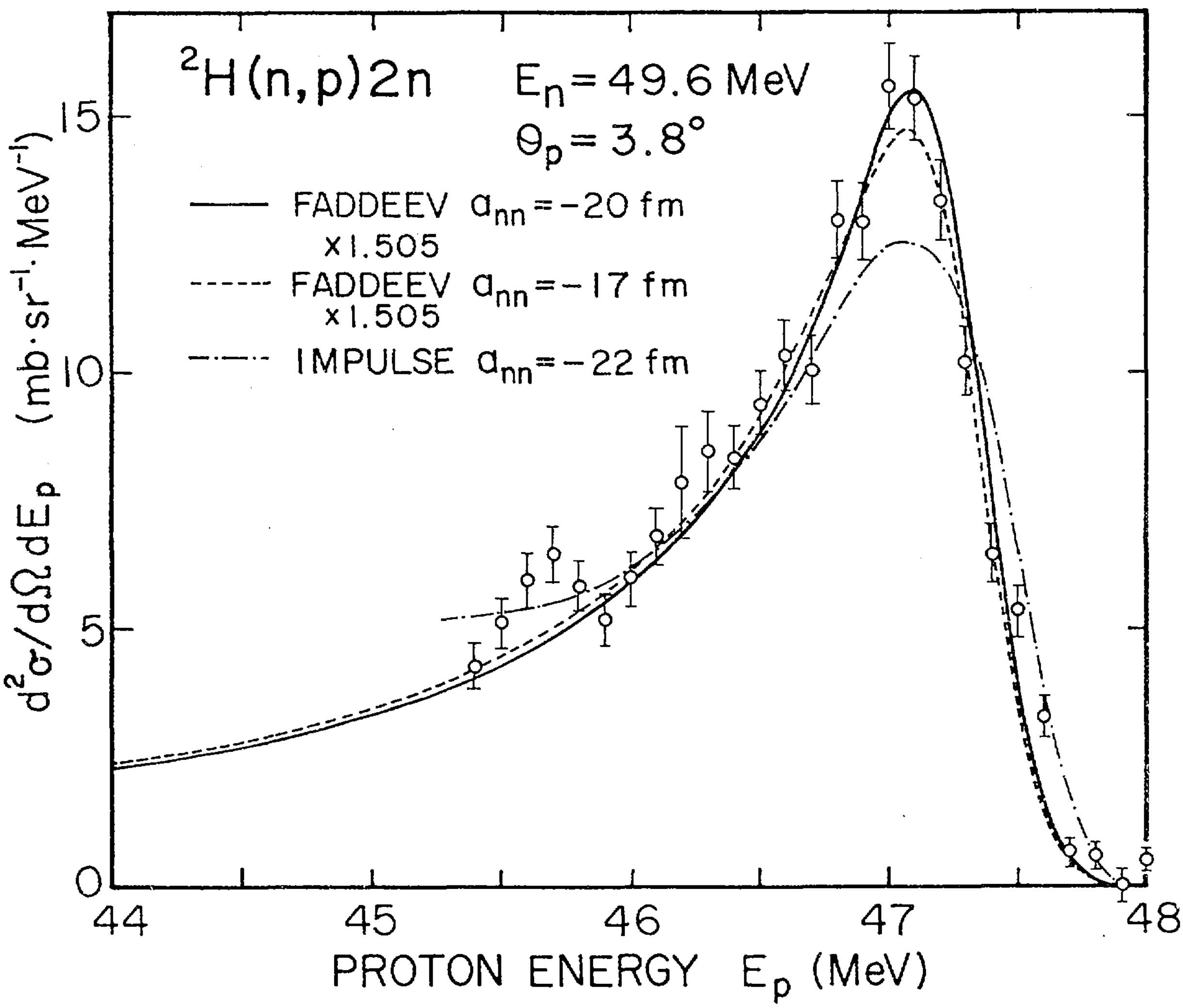

Fig. 1. Measured and calculated breakup proton spectra at the mean proton angle of 3.8°. The data and the impulse approximation calculation (dot-dashed line) are the results of Ref. 1.

Triton Spectra from the $^{7}Li(n,t)^{5}He$ Reaction at 14.1 MeV

I. Furutate, T. Kokubu, Y. Ando, T. Motobayashi and S. Shirato

The differential cross section for the $^{7}Li(n,t)^{5}He$ reaction was measured at several forward angles up to 70^{o} using 14.1 MeV neutrons. A natural lithium metal target of 12.44 mg/cm^2 thick and a counter telescope consisting of two gas proportional counters and two silicon detectors of 50 and 1500 μm thick were employed.

The measured triton energy spectra are shown in Fig. 1, after correction for energy losses of tritons in the target and the counter gas. The solid curves in the figure represent the simple three-body calculation based on the final-state interaction model using the n-α $P_{3/2}$- phase-shift. The result of this calculation, which was performed in the same way as those done in our $^{6}Li(n,d)^{5}He$ case[1), reproduces well the measured shape of triton spectra in the final-state interaction region. It is found that the measured shape of triton spectra is different in a low energy region from the calculation as well as previously measured deuteron spectra of the $^{6}Li(n,d)^{5}He$ case[1), indicating a considerable contribution from inelastic (and/or direct breakup) channels in the ^{7}Li case especially. The difference between measured triton and deuteron[1) spectra in a low energy region is due to different level structures in $^{7}Li^{*}$ and $^{6}Li^{*}$ leading to t+α and d+α in the final state after emission of an inelastic proton, respectively.

References:

1) S. Higuchi, K. Shibata, S. Shirato and H. Yamada, Nucl. Phys. A384 (1982) 51.

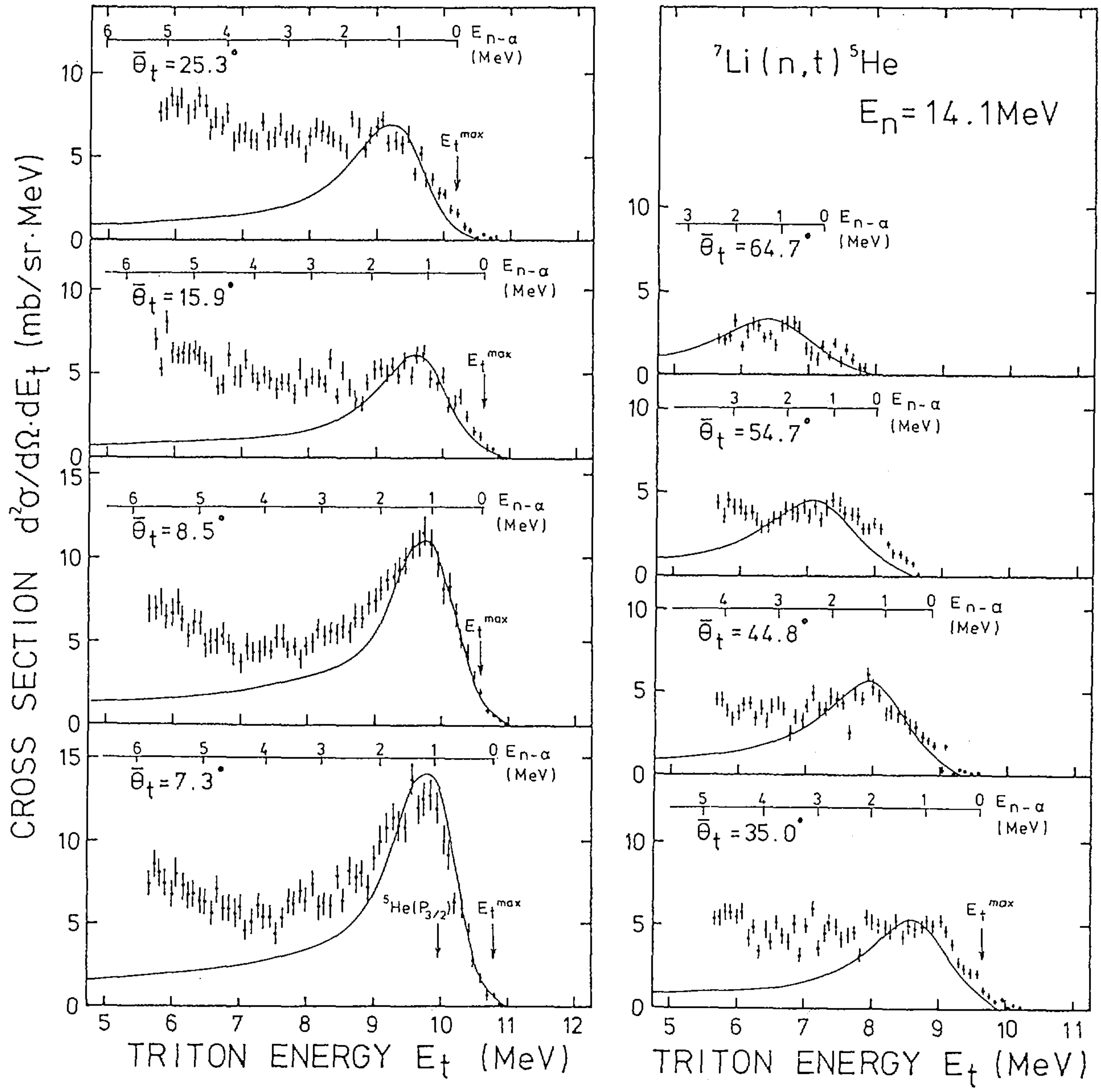

Fig. 1. Triton spectra from the $^{7}Li(n,t)^{5}He$ reaction at 14.1 MeV. The solid curves represent calculations using the n-α phase-shift.

IX. TOHOKU UNIVERSITY

Department of Nuclear Engineering

Faculty of Engineering

IX-1 Interction of Fast Neutrons with $^{6,7}Li$

S.Chiba*, M.Baba, H.Nakashima*, M.Ono, N.Yabuta,

S.Yukinori** and N.Hirakawa

A paper on this subjeect was presented at the International Conference on " Nuclear Data for Basic and Applied Science" (May 13-17, 1985, Santa Fe, USA) with the following abstract:

Energy-angle double-differential neutron emission cross sections (DDX) of lithium isotopes have been measured at incident energies of 4.2-6.0 and 14.2 MeV by the time-of-flight method. The $^{6,7}Li(n,2n)$ reaction cross sections were deduced. A coupled channel analysis was also made very successfully of the differential elastic and inelastic scattering cross sections measured at 9-14 MeV at TUNL. This work was performed for preparation of JENDL-3PR2.

---

* Present Address: Japan Atomic Energy Research Institute

** Present Address: Tokyo Institute of Technology

IX-2 Scattering of 14.1 MeV Neutrons from $^{10}B, ^{11}B$, C, N, O, F and Si

M.Baba, M.Ono, N.Yabuta, T.Kikuchi and N.Hirakawa

A paper on this subject was presented at the International Conference on "Nuclear Data for Basic and Applied Science" (May 13-17, 1985, Santa Fe, USA) with the following abstract:

We have measured the neutron emission cross sections using the time-of-flight technique for $^{10}B, ^{11}B$, C, N, O, F and Si at the incident neutron energy of 14.1 MeV, and for carbon at 18.2 MeV. The data were obtained at 10 or 12 laboratory angles between 25° and 150° over the secondary neutrons down to 0.4 MeV. The partial cross sections were obtained as well for elastic- and some inelastic-scattering processes.

IX-3 Double-Differential Neutron Emission Cross Sections of ^{6}Li and ^{7}Li at Incident Neutron Energies of 4.2,5.4,6.0 and 14.2 MeV

S.Chiba*, M.Baba, H.Nakashima*, M.Ono, N.Yabuta,

S.Yukinori** and N.Hirakawa

A paper on this subject will be published in Jour. Nucl. Sci. Tech. with the following abstract:

Energy-angle double-differential neutron emission cross sections of lithium isotopes were measured at incident neutron energies of 4.2, 5.4 and 14.2 MeV for ^{6}Li and of 5.4, 6.0 and 14.2 MeV for ^{7}Li using a time-of-flight spectrometer. Care was taken in background subtraction and in data correction for sample-size effects. Detaied comparison of the present results was made with the evaluated data in JENDL-3PR1. A spectrum fitting method was used to extract the $^{6,7}Li(n,n'x)\alpha$ and (n,2n) reaction cross sections. Neutrons emitted from the (n,2n) reactions were well described by the conventional evaporation model. A simple calculation with a final-state Coulomb interaction was effectively applied for the $^{6,7}Li(n,n'X)\alpha$ reactions. Angle-integrated cross sections of the $^{7}Li(n,n't)\alpha$ reaction were in good agreement with the JENDL-3PR1 data except the data measured at 6.0 MeV. The angular distributions of elastically and inelastically scattered neutrons were successfully analysed with the coupled-channel method at the incident neutron energy of 14.2 MeV.

* Present Address: Japan Atomic Energy Research Institute

** Present Address: Tokyo Institute of Technology

IX-4 Measurement of Fast Neutron Induced Fission Cross Sections of ^{232}Th, ^{233}U and ^{234}U Relative to ^{235}U

Kazutaka Kanda, Hiromitsu Imaruoka, Kazuo Yoshida,

Osamu Sato and Naohiro Hirakawa

A paper on this subject has been reported in International Conference on Nuclear Data for Basic and Applied Science, at Santa Fe, U.S.A.

Neutron induced fission cross section ratios relative to ^{235}U have been measured for ^{232}Th, ^{233}U and ^{234}U in the energy range from 0.5 to 7.0MeV. Experiments were carried out with the Dynamitron accelerator at Tohoku University. A tritium-titanium target was used to produce neutrons in the energy range from 0.5 to 3MeV by the T(p,n)^{3}He reaction. Neutrons in the range from 3 to 4 MeV and 4 to 7MeV were produced by the D(d,n)^{3}He reaction with a deuterium-titanium target and a deuterium gas target, respectively.

The fission chamber used in this study was a parallel plate type ionization chamber contained 90% Ar and 10% CH_4. The ^{235}U and another sample whose fission cross section ratio to be measured were placed back to back in the fission chamber. The samples were electroplated on platinum plates of 36mm in diameter by 0.3mm thick, then they were sintered into oxides to fix on the plates. The diameter of the deposition was 2.5cm.

To determine the number of fissionable nuclides in the samples three methods, the 2π alpha counting(^{232}Th), the low geometry alpha counting(^{233}U, ^{234}U) and thermal neutron irradiation (^{235}U) were utilized depending on characteristics of each nuclide.

Fission samples, placed perpendicular to the neutron beam, were irradiated at the locations of 3 to 8 cm from the target. Data acquisition at each energy point were composed two irradiation runs of approximately equal dose by changing the sample direction 180°. This procedure eliminated the need for many corrections such as neutron attenuation in backing plates. To measure background counts caused by room returned neutrons, the fission chamber was separated about 1m from the target and iron bar of 50cm thick was placed between them. A NE213 scintillation detector, 2" in diameter by 2" thick, located approximately 15m from the target, was used to measure mean energies and spreads of source neutrons at an angle of 0°.

Fission cross section ratios were obtained after corrections for background counts due to room returned neutrons and impurities in the samples, discriminated counts by bias settings, etc. were performed to measured raw data. Dominant sources of errors in the present results are the number of atoms in the sample (^{235}U 1.7%), estimation of lost counts by bias settings (^{233}U 1.5%, ^{234}U 1.0%) and counting statistics (^{232}Th 1%). Present results are compared with other measured data and evaluated data files in Figs. 1~3.

References:

1) J. W. Williams, "Fission cross section of 02, 23, 25, 28, 41, B-10 and Li-6", LA-520, Los Alamos National Laboratory (1946).

2) C. Nordborg, H. Conde and L. G. Stromberg, Proc. Int. Conf. Neutron Physics and Nuclear Data for Reactors and Other Applied Purposes, Harwell, p.910 (1978).

3) J. W. Meadows, Proc. Int. Conf. Nuclear Cross Sections for Technology, Knoxiville, NBS Publication 594, p.479 (1980).

4) J. W. Behrens, J. C. Browne and J. C. Walden, Nucl. Sci. Eng., 80, 383 (1982).

5) R. W. Lamphere, Phys. Rev., 104, 1654 (1956).

6) V. G. Nesterov and G. N. Smirenkin., Sov. J. At. Energ., 24, 185 (1967).

7) E. Pfletschinger and F. Kappeler, Nucl. Sci. Eng., 40, 375 (1970).

8) J. W. Meadows, Nucl. Sci. Eng., 54, 317 (1974).

9) G. W. Carlson and J. W. Behrens, Nucl. Sci. Eng., 66, 205 (1978).

10) P. H. White, Hodgkinson and G. W. Wall., Proc. Symp. Physics and Chemistry of Fission, Salzburg, 1, p.219 (IAEA, 1965).

11) P. H. White and G. P. Warner, J. Nucl. Energy, 21, 671 (1967).

12) J. W. Behrens and G. W. Carlson, Nucl. Sci. Eng., 63, 250 (1977).

13) J. W. Meadows, Nucl. Sci. Eng., 65, 171 (1978).

14) ENDF/B-4 : Data file for ^{235}U (MAT 1261) evaluation by L. Stewart, H. Alter and R. Hunter, ^{232}Th (MAT 1296) evaluation by Wittkopf, Roy and Livolski, ^{233}U (MAT 1260) evaluation by N. M. Steen, ^{234}U (MAT 1043) evaluation by Drake and Nicholson, National Neutron Cross Section Center, BNL (1974).

15) JENDL-2 : Japanese evaluated Nuclear Data Library Version-2, Japanese Nuclear Data Committee and Nuclear Data center, Japan Atomic Energy Research Institute (1980).

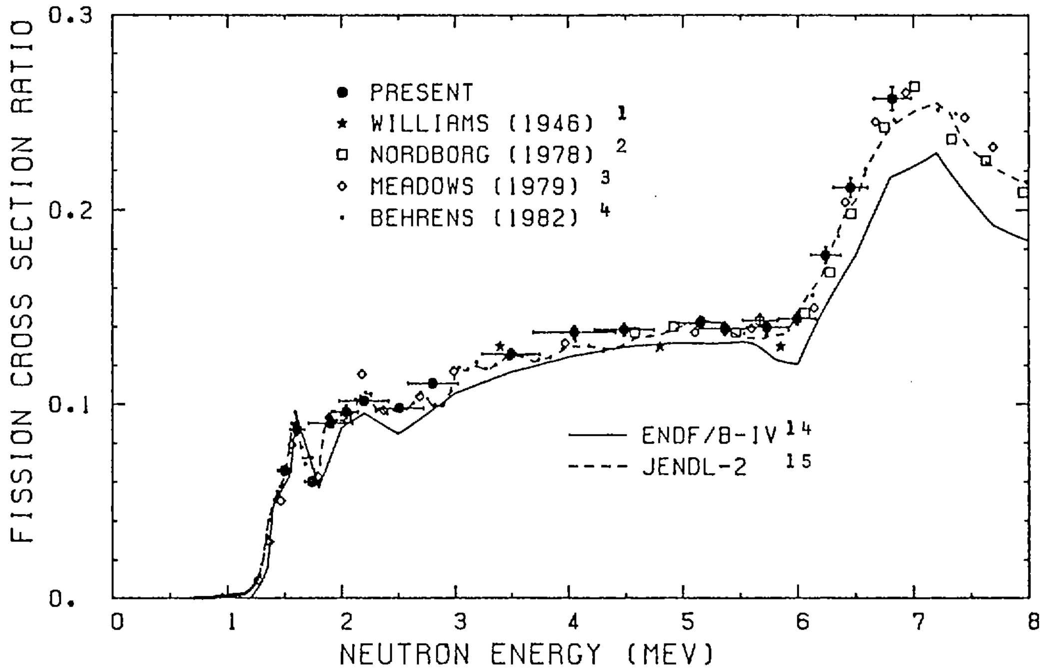

FIGURE 1 Fission cross section ratio of ^{232}Th to ^{235}U.

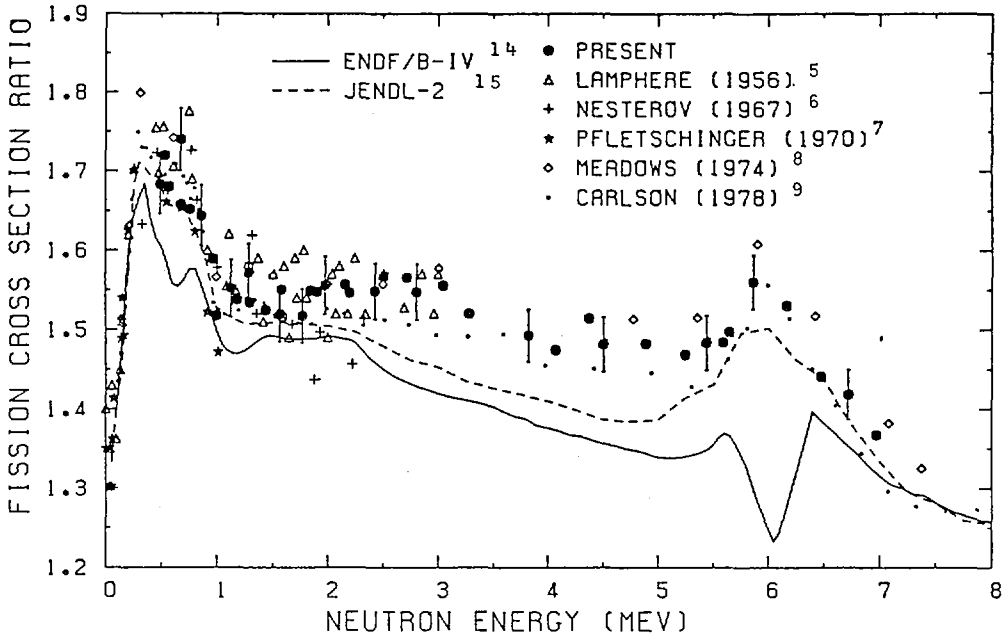

FIGURE 2 Fission cross section ratio of ^{233}U to ^{235}U.

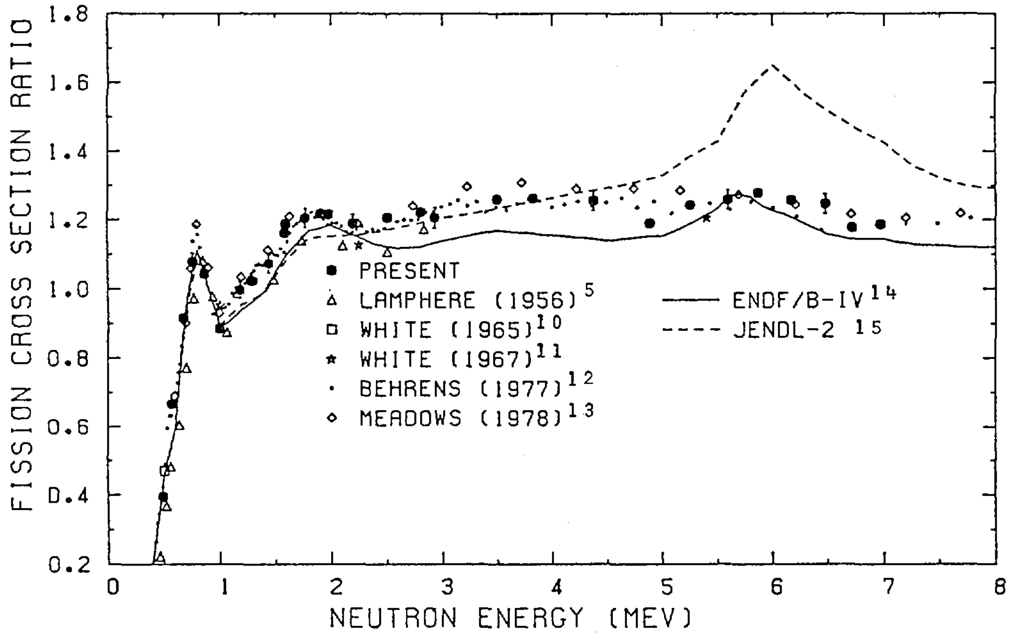

FIGURE 3 Fission cross section ratio of ^{234}U to ^{235}U.

X. TOKYO INSTITUTE OF TECHNOLOGY

Research Laboratory for Nuclear Reactors

X-1 Gamma-ray transitions following on p-wave neutron resonance capture and off-resonance capture by ^{28}Si

M.Shimizu, M.Igashira, K.Terazu and H.Kitazawa

We have measured gamma-ray spectra from 565-keV and 806-keV $p_{3/2}$-wave neutron resonance capture by ^{28}Si and from off-resonance capture with an anti-Compton NaI(Tl) detector, employing a time-of-flight technique. Particularly the latter resonance transitions were skillfully isolated from the 802-keV narrow resonance for the first time. Partial radiative widths of both p-wave resonances were obtained for the transitions to the ground $(1/2^+)$, 1273 keV$(3/2^+)$, 2028 keV$(5/2^+)$, 2425 keV$(3/2^+)$, and 3067 keV$(5/2^+)$ states in ^{29}Si. These widths cannot be reproduced by the Lane-Mughabghab optical model formulation of the valence model, even if the uncertainty of the optical potential parameters and spectroscopic factors which were used in the calculation is taken into account, but suggest that the core excitation in the resonance states is essential for an understanding of these reactions. Moreover, the results show that partial off-resonance capture cross sections are successfully predicted by the direct capture model in the distorted wave Born approximation.

X-2 Core-particle coupling model calculation of partial radiative widths for $p_{3/2}$-wave neutron resonances on ^{28}Si

H.Kitazawa, M.Ohgo, T.Uchiyama and M.Igashira

A core-particle coupling model was applied to the evaluation of radiative widths for the 565-keV and 806-keV broad $p_{3/2}$-wave neutron resonance on ^{28}Si. The calculation assumed the 2^+(1.78 MeV) and 3^-(6.88 MeV) one-phonon excitation of the core, and neglected the continuum nature of the resonance state wave function in the nuclear external region. The model wave functions were obtained from a coupled channel Schrödinger equation so as to reproduce the observed neutron escape widths, neutron binding energies, and spectroscopic factors. A reasonable agreement was achieved between the observed and calculated partial radiative widths for the transitions from both resonances to low-lying states in ^{29}Si. Moreover, it is emphasized that each of these resonances can be accounted for by a $J=3/2^-$ doorway states common to the $^{28}Si+n$ and $Si+\gamma$ channels, and that a dominant component of the doorway state wave function belongs the $[3^-\otimes 1d_{3/2}]$ configuration in which a single quasibound $1d_{3/2}$ neutron in ^{29}Si is coupled to the 3^- vibrational state of the ^{28}Si target.

X-3 Fast Neutron Spectrum in Lithium Fluoride Pile with D-T Neutron Source

D.-W. Lee*, H. Sekimoto and N. Yamamuro**

A paper on this subject was published in Journal of Nuclear Science and Technology, 22[1], pp.28~37 (January 1985). The abstract of this paper is as follows;

A lithium-fluoride pile was constructed by piling the lithium-fluoride ceramic blocks developed for the present study, and scalar neutron spectrum per source neutron in this pile was measured with a miniature NE213 spectrometer. The measured spectrum was unfolded with two window widths, a spectrometer resolution and one modified by one-time FORIST iteration. The measured spectrum was compared with ones calculated using the MORSE-GG Monte Carlo code with a modified point-detector estimator presented by Carter & Cashwell and the GICXFNS group cross-section set. The measured and calculated spectra agreed each other in their error bands, with the exception of the source energy peak.

* Present address: Busan National University, Busan, KOREA.

** Present address: Nippon Atomic Industry Group Co., Ltd., Ukishima-cho, Kawasaki-ku, Kawasaki 210.

X-4 Fast Neutron Spectrum Generated in Graphite Pile with D-T Neutron Source

H. Sekimoto, K. Hojo* and T. Hojo**

A paper on this subject was published in Journal of Nuclear Science and Technology, 22[3], pp.174~182 (March 1985). The abstract of this paper is as follows;

The scalar neutron spectrum normalized in reference to unit source neutron was measured with a miniature NE213 spectrometer at several positions along the centerline in a graphite pile irradiated with D-T neutrons. The measured spectra were compared with the results of calculation using the MORSE-GG Monte Carlo code with the modified point-detector estimator of Carter & Cashwell and GICXFNS group cross section set derived from the ENDF/B-V library. The measured and calculated spectra agreed within the errors estimated from the observed ranges of statistical error and of the folds on spectra due to response function error, except near the resonance peaks of the carbon total cross section at the deeper positions inside pile.

---

* Present address: Mitsubishi Heavy Industries, Ltd., Arai-machi, Takasago-shi 676.

** Present address: Mitsubishi Atomic Power Industries, Inc., Shiba-koen, Minato-ku, Tokyo 105.

X-5 Fast Neutron Spectrum in Water with a D-T Neutron Source

H. Sekimoto, K. Oishi*, T. Hojo** and K. Hojo***

A paper on this subject will be published in Nuclear Science and Engineering. The abstract of this paper is as follows;

Scalar neutron spectrum per source neutron was measured with a miniature NE213 spectrometer at several positions in water irradiated with D-T neutrons. The measured spectrum was compared with a calculated one using the MORSE-GG Monte Carlo code with a modified point-detector estimator presented by Carter and Cashwell and the GICXFNS group cross-section set processed from the ENDF/B-IV library. The measured and calculated spectra agreed within the errors estimated from the statistical error and the unfolding oscillations.

* Present address: Shimizu Construction Co. Ltd., Tokyo, Japan.

** Present address: Mitsubishi Atomic Power Industries, Inc., Tokyo, Japan.

*** Present address: Mitsubishi Heavy Industries, Ltd., Takasago, Japan.

X-6 Measurement and Calculation of Fast-Neutron Spectra in Water, Graphite and Lithium Fluoride Assemblies with a D-T Neutron Source

H. Sekimoto, D. Lee[1], K. Hojo[2], T. Hojo[3], K. Oishi[4],
T. Noura[5], M. Ohtsuka[6] and N. Yamamuro[7]

A paper on this subject will be published in Journal of Nuclear Materials. The abstract of this paper is as follows;

Scalar neutron spectra were measured with a miniature NE213 spectrometer at several positions in water, graphite, and lithium fluoride assemblies, which were irradiated with D-T neutrons. The n-γ discrimination was executed at each pulse height. The pulse height spectrum was unfolded to an energy spectrum with a modified FERDOR code.

The measured spectrum was compared with a calculated spectrum using the MORSE-GG Monte Carlo code with the GICXFNS group cross-section set processed from the ENDF/B-IV and V libraries.

The measured spectrum in the graphite assembly showed fine structure, and each peak and valley corresponds to a level-inelastic scattering and total cross-section resonance peak. The measured spectrum in the lithium-fluoride assembly was rather smooth. In general, all the measured spectra with the calculated ones in measurement and calculation error, though the error and oscillation of the unfolding were substantial.

---

1 Present address: Busan National University, Busan, Korea.

2 Present address: Mitsubishi Heavy Industries, Ltd, Takasago, Japan.

3 Present address: Mitsubishi Atomic Power Industries, Inc., Tokyo, Japan.

4 Present address: Shimizu Construction Co. Ltd, Tokyo, Japan.

5 Present address: Kobe Steel, Ltd, Kobe, Japan.

6 Present address: Hitachi Ltd, Hitachi, Japan.

7 Present address: Nippon Atomic Industry Group Co. Ltd, Tokyo, Japan.

X-7 A Simple Facility to Measure the Scalar Neutron Spectrum in an Assembly

H. Sekimoto, K. Hojo*, T. Hojo** and K. Oishi***

A paper on this subject was published in Nuclear Instruments and Methods in Physics Research A234 (1985) 148-151. The abstract of this paper is as follows;

An inexpensive, simple and safe facility was constructed to measure the neutron spectrum in an assembly, by setting a neutron source outside the assembly. A normalization technique for the neutron spectrum and error analyses are mentioned. The error of the calculated spectrometer efficiency is cancelled at the final spectrum normalization. The error caused by the present method is within acceptable levels.

* Present address: Mitsubishi Heavy Industries, Ltd., Takasago, Japan.

** Present address: Mitsubishi Atomic Power Industries, Inc., Tokyo, Japan.

*** Present address: Shimizu Construction Co. Ltd., Tokyo, Japan.

X-8 Some Characteristics of a Miniature Neutron Spectrometer

H. Sekimoto, K. Oishi*, K. Hojo** and T. Hojo***

A paper on this subject was published in Nuclear Instruments and Methods in Physics Research 227 (1984) 146-149. The abstract of this paper is as follows;

Some characteristics of an NE213 miniature spherical spectrometer for in-assembly fast-neutron spectrometry were measured. As the bubbling time changed, the pulse-height did not change appreciably, but the n-γ discrimination characteristics changed considerably. As the count rate changed, the pulse-height did not change appreciably, and the change of the n-γ discrimination characteristics was acceptable. The neutron response function was measured to be almost isotropic except for the backward direction.

X-9 An Unfolding Method Leading to a Positive Solution Only

H. Sekimoto

A paper on this subject was published in Nuclear Instruments and Methods in Physics Research 228 (1984) 129-132. The abstract of this paper is as follows;

A new unfolding method has been developed to minimize an objective function by adjusting the logarithm of the spectrum. This method gives a positive solution over the whole energy region. The solution oscillates much less than conventional solutions using the linear least-squares method, such as FERDOR, even without an oscillation damping term.

---

* Present address: Shimizu Construction Co. Ltd., Tokyo, Japan.

** Present address: Mitsubishi Heavy Industries, Ltd., Takasago, Japan.

*** Present address: Mitsubishi Atomic Power Industries, Inc., Tokyo, Japan.

X-10 High-Resolution Measurements of Compound States in ^{53}Mn

Y. Ozawa, Y. Oguri and E. Arai

In the present work excitation functions for elastic and inelastic scattering from ^{52}Cr were measured using a high-resolution beam over proton energies ranging from 3.20 to 4.76 MeV. At the low-energy end our data overlapped slightly with the results of Moses et al.[1)] The inelastic scattering data were helpful in determining J^{π} values of the compound states in the higher energy region.

1. Experimental procedure

The proton beam used in the experiment was obtained from the Tokyo Institute of Technology 4.75 MV Van de Graaff. The procedure of the automatic measurements of excitation functions and the method of improving the beam energy resolution have been described in detail by Ogawa et al.[2)]. The beam energy resolution was determined to be 200 eV (FWHM). The finite target thickness has introduced an additional broadening in the beam energy spread, and the overall resolution became 300-600 eV (FWHM) in actual experiments. The beam energy calibration was accomplished with the measured threshold energy in the reaction ^{19}F(p,n)^{19}Ne (E_{th} =4.2340 MeV). Absolute energies are believed accurate to ±3 keV, while relative energies over a small energy range are reproducible to a few hundred eV.

The energy mesh size was normally 300 eV but reduced to 200 eV in the region where the level density was high. An integrated charge of 300 μC was accumulated per point to obtain good statistical accuracy (1-3%).

The measured cross sections were fitted to theoretical results obtained from a multilevel, multichannel R-matrix calculation to extract resonance parameters. The only non-elastic channel included was inelastic scattering to the 2^+ first excited state at 1.4336 MeV in ^{52}Cr. The measured spectrum of protons scattered by the ^{52}Cr target supports this assumption. In the higher energy region, there was a large number of closely-spaced strong resonances and it was difficult to determine the resonance parameters from the elastic cross sections alone. In such cases, the inelastic scattering data were very helpful in estimating resonance parameters for the elastic cross sections.

Values of channel-spin-dependent partial width $\Gamma_{s'l'}$ were determined from the angular distributions of inelastic protons. (s' is the channel spin of the exit channel and l' is the orbital angular momentum of the emitted particle.) The analysis was based on the theory of Blatt and Biedenharn[3). For convenience we define the coefficients $a^2_{s'l'}$ as follows:

$$\Gamma_{s'l'} = a^2_{s'l'}\Gamma_{p'} \quad (\sum_{s'} \sum_{l'} a^2_{s'l'}=1),$$

where $\Gamma_{p'}$ is the inelastic partial width. By changing the coefficients $a^2_{s'l'}$ for possible outgoing channel spins and orbital angular momenta, the best fit was sought for each angular distribution of inelastic protons.

2. Results and discussion

Fig. 1 shows one part of the measured (points) and calculated (curves) values of proton elastic and inelastic cross sections at lab scattering angles of 90°, 120°, 135° and 160°. We have observed about 550 resonances in the whole energy region. Due to the penetrability effect, only few levels with l-values larger than two are seen. Except for a shift of 6.3 keV in the absolute proton energy scale, our data agree rather well with the Duke result[1)] in the overlapping region (our resonance energies are higher than the other data).

With the large number of levels observed and analyzed it is suitable to perform a statistical analysis. The reduced width distributions and the proton strength functions are investigated. The results are presented in the following subsections.

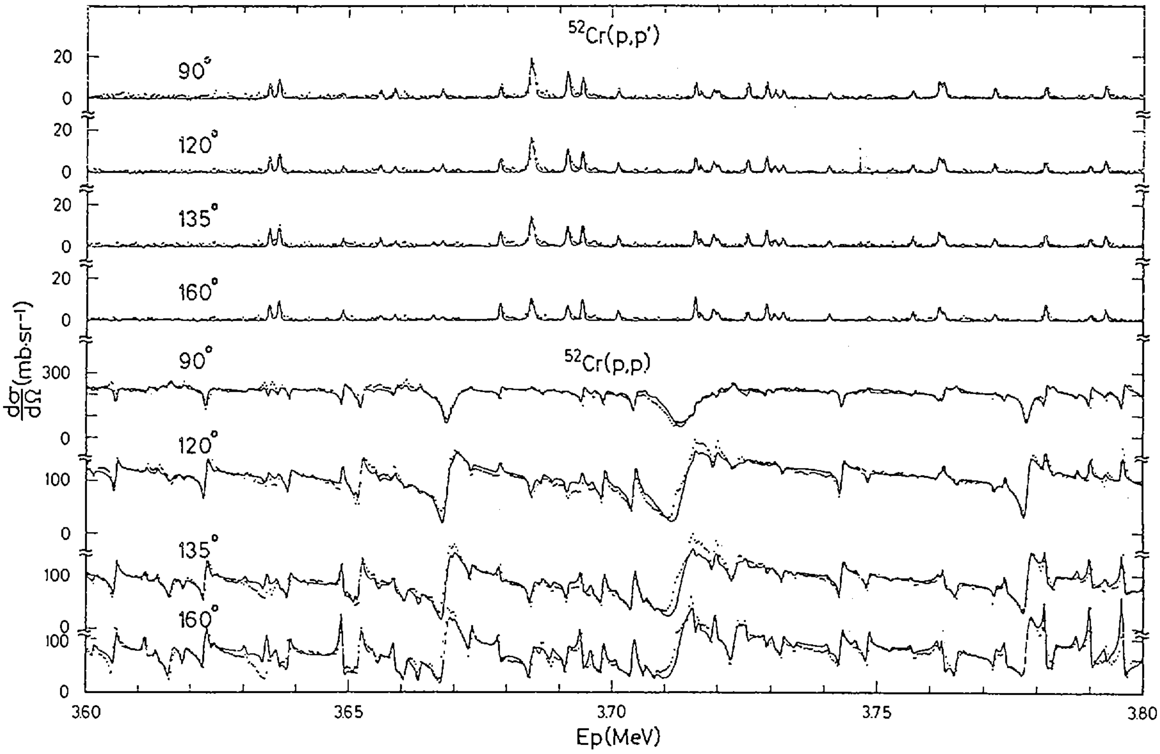

Fig. 1 Differential cross sections for elastic and inelastic scattering of protons from ^{52}Cr at lab angles of 90°,120°,135° and 160°. The solid lines are fits to the experimental values as described in the text.

2.1 Reduced width distributions. If the reduced-width amplitude distribution is a gaussian with zero mean, then the reduced widths follow the Porter-Thomas distribution

$$p(y) = \exp(-\frac{1}{2}y)/\sqrt{2\pi y}, \qquad y = \gamma^2/\langle\gamma^2\rangle.$$

Theoretical values are compared with the observed reduced widths where an integrated form is adopted. (The analogue resonances were eliminated from the experimental data.) Good agreements are obtained for each J^π values. From this best fit we have estimated numbers (fractions) of missing levels and average values of reduced widths for J^π up to $\frac{5}{2}^+$. The results are summarized in table 1.

2.2 Proton strength functions. We have calculated proton strength functions $s\equiv\langle\gamma^2\rangle/\langle D\rangle$ for two energy regions E_p=3.20-4.76 MeV and E_p=2.10-3.23 MeV, from the data of the present work and from the data of Moses et al., respectively. The results are summarized in Table 2. The missing fractions have been taken into account. The analogue resonances have been eliminated from the data to obtain pure "background" strength functions. The error was deduced from the statistical fluctuation due to the Porter-Thomas width distribution. The fractional error is given by $\sqrt{2/n}$, where n is the number of observed levels.

TABLE 1

Numbers(fractions) of missing levels and average values of reduced widths

J^{π}	The number of missing levels[a]	The average value of reduced widths[keV]
$\frac{1}{2}^{+}$	23(17%)	1.10
$\frac{1}{2}^{-}$	14(21%)	0.37
$\frac{3}{2}^{-}$	79(52%)	0.10
$\frac{3}{2}^{+}$	75(32%)	0.46
$\frac{5}{2}^{+}$	63(34%)	0.38

[a] The missing fraction is presented in perentheses.

TABLE 2

Proton strength functions for ^{52}Cr+p(the theoretical values are also listed in the last column)

J^{π}	Present work E_p=3.20-4.76 MeV	Moses et al.[1] E_p=2.10-3.23 MeV	Theory[4] E_p=3.00 MeV
$\frac{1}{2}^{+}$	0.093±0.012	0.067±0.015	0.052
$\frac{1}{2}^{-}$	0.014±0.003	0.044±0.009	0.031
$\frac{3}{2}^{-}$	0.010±0.002	0.010±0.004	-
$\frac{3}{2}^{+}$	0.068±0.008	0.009±0.004	-
$\frac{5}{2}^{+}$	0.044±0.006	0.041±0.010	-

In table 2, we see some indication of the energy dependence of the strength function. For $J^{\pi}=\frac{1}{2}^{-}$, the calculated value from the present data is smaller than the low-energy result. This is probably due to the fact that the $2p_{1/2}$ single particle state is located below our energy range. For $J^{\pi}=\frac{3}{2}^{+}$, the value of the present work is larger than the low-energy result. This indicates that the $2d_{3/2}$ single-particle state lies within our energy range. These two energy dependences are also found in the proton strength functions for ^{50}Cr.

Matuzaki and Arai[4] have calculated theoretical values of proton strength functions at an incident proton energy of 3 MeV for the target mass region between 30 to 70. The results for the ^{52}Cr target are compared with the present data in Table 2. The data of Moses et al. show reasonable agreement with the theoretical values, whereas the data of the present work show clear disagreement. This discrepancy also may be explained by the energy dependence of the proton strength function.

For complete discription see ref.[5].

References

1) J. D. Moses, H. W. Newson, E. G. Bilpuch and G. E. Mitchell, Nucl. Phys. A175(1971) 556.

2) M. Ogawa, T. Matsuzaki, Y. Ozawa and E. Arai, Nucl. Instr. Meth. 215(1983) 167.

3) J. M. Blatt and L. C. Biedenharn, Rev. Mod. Phys. 24(1952)258.

4) T. Matsuzaki and E. Arai, Z. Phys. A313(1983)293.

5) Y. Ozawa, Y. Oguri and E. Arai, Nucl. Phys. A440(1985)13.

XI. UNIVERSITY OF TOKYO

Institute for Nuclear Study

XI-1 Neutron Yield and Energy Spectrum Produced from Thick Targets by Light-Mass Heavy Ions

Takashi Nakamura

A paper on this subject is to be published in Nuclear Instruments and Methods[1).

The neutron yields and energy spectra produced from thick targets by light-mass heavy ion beams are evaluated. The neutron energy spectra are fitted to two(in low energy region of incident projectile energy lower than 100 MeV) and three (in high energy region of incident projectile energy higher than 100 MeV) Maxwellian-shape components. The lowest energy component corresponds to the evaporation neutrons from a compound nucleus having a nuclear temperature, T, independent to the neutron emission angle and the higher two components to the pre-equilibrium neutron emission having a nuclear temperature, T'(θ), depending on the angle, θ. The estimated values of T and T'(θ) are listed in Table 1. The lower T'(θ) values are around 5 to 10 MeV and almost independent to θ, but the higher T'(θ) values are several tens MeV and strongly dependent to θ.

The total neutron yields are evaluated by surveying several published papers. The surveyed results for several projectile and target combinations are shown in Fig. 1 as a function of projectile energy[2]. The total neutron yield generally increases with the incident projectile energy and mass and the target mass.

References:

1) T. Nakamura, to be published in Nucl. Instrum. Methods.
2) T. Nakamura, Genshikaku Kenkyu, 29 (1985) 55.

Table 1 Nuclear Temperature T for the Equilibrium State and T' for the Preequilibrium State for Each Projectile-Target Combination

Projectile	Energy E_0 (MeV)	Target	Nuclear Temperature: Equilibrium T (MeV)	Preequilibrium T' (MeV): 0°	15°	30°	45°	60°	75°	90°	120°	135°	150°
p	30	C	1.7	---	---		---		---			---	
		Cu	1.5	4.7	4.6		3.9		3.6			2.6	
		Pb	1.0	4.4	4.3		4.1		3.8			3.3	
d	33	C	2.3	9.3	7.0		5.0		3.9			---	
		Cu	1.5	6.9	5.9		4.3		3.3			2.7	
		Pb	1.1	5.0	4.9		4.3		3.3			3.3	
^{3}He	65	C	2.8	11.2	9.8		8.3		6.3			4.2	
		Cu	2.1	9.8	9.0		6.9		---			---	
		Pb	1.5	10.2	8.2		5.8		---			---	
α	65	C	2.8	7.4	5.5		4.6		4.6			3.0	
		Cu	2.1	7.3	6.8		6.7		5.9			3.5	
		Pb	1.5	6.2	5.4		5.0		4.7			3.6	
p	590	Pb	1.7			(9 53				(9 40			(8 36
p	750	U	1.8				(--- 38*					(--- 16**	
α	640	Pb	1.5	---	---	---	---	---		---	---		---
α	710	C	3.2	--- ---	(7 48	(7 35	(7 30	(7 27		(7 16	(--- 10		(--- 8
		Fe	2.2	--- ---	(7.5 48	(7.5 33	(7.5 29	(7.5 25		(7.5 20	(--- 13		(--- 9
		Pb	1.7	--- ---	(6.5 43	(6.5 32	(6.5 26	(5.5 23		(5.5 17	(--- 13		(--- 9

* θ = 50° , ** θ = 130°.

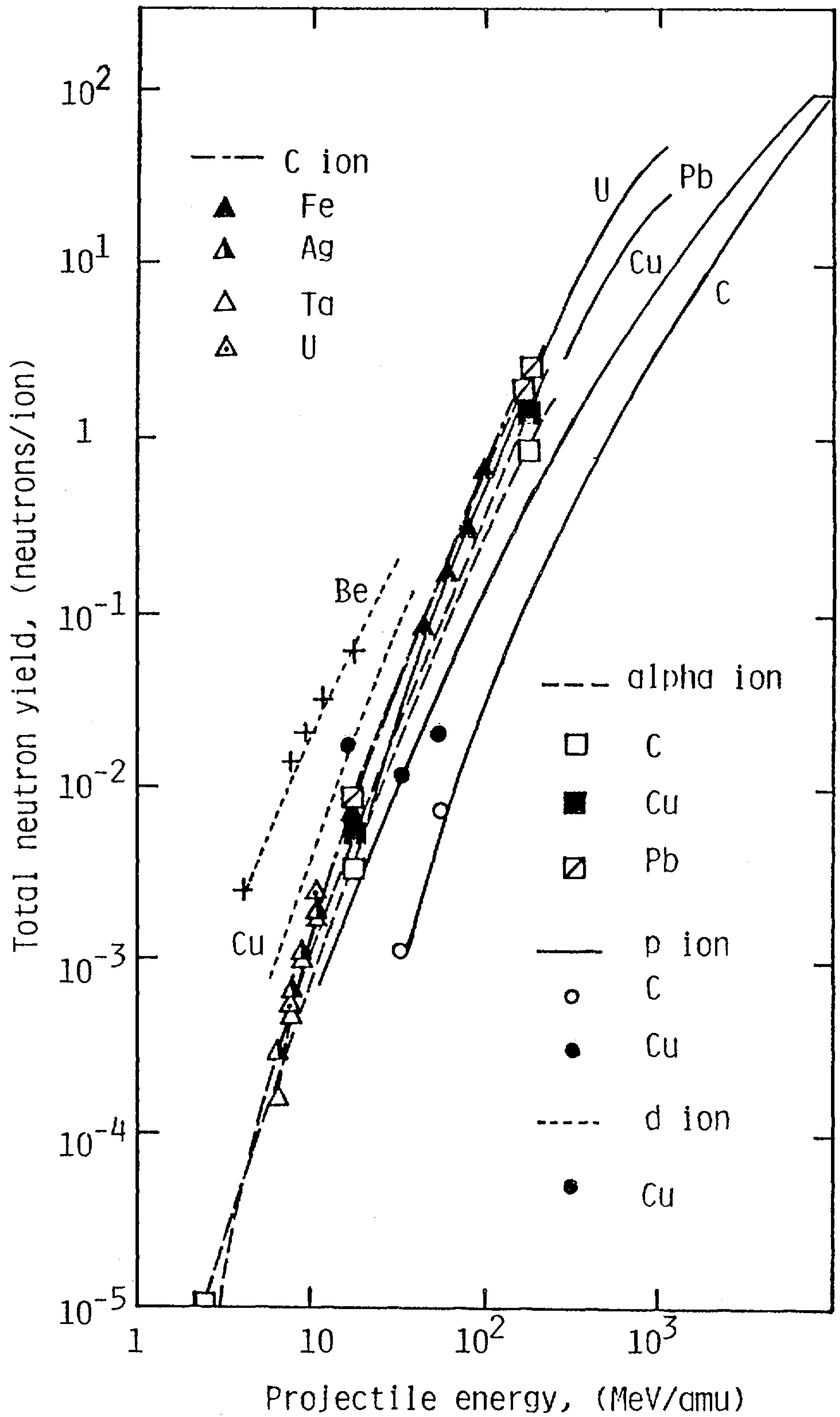

Fig. 1 Total neutron yields per incident ion for various projectile-target combinations[2)]